UNIVERSITY OF HAWAII
LIBRARY
MAY 9 '51

# The
# PHILOSOPHICAL MAGAZINE

FIRST PUBLISHED IN 1798

. 42 SEVENTH SERIES No. 327 April, 1951

## A Journal of Theoretical Experimental and Applied Physics

EDITOR
PROFESSOR N. F. MOTT, M.A., D.Sc., F.R.S.

EDITORIAL BOARD
SIR LAWRENCE BRAGG, O.B.E., M.C., M.A., D.Sc., F.R.S.
ALLAN FERGUSON, M.A., D.Sc.
SIR GEORGE THOMSON, M.A., D.Sc., F.R.S.
PROFESSOR A. M. TYNDALL, C.B.E., D.Sc., F.R.S.

PRICE 12s. 0d.
Annual Subscription £6 0s. 0d. payable in advance.

AND PUBLISHED BY TAYLOR & FRANCIS LTD., RED LION COURT, FLEET ST., LONDON, E.C.4.

# *Early Scientific Publications*

## DIARY OF ROBERT HOOKE, M.A., M.D., F.R.S.
1672-1680

**25/-**
net

Edited by **H. W. ROBINSON** and **W. ADAMS**
**Recommended for publication by the Royal Society, London**

"This vivid record of the scientific, artistic and social activities of a remarkable man during remarkable years has too long remained in obscurity."—Extract from foreword by Sir Frederick Gowland Hopkins, O.M., President of the Royal Society.

## MATHEMATICAL WORK OF JOHN WALLIS, D.D., F.R.S.

**12/6**
net

By **J. F. SCOTT, Ph.D., B.A.**

"His work will be indispensable to those interested in the early history of The Royal Society. I commend to all students of the Seventeenth Century, whether scientific or humane, this learned and lucid book."—Extract from foreword by Prof. E. N. da C. Andrade, D.Sc., Ph.D., F.R.S.
**Recommended for publication by University of London**

## CORRESPONDENCE AND PAPERS OF EDMOND HALLEY

**21/-**
net

Arranged and Edited by **EUGENE FAIRFIELD MACPIKE**

First published on behalf of The History of Science Society by Oxford University Press. Now re-issued by Taylor & Francis, Ltd.

## MEMOIRS OF SIR ISAAC NEWTON'S LIFE

**5/-**
net

By **WILLIAM STUKELEY, M.D., F.R.S., 1752**
From an Original Manuscript
Now in the possession of the Royal Society, London

## HEVELIUS, FLAMSTEED AND HALLEY

**12/6**
net

Three Contemporary Astronomers and their Mutual Relations
By **EUGENE FAIRFIELD MACPIKE**
**Published by arrangement with The History of Science Society**

Established
over 150 years

**TAYLOR & FRANCIS, LTD.**
**RED LION COURT, FLEET ST., LONDON E.C**
**PRINTERS & PUBLISHERS OF SCIENTIFIC BOOKS**

# XXXVI. *A New Method of Determining the Charge and Energy of Heavy Nuclei in the Cosmic Radiation.*

By A. D. Dainton, P. H. Fowler and D. W. Kent,
H. H. Wills Physical Laboratory, University of Bristol*.

[Received February 5, 1951.]

## Summary.

The charge and energy of a heavy particle in cosmic radiation may be determined from the frequency of the accompanying delta rays and the multiple scattering in its path through an emulsion. The method is illustrated by the charge spectrum of 226 tracks in emulsions exposed at 95,000 feet.

## §1. Introduction.

Since the discovery of the presence of heavy nuclei in the cosmic radiation (Freier *et. al.* 1948), several experimenters have employed the photographic method to determine the magnitude of the charges of the individual particles. The problem is of great importance because a knowledge of the "charge spectrum" of the primary radiation is essential for any discussion of its origin (Bradt and Peters 1950 a and b).

The method employed hitherto has been based on the measurement of, (*a*), the frequency of occurrence, $N_\delta$, per unit length of the track, of $\delta$-rays with energies in excess of a certain minimum value ; together with, (*b*), the ranges of the particles in the assembly of glass and emulsion constituting the photographic plates employed to record the tracks. At geomagnetic latitudes less than 30°, most of the primary particles are moving at relativistic velocities. For such particles, $N_\delta$ varies as $Z^2$ and this relation is independent of the precise value of the energy. The charge can therefore be deduced from the observed value of $N_\delta$ without an exact knowledge of the range, except in the few cases where an observable change of $N_\delta$ with range indicates that a particle is of lower energy.

Bradt and Peters (1950 b) have recently refined this method by using insensitive emulsions. The grain-density in the tracks of multiply charged particles is then so reduced that it can be determined by grain counts. Such observations give a measure of the ionization of the particle with a much greater statistical weight than a determination of $N_\delta$ deduced from an equal length of track.

For particles of lower energy, which occur frequently in the primary radiation at geomagnetic latitudes greater than 45°, the above methods suffer from the fact that, in general, the charge and the energy can be accurately determined only if the particle happens to reach the end of its range in one of the emulsions of the assembly. It is therefore important to develop other modes of attack, and for this purpose we have found it possible to modify the methods employed in this laboratory in determining the energy of fast protons and other particles of charge $|e|$.

---

* Communicated by Prof. C. F. Powell, F.R.S.

In the observation on the tracks of fast protons, the energy of a particle can be determined, and its identity established in favourable cases, by measuring, (*a*), the grain density, $g$, in the track; and, (*b*), the average angular deviation in the direction of motion, $\bar{\alpha}$, per unit length of the track, due to multiple coulomb scattering. In extending this method to the heavy particles, we have made similar observations on the scattering, but instead of the grain-density in the track, we determine $N_\delta$ the frequency of occurrence of $\delta$-rays. By these observations it is possible to determine the charge and energy of a particle if its track in a single emulsion is long enough to allow measurement of $\bar{\alpha}$ and $N_\delta$ to be made with sufficient statistical weight. A knowledge of the range of the particle is unnecessary. Further, the method appears to be sufficiently precise to allow elements of low atomic number to be identified with little ambiguity, so that the charge spectrum shows clearly resolved peaks due to the different elements.

Fig. 1.

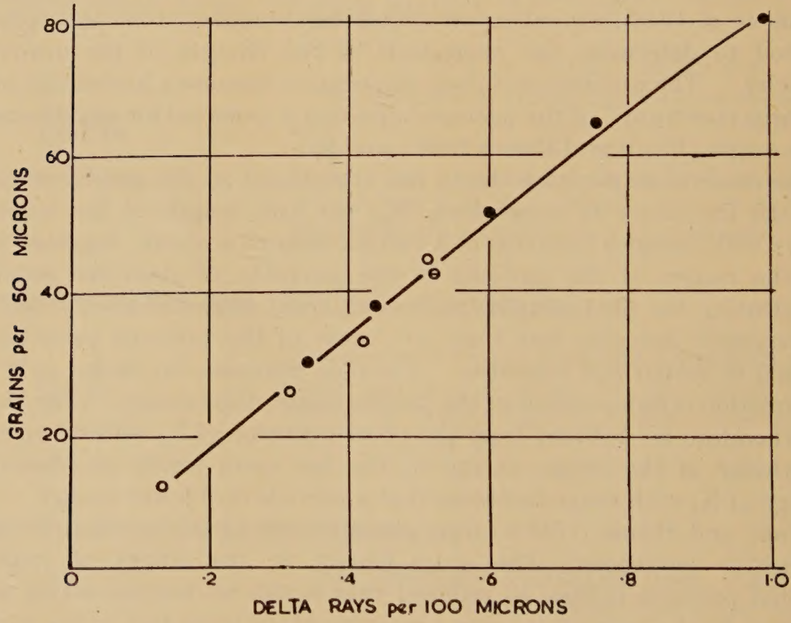

Relation between grain-density, $g$, and delta-ray density, $N_\delta$, in the trajectory of particles of charge $|e|$. Measurements on $\pi$-mesons are shown thus : ● ; on protons and deuterons, thus : ○ ; and on fast $\alpha$-particles, thus : θ .

## §2. Relation Between $N_\delta$ and Velocity for Particles of Different Charge.

In order to determine the relationship between the $\delta$-ray density in the track of a particle of known charge and its velocity, we have made observations on particles of charge $|e|$. For these particles, the relationship between residual range and velocity, and between grain-density and velocity, is now well established, for the type of emulsion in which the present tracks are recorded.

In the first instance, we made measurements on the tracks of $\pi^+$ or $\pi^-$ particles of which the range in the emulsion was about 8 mm., and which were identified by the secondary effects observed at the end of their range; viz., either $\mu$-decay, or the nuclear absorption of the particle and the formation of a " star " with two or more branches. The observed values of $N_\delta$ were plotted against the corresponding values of grain-density in the track, for various values of the residual range, and the results are shown in fig. 1. In making the observations, only $\delta$-rays giving rise to a track containing four or more grains were accepted.

Similar observations of greater statistical weight were made on the tracks of fifty protons and deuterons emitted from nuclear explosions occurring in the emulsion, particles of which the identity had been established by the methods previously described (Fowler 1950). It will be seen from fig. 1, that for particles of charge $|e|$, moving at velocities for which the grain-density is less than five times the minimum value ($g<5g_{\text{min}}$), the values of $N_\delta$ are proportional to the grain-density. On the basis of these observations, curves can be drawn showing the relation between $N_\delta$ and the scattering parameter $\bar{\alpha}$—for particles with any value of the charge $Ze$, and mass, A—using the relation between $\bar{\alpha}$ and $g$ established for $\pi$-particles (Camerini *et al.* 1950).

Fig. 2.

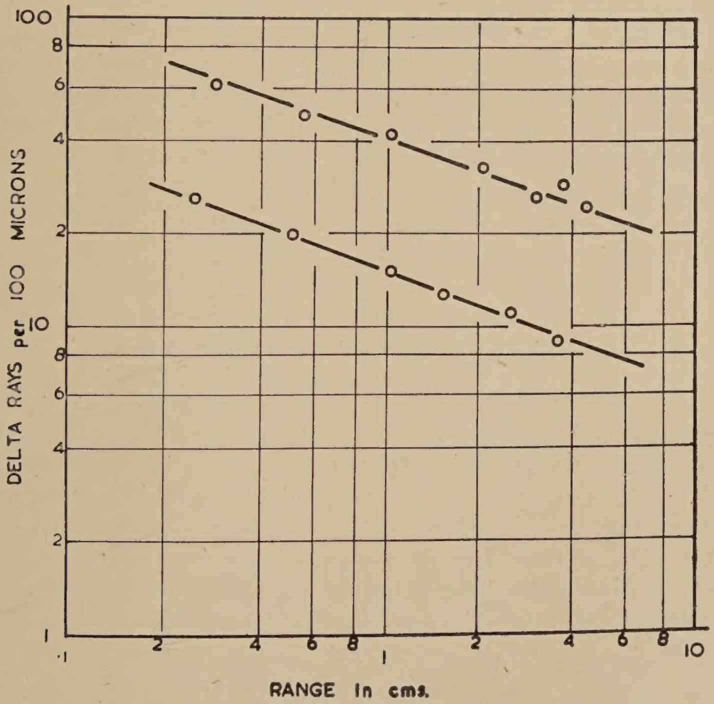

Variation of delta-ray density with range for tracks of a carbon and of a magnesium nucleus which reach the end of their range in the emulsion. The nuclei were identified by observations of $N_\delta$ and range.

As a check on equation (1), values of $N_\delta$ were determined by observations on long tracks of magnesium and carbon nuclei which came to rest in the emulsion, and which could be identified by the original method based on determinations of $N_\delta$ and range. The observations showed that

$$N_\delta \propto R^{0\cdot 42}, \quad . \quad . \quad . \quad . \quad . \quad . \quad . \quad . \quad . \quad . \quad (1)$$

where R is the residual range; see fig. 2. Using this result and the established relation between range and energy for particles moving in a photographic emulsion,

$$E \propto R^{\cdot 578}, \quad . \quad . \quad . \quad . \quad . \quad . \quad . \quad . \quad . \quad . \quad (2)$$

the relation between $N_\delta$ and $\beta$ was computed*. The result thus obtained was found to be consistent, within the limits of experimental error, with the calculated family of curves.

## §3. OBSERVATIONS ON THE SCATTERING OF HEAVY NUCLEI.

The measurements of the deviations in the tracks of heavy nuclei due to multiple coulomb scattering present no particular difficulties and have been carried out in the manner described by Fowler (1950). The thickness of the track gives rise to larger reading errors than in the case of similar observations with fast protons or α-particles, but these are not important. In order to evaluate the mean angle of scattering from the readings taken on the microscope, we have corrected for reading errors, stage " noise " and distortion, by the procedures to be described in a later communication. If A is the mass number and Z the charge number of the nucleus, its energy, corresponding to a given value of $\bar{\alpha}$, can be calculated from the relation :—

$$\bar{\alpha} = Zk/Apv, \quad . \quad . \quad . \quad . \quad . \quad . \quad . \quad . \quad . \quad . \quad (3)$$

where $p$ is the momentum of the nucleus per nucleon. With the units commonly employed, the scattering constant $k$ is taken as 26, a value indicated by a preliminary determination made in this laboratory. With the present exposures, " noise " and distortion prevent any accurate measurement of energies greater than 3 BeV./nucleon. It may, however, be possible to refine the processing technique in order to diminish the distortion errors and thus to improve the precision of the measurements.

## §4. CHARGE SPECTRUM OF HEAVY NUCLEI.

The present methods were employed in a study of the charge distribution of the heavy nuclei recorded in an assembly of Ilford G5 plates exposed by means of free balloons at an altitude of 95,000 ft., 40 c.c. of the emulsion of these plates were searched for tracks of which the length in any one emulsion was greater than 6 mm., and in which the value of $N_\delta$ was greater than 1·0 per 100 $\mu$. For each of these tracks the values of $\bar{\alpha}$ and $N_\delta$ were determined. The results thus obtained are represented in fig. 3.

---

* Equation (3) is not seriously invalidated, for particles with values of the energy with which we are here dealing, by the processes of " capture and loss " of electrons occurring at the end of the range of the heavy particles.

The family of full lines in fig. 3 represent the expected relation between $N_\delta$ and $\bar{\alpha}$ for different values of the charge number Z. They have been calculated on the assumption that the mass number of a nucleus, A, is equal to 2Z. This assumption is approximately justified for stable nuclei up to Z∼20; any nuclei of greater charge seldom occur in the primary radiation. Further, it seems very unlikely that any but stable or very long-lived isotopes will have survived the long periods believed to be involved in the acceleration process which produces the primary particles.

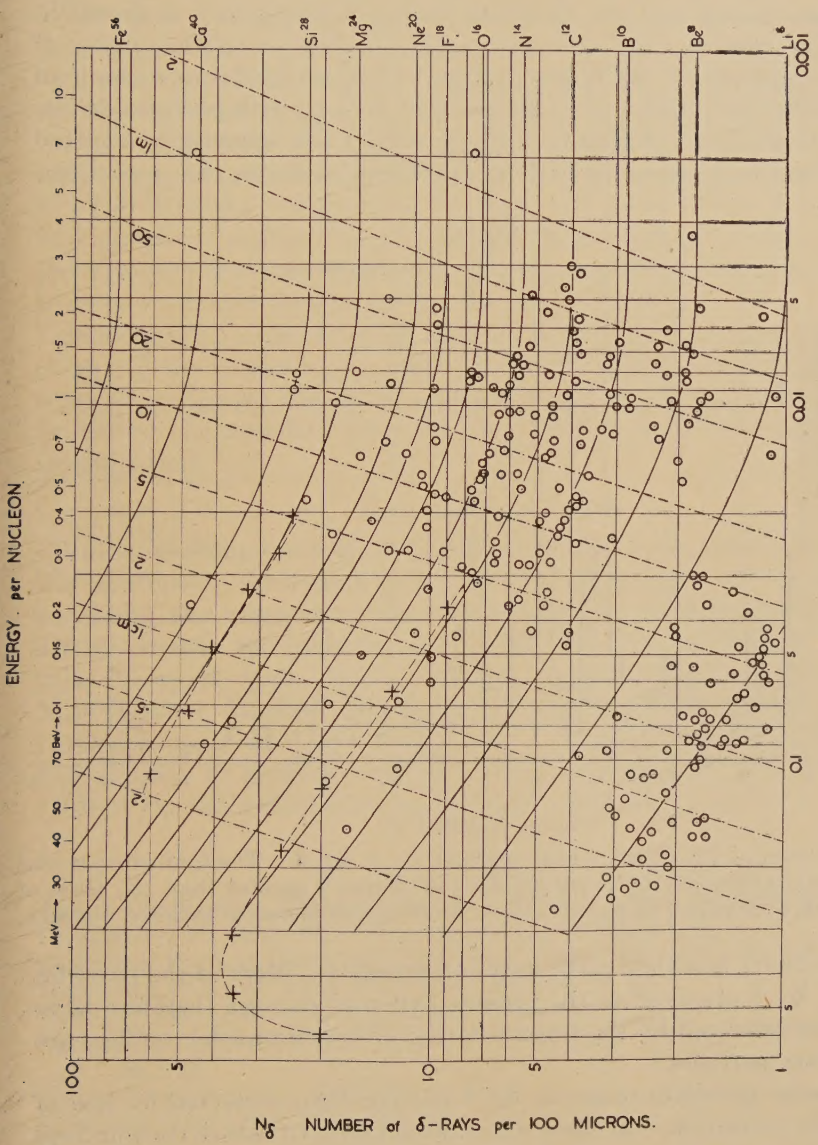

Relation between $N_\delta$ and $\bar{\alpha}$ (100$\mu$) for the tracks of 230 particles. Observations on tracks found in a systematic survey of 40 c.c. of emulsion are shown thus :—○. Measurements on two tracks which terminate in the emulsion after travelling over 4 cm. in a single plate (see fig. 2), are shown thus :— +--+. The full lines represent lines of constant charge, whilst the dashed lines are lines of constant range. An energy scale is included at the top of the figure.

The approximation is therefore adequate, with the present state of precision of the mass measurements, in the case of the primary particles. The greatest errors are likely to occur in the case of nuclei of lithium and beryllium, but they can hardly be serious.

From the results, the value of the charge for each individual particle can be determined and the resulting charge "spectrum" is shown in fig. 4. The spectrum includes results due to slow α-particles, many of which are products of the fragmentation of heavier nuclei as a result of nuclear collisions. Lithium nuclei are also present with energies as low as 60 MeV./nucleon. Energetic lithium nuclei are sometimes emitted from nuclear explosions caused by protons, neutrons, or α-particles

Fig. 4.

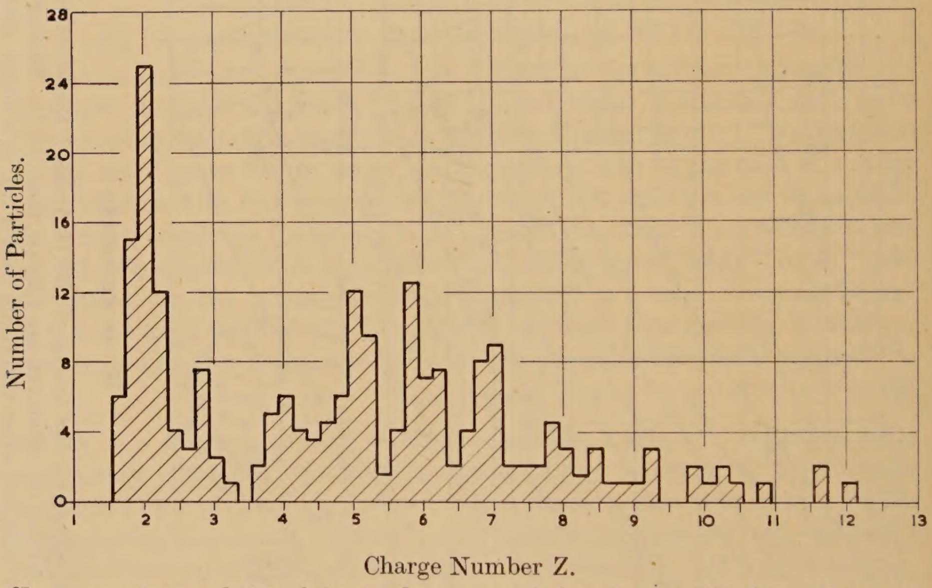

Charge spectrum of 226 of the tracks represented in fig. 3. The four other tracks observed in the systematic survey were of charge Z greater than 12; three of them were identified as due to silicon, and the fourth due to acalcium nucleus.

(Sörensen 1951), but they occur very infrequently. Most of the particles of charge $Z=3$ observed in the present experiment must therefore have been either produced by the fragmentation of heavier nuclei, or they are true primary particles.

The charge spectrum shown in fig. 4 has not been corrected for loss of particles by ionization—an effect which would tend to reduce the numbers of more massive nuclei observed—or for the general degradation in charge due to nuclear collisions in the atmosphere above the plates. Even after making allowance for these factors, however, it is difficult to account for the observed numbers of beryllium and boron nuclei if these elements are absent from the primary radiation at this latitude. Such a result, if it can be manitained by observations of greater statistical weight, would appear to be at variance with those of other observers working at a geomagnetic latitude of 30° N. (Bradt and Peters 1950 b).

## §5. APPRAISAL OF THE METHOD.

The most important advantage of the present method of determining the charge of fast atomic nuclei over those previously employed is that, at high geomagnetic latitudes, if the track of a particle is of sufficient length, the observations on it can be confined to a single emulsion. Further, for values of Z between three and six inclusive, the accuracy of the measurements appears to be greater than that previously attained (Bradt and Peters 1950 a, Hoang 1950, Dainton and Kent 1950). It is difficult, for example, to evaluate the charge of such particles, even when they are of low velocity, from the changes in the values of $N_\delta$ as the particle passes from one emulsion to another in traversing the stack.

In addition to the determination of the charge, the method gives the energy of the particles as a result of the same limited observations and a scale of energy per nucleon is included in fig. 3. It would be premature to discuss the detailed features of the observations at this stage of the investigation.

## ACKNOWLEDGMENTS.

In conclusion, we wish to thank Professor C. F. Powell, F.R.S., for his continued encouragement; Dr. M. M. Shapiro for assistance in obtaining the exposure; Mr. U. Camerini for helpful discussions, and Dr. H. Heitler for technical assistance. We also extend our thanks to Miss Margaret Stott, who made the scattering measurements, and to Miss Eleanor James, who scanned the plates. The investigation was carried out as part of a programme of research supported by the Department of Scientific and Industrial Research, to whom one of us (A.D.D.) is also indebted for a maintenance grant.

## REFERENCES.

BRADT and PETERS, 1950 a, *Phys. Rev.*, **77**, 54; 1950 b, *Ibid.*, **80**, 943.

CAMERINI *et al.*, 1951, *Phil. Mag.* (in course of publication).

CAMERINI, FOWLER, LOCK and MUIRHEAD, 1950, *Phil. Mag.*, **41**, 413.

DAINTON and KENT, 1950, *Phil. Mag.*, **41**, 963

FOWLER, 1950, *Phil. Mag.*, **41**, 169.

FREIER, LOFGREN, NEY, OPPENHEIMER, BRADT and PETERS, 1948, *Phys. Rev.*, **74**, 213.

HOANG TCHANG-FONG, 1950, *Thesis*, Paris.

SÖRENSEN, 1951, *Phil. Mag.*, **42**, 188.

# XXXVII. *An Interferometric Study of Cleavage Surfaces of Artificially Grown Crystals of Sodium Chloride.*

By S. Amelinckx,
University of Ghent, Belgium*.

[Received January 30, 1951.]

[Plate XIV.]

## Abstract.

Cleavage surfaces of an artificially grown crystal of sodium chloride are examined by multiple-beam interferometry. Two main features are noted, namely long narrow, more or less parallel strips, and superposed on this is a secondary fine grain structure. Silver films on sodium chloride are found to be unstable and apparently photosensitive. The cleavage mechanism is discussed.

Cleavage faces of an artificially grown crystal of NaCl have been examined by means of optical interference methods, using both multiple-beam Fizeau fringes and fringes of equal chromatic order (Tolansky 1948). The silvered specimen was matched against a high-grade silvered optical flat accurate to within $\lambda/40$.

Cleavage was induced in a large clear crystal (grown by Hilger) by striking perpendicular to a face with a razor blade. Rocksalt shows three cleavage directions parallel to (001), (010) and (100), which are considered as crystallographically equivalent. This was confirmed since no specific difference could be detected between them.

Although the cleavage is generally described as " perfect ", interferometric examination revealed a rather complex structure on these faces. The Fizeau fringes ($\lambda$ 5461) for a typical low magnification of a well-cleaved specimen is shown on fig. 1 *a*. This shows the presence of narrow strips, generally more or less parallel to each other and radiating out from the point where the cleavage was induced. There is a close resemblance between this picture and that of the calcite cleavage plane reported by Tolansky and Khamsavi (1946).

The strip widths vary from 1/100 to 1/10 mm. and their lengths are of the order of 1 mm. The planes of the strips are not always parallel but are sometimes inclined one to another as in the case of selenite (Tolansky 1945). In fig. 1 *a* the strip AB is inclined to the strip CD at an angle of $1{\cdot}33 \times 10^{-4}$ radians.

Another fact of interest is clearly visible. The part of the cleavage face in the right bottom corner (below the line A′B′) is inclined to the adjacent

---

* Communicated by Professor Tolansky.

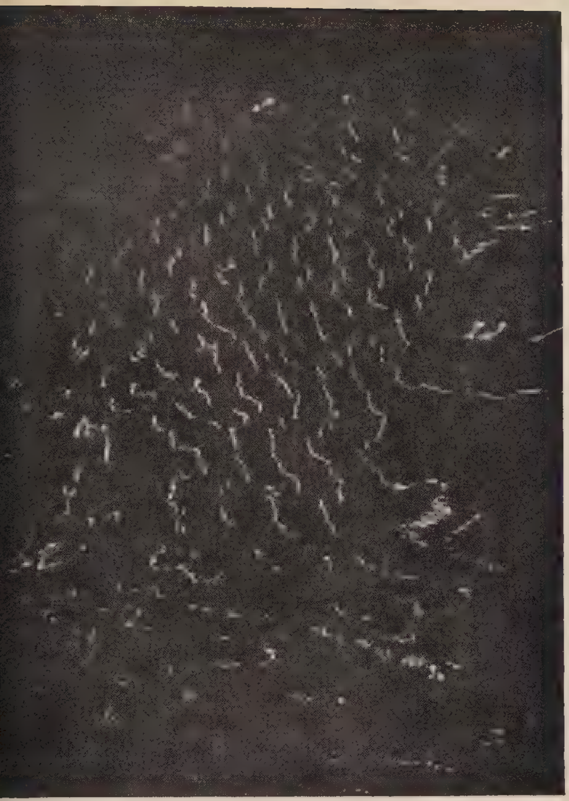

×48

(b)

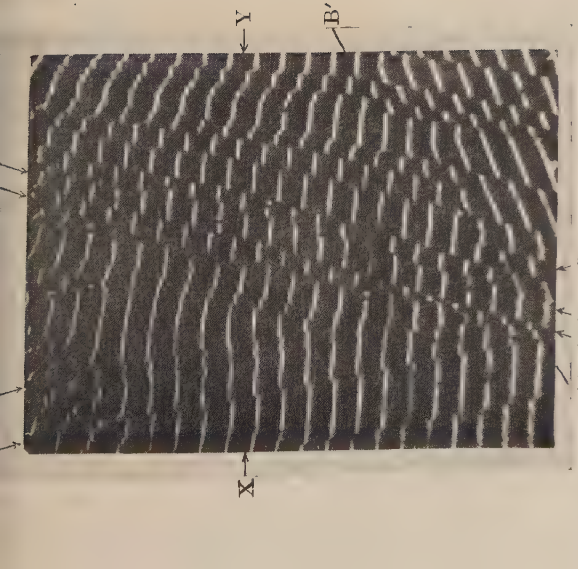

×60

(a)

×130

(e)

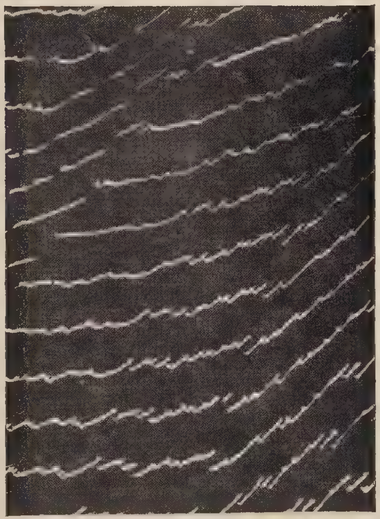

×100

(d)

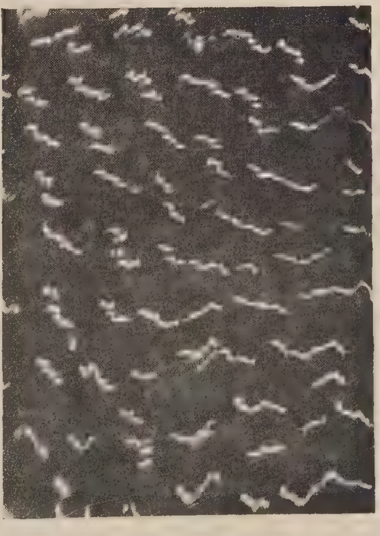

×90

(c)

region above A′B′ at an angle of $2{\cdot}11 \times 10^{-3}$ radians. The part of the crystal face to the left of the strip CD consists of strips all very nearly parallel to the strip CD; whereas the part to the right of AB consists of strips all very nearly parallel to AB.

The strips CD and AB themselves are inclined one to another. The part of the crystal face shown here consists consequently of three main regions which are inclined one to another over very small angles.

Fig. 2

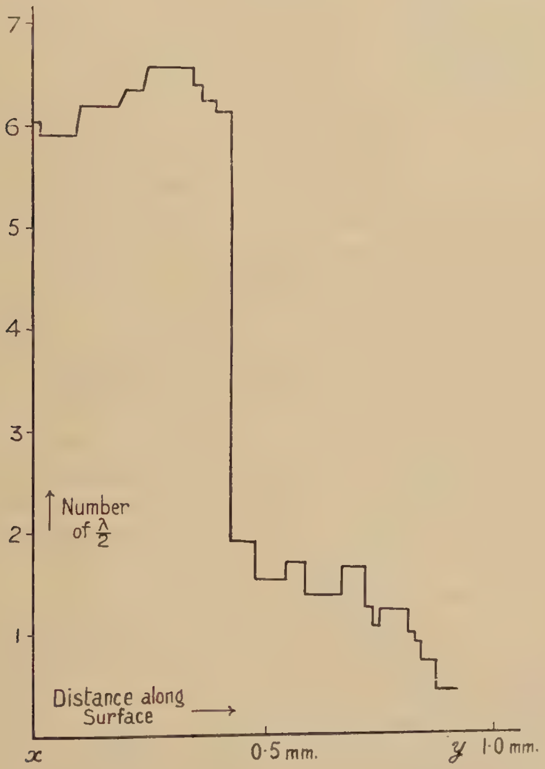

Fig. 1 (Pl. XIV.) shows some other characteristics of the rocksalt cleavage structure rarely seen on other cleavage structures investigated such as mica (Tolansky 1945, Tolansky and Morris 1947), selenite and calcite (*loc. cit.*). Besides well defined steps the change in level sometimes takes place gradually as can be seen along the lines ED and FG on fig. 1 *a*. Fig. 2 represents a cross-section along a line XY, overlapping order allocations being ascertained by using several wavelengths of light. The gradual changes in level are probably due to the non-resolution of very small steps. The elementary distance, perpendicular to the face as given by X-ray diffraction, is $d_{100} = 5{\cdot}63$ A. which is beyond the resolving power of the method.

Although in general within a narrow strip cleavage must probably proceed along a lattice plane, in some cases curved strips were seen (fig. 1 *b*). Some radii of curvature calculated by using the approximation: $R = 1/2\lambda[d_1 d_2(d_1 + d_2)]/[d_1 - d_2]$, where $d_1$ and $d_2$ are the distances between three adjacent fringes, are for example, R=1·58, 2·02 and 3·29 metres respectively.

Uniform areas are rare and very small and in general high dispersion gives ragged fringes, indicating a complicated fine structure as in figs. 1 *c* and 1 *d*. This fine structure, probably also due to non-resolved steps, corresponds to level changes up to 200 A.

Fig. 1 *b* shows another striking feature of the rocksalt cleavage. The surface is striated in two directions: one parallel to (100) and the other parallel to the cleavage lines. The striations lead to the dotting of the fringes.

The following proposed cleavage mechanism is suggested by the fringe patterns. When a knock is applied to a crystal face, cleavage starts in the plane under the razor blade's edge containing the largest number of dislocations or defects. Cleavage will proceed along this plane until reaching the immediate neighbourhood of some other plane which contains a higher concentration of dislocations. Cleavage then jumps and continues along that new plane. The result is a repeated change of level and the production of steps. This mechanism would probably account for the smaller steps only. The higher steps could be associated with inner cracks existing previously in the crystal or with the boundaries of the separate blocks which build up a coarse mosaic structure of the crystal. Evidence in favour of this last argument may be found in the fact that the large step of fig. 2 occurs in the immediate neighbourhood of the border between two inclined crystal-blocks.

According to this view the quality of a cleavage would depend on the concentration of lattice defects and on their distribution in the crystal and consequently on growth conditions. This view is supported by fig. 2 of Tolansky and Khamsavi's paper on calcite (1946).

This investigation of the rocksalt cleavage involved certain difficulties. As rocksalt is hygroscopic it was necessary to silver the specimens immediately after cleavage. Keeping the silvered specimens in a desiccator filled with $P_2O_5$ was not sufficient to prevent the immediate attack on the rocksalt. One hour only is needed to make this effect visible. It results in a decrease of reflectivity and an increase of the absorption of the silver layer. A specimen is completely spoiled and unusable for examination some twelve hours after silvering.

The break-up of the film is much more visible with reflection fringes than with transmission, as the local loss of reflectivity is then seen as a dark region on a bright background. In transmission on the contrary the effect is seen only as an interruption in the bright fringes. The disintegration could therefore be studied much easier in reflection. There is some indication that it starts in regions of maximum illumination which, as Holden (1949) has shown is asymmetrically on one side of the dark reflection fringe. It appears to spread out in the direction of the illuminated region and stops abruptly when a cleavage line is reached (fig. 1 *e*).

Although the silver break-up is undoubtedly partly due to the hygroscopic character of rocksalt, it may be that a photosensitive effect contributes if it be supposed that the silver in contact with the sodium chloride forms a certain amount of silver chloride, which is photosensitive.

Further evidence in favour of this hypothesis is this: the rocksalt specimens when subjected to a glow discharge turned yellow, in accordance with known expectations. It is found that yellowish specimens were spoiled much more quickly than the others. Fig. 1 *e* referring to such a specimen, the picture being taken approximately half an hour after the exposure to the glow discharge followed by silvering.

In terms of Mott's explanation (1940) of Pohl's experiments the formation of silver chloride can be explained in the following way. The glow discharge results in a stochiometric excess of the metal. As a consequence a certain amount of chlorine becomes available. When afterwards the silver is deposited some silver chloride will be formed, which has a low photosensitivity. If exposed only to low intensity daylight, the darkening takes place slowly, but under the influence of the very intense Hg source of illumination, used in interferometry, the silver chloride shows the " print-out " effect which causes the dark stains in the picture. This picture was taken a very short time after the specimen was silvered, it was completely clean when putting it in the light beam. Once in the interferometer the fringe system was kept fixed. As a result one can see the preferential darkening on one side of the dark fringes, *i. e.* on the side at which the light has a reflection maximum. If this is indeed the correct explanation then the effect is highly critical since the maximum on the side of the fringe is but a few per cent above that of the intensity between fringes.

This work has been carried out whilst holding a Fellowship from the " Centre National Belge de Chimie Physique Moleculaire ", and a visit to the laboratory at Royal Holloway College, London, was made possible with aid from the " Fonds pour les relations culturelles Anglo-Belges ". I am very much indebted to Professor S. Tolansky; without his constant advice and encouragement this work would have been impossible.

## REFERENCES.

HOLDEN, J., 1949, *Proc. Phys. Soc.* B., **62,** 405.
MOTT, N. F., 1940, *Electronic processes in Ionic Crystals,* (Oxford University Press), p. 111.
TOLANSKY, S., 1945, *Proc. Roy. Soc.* A, **184,** 51; 1948, *Multiple-beam Interferometry of Surfaces and Films,* Clarendon Press, Oxford, p. 96.
TOLANSKY, S., and KHAMSAVI, A., 1946, *Nature,* **157,** 661.
TOLANSKY, S., and MORRIS, P. G., 1947, *Min. Mag.* XXVIII, **198,** 137.

# XXXVIII. *The Hydrogen and Carbon Total Cross-Sections for Neutron Energies between* 39 *MeV. and* 156 *MeV.*

By A. E. Taylor, T. G. Pickavance, J. M. Cassels and T. C. Randle,
Atomic Energy Research Establishment, Harwell*.

[Received January 30, 1951.]

## Abstract.

The total cross-sections of carbon and hydrogen have been measured at neutron energies of 39, 64·5 and 97 MeV., using a recoil proton telescope as a neutron detector. At these three energies the hydrogen cross-sections are $223 \pm 7{\cdot}6$, $126 \pm 3$ and $73{\cdot}9 \pm 3{\cdot}0 \times 10^{-27}$ cm.$^2$ respectively. The corresponding carbon cross-sections are $1100 \pm 20$, $784 \pm 5$ and $508 \pm 5 \times 10^{-27}$ cm.$^2$.

## Introduction.

Neutron beams, produced by proton bombardment of internal beryllium targets at various radii in the 110-inch Harwell cyclotron, have been used to measure the n–p total cross-section at 39 MeV., 64·5 MeV., and 97 MeV. The method employed was similar to that used at 156 MeV. (Taylor, Pickavance, Cassels, and Randle 1950, 1951).

The collimation of the neutron beam and geometrical layout of the apparatus differed little from the previous arrangements, but at each new energy a change was needed in the polythene radiator and carbon absorber of the triple coincidence telescope. The thicknesses of these are included in the summary of the results.

## Effective Energy.

As before, only the high energy end of the neutron spectrum was used (see Table), and the limits of detection were now such that not less than 98 per cent of the recoiling protons counted came from the hydrogen content of the polythene radiator. The effective energy was determined in a subsidiary experiment at each energy by counting the number of recoiling protons as a function of absorber thickness in the telescope and hence as a function of energy. The maximum neutron energy determined this way was compared with the value expected knowing the energy of the internal proton beam and the geometrical arrangement. These results were used to check the range energy relation, and so an estimate of the error in the effective energy was obtained.

To test for " hardening " of the neutron beam in the attenuator, the effective energy after passing through the carbon was determined in the course of the 64·5 MeV. experiment. Since this differed from the effective energy of the unattenuated beam by less than 1 MeV., no appreciable hardening was taking place. The mean of the two values was taken as the effective energy.

---

* Communicated by the Authors.

### ATTENUATORS.

The carbon and polythene $2\frac{1}{2}$-inch diameter bars were of such lengths that the polythene attenuator contained the same number of carbon atoms as the carbon attenuator and the attenuation produced by the hydrogen content varied between exp (0·5) and exp (0·8). Details of the attenuators are given in the Table.

### RESULTS.

The results, including those at 156 MeV., are presented in the Table. The hydrogen total cross-section, $\sigma_H$, is plotted as a function of energy in the figure (p. 330).

TABLE.

| | | | | |
|---|---|---|---|---|
| Effective energy (MeV.) | 39 | 64·5 | 97 | 156 |
| Estimated error in effective energy (MeV.) | ±1 | ±1·6 | ±1·5 | ±3 |
| Upper energy limit of neutrons in the beam (MeV.) | 45·7 | 74 | 107 | 169 |
| Lower energy limit of detection (MeV.) | 34·5 | 59 | 91 | 149 |
| Absorber in telescope (gm. cm.$^{-2}$ of carbon equivalent) | 1·14 | 3·01 | 6·49 | 15·8 |
| Radiator thickness (gm. cm.$^{-2}$ of polythene) | 0·29 | 0·63 | 0·87 | 1·7 |
| Carbon attenuator (gm. cm.$^{-2}$) | 23·51 | 70·76 | 70·76 | 120·23 |
| Polythene attenuator (gm. cm.$^{-2}$) | 27·50 | 82·41 | 82·41 | 136·93 |
| Hydrogen total cross-section $\times 10^{27}$ (cm.$^2$) | 223<br>±7·6 | 126<br>±3·0 | 73·9<br>±3·0 | 46·4<br>±1·2 |
| Carbon total cross-section $\times 10^{27}$ (cm.$^2$) | 1100<br>±20 | 784<br>±5 | 508<br>±5 | 330<br>±3 |

### DISCUSSION.

The value obtained for the hydrogen total cross-section at 97 MeV. is in good agreement with the most accurate experiment at Berkeley, in which the effective energy was 95 MeV. (DeJuren and Knable 1950). However, the result at 39 MeV. is greater than that expected from earlier Berkeley measurements at 40 MeV. (Hadley, Kelly, Leith, Segrè, Wiegand, and York 1949), but in good accord with the more recent determination at 42 MeV. (Hildebrand and Leith 1950).

It may be of interest that a simple empirical relation can be used to fit the results within the experimental errors quoted, namely,

$$\sigma_H = \frac{10{,}342}{E} - 45{\cdot}7 + 0{\cdot}157E,$$

where $\sigma_H$ is in units of $10^{-27}$ cm.$^2$ and E in MeV. This relation also gives agreement with the results at 14 MeV. (Salent and Ramsey 1940), 25 MeV. (Sherr 1945), and 280 MeV. (Fox, Leith, Wouters, and MacKenzie 1950).

## ACKNOWLEDMENTS.

Thanks must be expressed to Mr. E. Wood for help in carrying out the measurements and to the cyclotron crew for their cooperation.

This paper is published by the permission of the Director, Atomic Energy Research Establishment, Harwell.

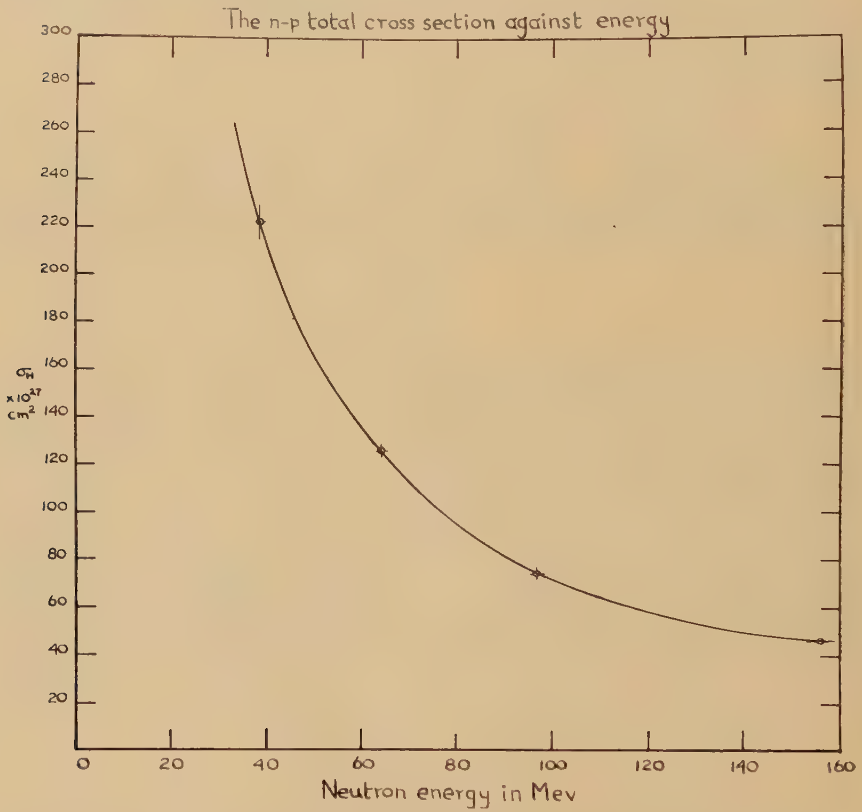

## REFERENCES.

DEJUREN, J., and KNABLE, N., 1950, *Phys. Rev.*, **77,** 606.
FOX, R., LEITH, C., WOUTERS, L., and MACKENZIE, K. R., 1950, *Phys. Rev.*, **80,** 23.
HADLEY, J., KELLY, E., LEITH, C., SEGRÈ, E., WIEGAND, C., and YORK, H., 1949, *Phys. Rev.*, **75,** 351.
HILDEBRAND, R. H., and LEITH, C. E., 1950, *Phys. Rev.*, **80,** 842.
SALENT, E. O., and RAMSEY, N. F., 1940, *Phys. Rev.*, **57,** 1075.
SHERR, R., 1945, *Phys. Rev.*, **68,** 240.
TAYLOR, A. E., PICKAVANCE, T. G., CASSELS, J. M., and RANDLE, T. C., 1950, *Nature Lond.*, **165,** 967 ; 1951, *Phil. Mag.*, **42,** 20.

# XXXIX. *Rate of Production of Neutrons in Ice by Cosmic Rays.*

By S. LATTIMORE,
Imperial College, London*.

[Received January 30, 1951.]

## ABSTRACT.

The rate of production in ice of fast neutrons is given. It is shown that the number of fast neutrons produced at any point in the ice is approximately proportional to the number of cosmic ray stars at that point. The results are compared with those of other investigations, and it is pointed out that many previous results are too low due to the misuse of a formula given by Bethe *et al.* (1940).

## INTRODUCTION.

DURING recent years there have been many experiments to find the absolute rate of production of neutrons by cosmic rays, and the variation of this rate with the height of production. In general the results of these experiments have been in agreement only as far as the height variation is concerned, the values found for the rates of production varying by a factor as large as five. It has been found that the variation with height over the lower part of the atmosphere is exponential, the rate of production at a depth $x$ gm./cm.$^2$ below the top of the atmosphere being proportional to $\exp(-x/\lambda)$ where $\lambda$ is 140–150 gm./cm.$^2$. This height variation is the same as that found for stars observed in photographic emulsions.

For measurements on slow neutrons, the use of boron loaded nuclear emulsion has a great advantage over counter or ionization chamber technique, in that the boron disintegrations

$$B_5^{10}+n_0^1 \rightarrow Li_3^7+He_2^4$$

can actually be observed and there is therefore no doubt as to what is being measured. In the electronic devices, on the other hand, elaborate precautions must be taken to eliminate background counts, and one can never be certain that no spurious events are counted, or that all true counts are recorded. The photographic plate, however, requires long exposures, of the order of 50 days, and cannot, therefore, be used to examine short term fluctuations, such as have recently been observed by Adams (1950) and others, using electronic devices, after intense solar activity.

---

* Communicated by Sir George Thomson.

## EXPERIMENTAL.

The plates used were Ilford 100$\mu$ C.2 boron loaded emulsion and were exposed vertically, at depths of 0, 0·5, 1, 2 and 3 metres below the surface of the glacier ice at 3600 m. elevation at the Jungfraujoch. The geometry was excellent, the plates being contained in an iron pipe, internal diameter $2\frac{1}{8}$ inch., wall thickness $\frac{1}{8}$ inch., which had been sunk into the ice. The glacier ice was covered with approximately 15 gm./cm.$^2$ of snow.

The results are shown in fig. 1, where the numbers of boron disintegrations observed (in arbitrary units) are plotted logarithmically against the depth below the glacier ice. As can be seen, the results are consistent with an exponential absorption. The best values for the range in ice and the number of disintegrations at the surface of the ice were calculated by the method of least squares, and were found to be :

Fig. 1.

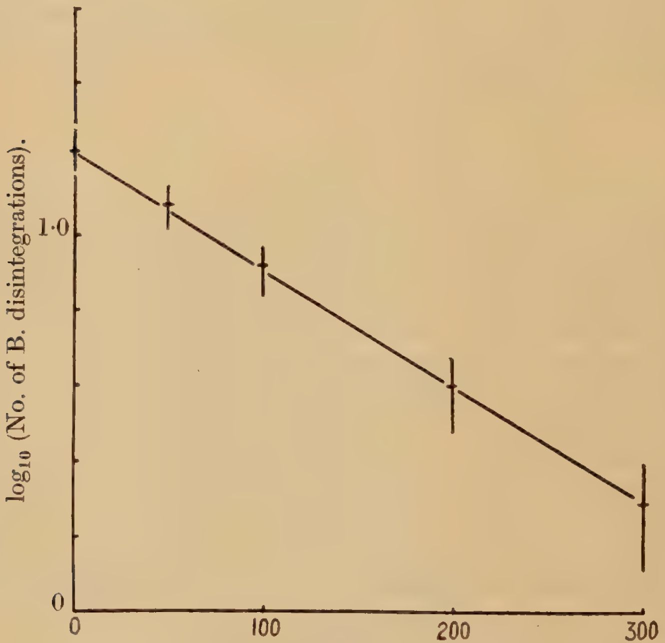

Depth in glacier ice in cms.

Range in ice=126 gm./cm.$^2$.

No. of boron disintegrations at the surface of the ice =893/c.c. of emulsion/day.

## INTERPRETATION OF RESULTS.

In the following paragraphs we shall show how the number of neutrons captured at any point, which is the quantity we measure, is related to the number of neutrons produced at that point.

The boron disintegrations are produced by thermal and near-thermal neutrons only, since it is only in this region that the cross section is large. The neutrons will be slowed down to thermal energies by elastic collisions with the hydrogen in the ice. It seems probable that the neutrons will be produced in cosmic ray stars in the ice. We shall assume that (1) the neutrons are produced in stars, and that the mean number of neutrons/star is independent of the depth in the ice. In this case, the neutron production will decrease exponentially with depth in the ice, with a range of 130 gm./cm.$^2$ (Harding 1950). (2) the neutrons can be divided into two groups, one group consisting of those neutrons that are evaporated from stars, the second of those neutrons that correspond to the high energy tail (Perkins 1947) observed in the proton spectrum. The evaporated neutrons will have an energy spectrum given by the formula

$$\mathrm{P(E)}\,d\mathrm{E}=\mathrm{A}\,\frac{\mathrm{E}}{\mathrm{T}^2}\exp(-\mathrm{E/T})\,d\mathrm{E}, \quad . \quad . \quad . \quad . \quad . \quad (1)$$

where P(E) is the number of neutrons emitted with energies between E and E$+d$E, A is the total number of neutrons emitted, and T is a constant, with the dimensions of an energy. From a study of the protons it has been found that for stars of three or more visible tracks, T is equal to 4 MeV. It has further been found that the evaporated protons are emitted isotropically, (Harding *et al.* 1949), and we shall suppose that this is also true for the evaporated neutrons. Now, from formula (1), we can calculate that 96 per cent of the evaporated neutrons will have energies less than 20 MeV. We shall therefore assume that all those neutrons with energies below 20 MeV. are evaporated, and have an isotropic angular distribution, while none of those with energies greater than 20 MeV. are evaporated, but they are all strongly collimated downwards. We shall deal with these two groups separately.

## EVAPORATED NEUTRONS.

Bethe *et al.* (1940) have shown that the mean square distance $\bar{r}^2$ travelled by a neutron in losing energy from E$_1$ to E$_2$ is given by

$$\bar{r}^2=\mathrm{M}\int_{\mathrm{E}_2}^{\mathrm{E}_1} l^2(\mathrm{E})\,\frac{d\mathrm{E}}{\mathrm{E}}, \quad . \quad . \quad . \quad . \quad . \quad . \quad . \quad . \quad (2)$$

where M is the atomic weight of the moderating material and $l$(E) is the mean free path at an energy E. If we put E$_1$ and E$_2$ equal to 20 Mev. and 1 eV. (thermal energies) and neglect the scattering with the oxygen, we find

$$\bar{r}^2=120\ (\mathrm{gm./cm.}^2)^2.$$

This value will be greater than the true value because of the neglect of the oxygen scattering. We should note that the value of $\bar{r}^2$ decreases as E$_1$ decreases.

Bethe *et al.* have also shown that the distribution, after the slowing down process of neutrons produced at a depth $x_0$, is given by

$$N(x)\,dx=\pi^{-\frac{1}{2}}L^{-1}\exp\left[-(x-x_0)^2/L^2\right]dx, \quad . \quad . \quad . \quad . \quad (3)$$

where $N(x)\,dx$ is the fraction of the neutrons that will be found between $x$ and $x+dx$ as thermal neutrons and L is given by

$$L=\left(\frac{\overline{r^2}}{3}\right)^{\frac{1}{2}}=7 \text{ gm./cm.}^2 \text{ for 20 MeV. neutrons.}$$

It must be emphasized that formula (3) holds only if the neutrons are emitted isotropically.

Now, the number $n'(x)$ of evaporated neutrons produced at a depth $x$ in the ice can be written

$$n'(x)=n'(o)\exp(-x/\lambda)/\text{gm./sec.} \quad . \quad . \quad . \quad . \quad . \quad . \quad (4)$$

where $\lambda=130$ gm./cm.$^2$.

Using equations (3) and (4), we find that $B'(x)dx$, the number of neutrons of the first group, assumed all to have energies of 20 MeV., reaching thermal energies/sec. between depths $x$ and $x+dx$ is given by

$$\begin{aligned} B'(x)\,dx &= dx\,\frac{n'(o)\exp(-x/\lambda)}{\pi^{\frac{1}{2}}L}\int_{-\infty}^{x}\exp(y/\lambda)\exp(-y^2/L^2)\,dy \\ &= dx\,\frac{n'(o)\exp(-x/\lambda)}{\pi^{\frac{1}{2}}L}\exp(L^2/4\lambda^2)\int_{-\infty}^{x}\exp(-y^2/L^2)\,dy. \end{aligned} \quad . \quad . \quad . \quad (5)$$

Now, for $L=7$ gm./cm.$^2$, we find that the upper limit of the integral in equation (5) can be replaced by $\infty$ with less than 3 per cent error for all values of $x>10$ gm./cm.$^2$.

Then we find

$$B'(x)=n'(o)\exp(-x/\lambda)\exp(L^2/4\lambda^2),$$

and for $L=7$ gm./cm.$^2$, $\lambda=130$ gm./cm.$^2$, $\exp(L^2/4\lambda^2)$ is very nearly unity (0·999), so therefore we can write

$$B'(x)=n'(o)\exp(-x/\lambda)=n'(x) \quad . \quad . \quad . \quad . \quad . \quad . \quad (6)$$

We have derived equation (6) by considering all the evaporated neutrons to be emitted with an energy of 20 MeV. In fact, the majority of the neutrons will have energies of only three or four MeV. For these lower energy neutrons, $\overline{r^2}$, and therefore L, will be reduced. This will make the contribution between $y=\pm10$ gm./cm.$^2$ to the integral in equation (5) even larger than 97 per cent, and will make $\exp(L^2/4\lambda^2)$ nearer unity, therefore equation (6) will still hold.

## HIGH ENERGY NEUTRONS.

The scattering mean free path in ice for neutrons of energy greater than 20 MeV. is largely governed by the oxygen cross section, and further, varies only slowly with the energy. For a 50 MeV. neutron the mean free path is of the order of 20 gm./cm.$^2$. Now, since the oxygen nucleus is massive compared to the neutron the scattering is very large, and therefore, after one collision the neutrons will have an isotropic angular distribution. We will take the mean energy of the fast neutrons as 50 MeV. and suppose that all the neutrons have this energy. Let the number of fast neutrons produced at a depth $x$ be given by

$$n''(x)=n''(o)\exp(-x/\lambda) \quad . \quad . \quad . \quad . \quad . \quad . \quad (7)$$

where $\lambda$ is again equal to 130 gm./cm.$^2$.

Then the number of fast neutrons produced *isotropically* at a depth $x$ will be approximately equal to the number of fast neutrons produced from stars a distance 20 gm./cm.$^2$ above $x$, since these fast isotropic neutrons are produced after one collision from the fast collimated neutrons.

We can now apply equations (2), (3) and (5) to these isotropic neutrons, and we then find that

$$\bar{r}^2=6{,}500\ (\text{gm./cm.}^2)^2,$$

$$\text{L}=30\ \text{gm./cm.}^2$$

and that

$$\text{B}''(x)=n''(x-20), \quad . \quad . \quad . \quad . \quad . \quad . \quad . \quad . \quad (8)$$

provided $x$ is greater than 50 gm./cm.$^2$.

$\text{B}''(x)\,dx$ is the number of neutrons, which were originally fast collimated neutrons, that reach thermal energies between $x$ and $x+dx$. For values of $x$ less than 50 gm./cm.$^2$, $\text{B}''(x)$ will not have the full contribution from the neutrons produced in the ice, but this will be compensated for by the entry of fast neutrons from the air.

From this analysis, we can say that, for depths of more than 50 gm./cm.$^2$ of ice, the total number of neutrons reaching thermal energies/sec. at a depth $x$ is given by

$$\text{B}'(x)+\text{B}''(x)=n'(x)+n''(x-20),$$

and that for values of $x$ between 15 and 50 gm./cm.$^2$, we will have the full contribution to $\text{B}'(x)$, but a reduced contribution to $\text{B}''(x)$ from neutrons produced in the ice, which will be compensated to some extent by neutrons produced in the air. This view is strengthened by a study of fig. 1, which shows that all the experimental points lie on a straight line, with a slope corresponding very closely to that expected for a value of $\lambda=130$ gm./cm.$^2$.

We can now find $\text{B}'(x)+\text{B}''(x)$ for $x$ 15 gm./cm.$^2$. Bethe *et al.* show that if $\rho(x)$ is the number of boron disintegrations/c.c. day at a depth $x$ gm./cm.$^2$, then

$$p(x)=\frac{\text{D}'}{\text{D}}\frac{\sigma_0^1}{\sigma_0}(\text{B}'(x)+\text{B}''(x))\rho,$$

where D′ and D are the number of boron atoms/c.c. of emulsion and the number of hydrogen atoms/c.c. of ice respectively, $\rho_0^1$ and $\rho_0$ the atomic capture cross sections of boron and hydrogen respectively, and $\rho$ the density of ice. It is assumed that no capture occurs in the oxygen. Putting

$$\left.\begin{aligned}\sigma_0^1&=115\text{ borons},\\ \sigma_0&=0{\cdot}049\text{ borons},\end{aligned}\right\}\text{ R. K. Adair (1950)}$$

we find

$$B'(15)+B''(15)=20/\text{gm./day in ice.}$$

Fig. 2.

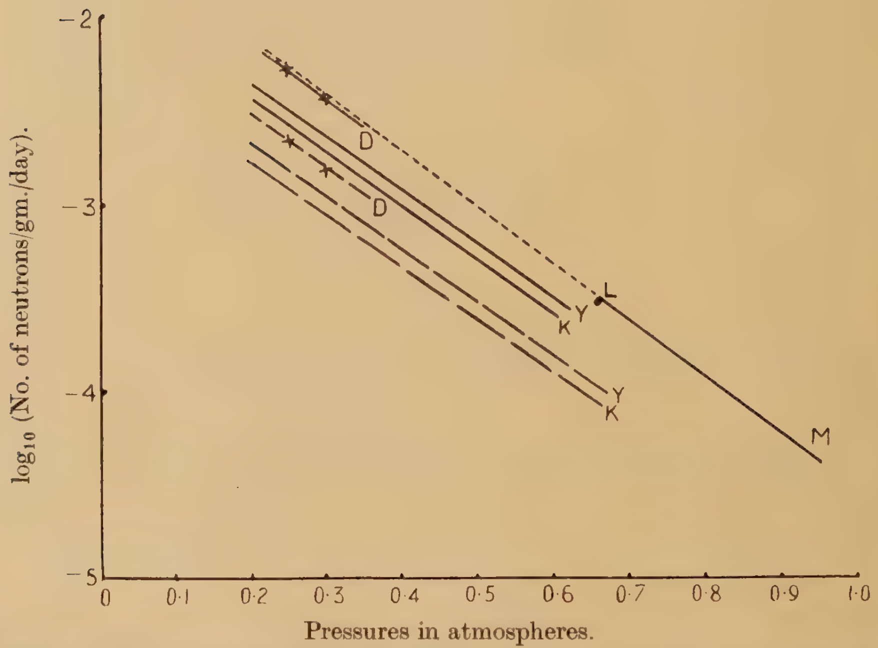

This figure shows some results obtained for the rate of neutron production as a function of the atmosphere depth, both before (dashed lines) and after (full lines) the corrections given in this paper have been applied.

D—Davis (1950).
K—Korff and Hamermesh 1946.
L—Lattimore (present results).
M—Montgomery and Tobey 1949 (no corrections required).
Y—Yuan 1946.

If we assume that only the oxygen in the ice produces neutrons, and also correct for the absorption in the 15 gm./cm.$^2$ of snow by multiplying by exp (15/130), we find

$$B'(0)+B''(0)=25/\text{gm. of oxygen/day}$$

at an elevation of 3600 m. Now,

$$\begin{aligned}B'(x)+B''(x)&=n'(x)+n''(x-20)\\ &=n'(x)+1{\cdot}15n''(x),\end{aligned}$$

since $n''(x-20)=\exp(20/130)\,n''(x)$. (See equation (7).)

If we assume that the neutron and proton spectra are similar, $n''(x)/n'(x)$ is of the order of $\frac{1}{3}$, and we can therefore write

$$n'(x)+1{\cdot}15n''(x)=1{\cdot}04(n'(x)+n''(x)),$$
$$B'(0)+B''(0)=1{\cdot}04(n'(0)+n''(0)),$$

and therefore the rate of production of fast neutrons in oxygen at 3600 m. is given by 25 divided by 1·04 which is equal to 24/gm./day.

Rate of production of fast neutrons =24/gm. of oxygen/day at 3600 m.

## DISCUSSIONS OF RESULTS.

The value obtained for the absorption of the neutron producing primaries, namely 126 gm./cm.$^2$ of ice, is in excellent agreement with that found by Harding (1950) for the star producing radiation. The rate of production also agrees well with that found in carbon at the same elevation by Montgomery and Tobey (1949), who used a similar method to that used here, that is to say, they surrounded an ionization chamber with large masses of paraffin wax. These two values are, however, greater by a factor of about two than those given for air by several other investigators. As had been pointed out in another paper (Lattimore 1951), this is probably due to the misuse of a formula given by Bethe *et al.* (1940) which involves the nitrogen cross section/*molecule*. In many cases the cross section/*atom* has been used, which gives a rate of production of only half the true value. In fig. 2 is shown some corrected values, and it can be seen that the agreement between these and the results presented here is much improved.

## ACKNOWLEDGMENT.

I must express my thanks to Professor Sir George Thomson for much helpful advice during the course of this work.

## REFERENCES.

ADAIR, 1950, *Rev. Mod. Phys.*, **22,** 3, 249.
ADAMS, N., 1950, *Phil. Mag.*, **41,** 503–5.
BETHE, H. A., KORFF, S. A., and PLACZEK, G., 1940, *Phys. Rev.*, **57,** 573.
DAVIS, W. D., 1950, *Phys. Rev.*, **80,** 150.
HARDING, J. B., 1950, (unpublished).
HARDING, J. B., LATTIMORE, S., and PERKINS, D. H., 1949, *Proc. Roy. Soc.* A, **196,** 325–43.
KORFF, S. A., and HAMERMESH, B., 1946. *Phys. Rev.*, **69,** 155.
LATTIMORE, S., 1951, *Phys. Rev.* (in the press).
MONTGOMERY, G. G., and TOBEY, A. R., 1949, *Phys. Rev.*, **76,** 1478–81.
PERKINS, D. H., 1947, *Nature*, **160,** 299.
YUAN, L. C. L., 1946, *Phys. Rev.*, **74,** 504.

# XL. *The Binding Energies of Three- and Four-particle Nuclei.*

By J. Irving,
Department of Natural Philosophy, The University of Glasgow*.

[Received January 30, 1951.]

## Abstract.

The binding energies of the nuclei $H^3$, $He^3$ and $He^4$ are calculated, using the standard variation method with a simple two-parameter wave-function of a new form. Purely central interactions of the Yukawa and exponential types are considered. It is found that, when the nuclear parameters are chosen to fit the low-energy scattering and deuteron data, reasonable values are obtained for the three-particle nuclei, but the $\alpha$-particle binding energy is too high. This result is in agreement with the calculations of Rarita and Present for the exponential potential, and those of Svartholm for the Yukawa potential. In contrast with Svartholm's method of calculation, the potential and kinetic energies of the nuclei are obtained explicitly. In the case of the $\alpha$-particle, the Yukawa potential yields exceptionally high values for these quantities, and results also in a very concentrated nucleus. The exponential potential, on the other hand, does not give rise to such high values for the potential and kinetic energies nor does it concentrate the nucleus to the same extent as the former potential†.

## § 1. Introduction.

Numerous investigations have been made on the binding energies of the three- and four-particle nuclei, using a central two-body interaction with various forms of potential well. The methods of calculation adopted in these investigations and the conclusions arising therefrom have been summarized by Rosenfeld (1948). The so-called consistency problem may be stated as follows :—

(1) A set of parameters compatible with the deuteron and low-energy scattering data, and with the binding energy of the triton, yields too large a binding energy of the $\alpha$-particle.

(2) A set of parameters yielding the correct binding energy of $H^2$, $He^3$ and $He^4$ involves a longer range than allowed by the $p-p$ data and gives rise to a bound $^1S$ state of the deuteron.

In this paper the problem is approached from the point of view of the first statement.

The standard variation method is used with a new two-parameter wave-function of simple form for both the Yukawa and exponential central interactions. The wave-functions chosen give rise to relatively simple mathematical analysis, no approximations being necessary in the evaluation of the integrals involved. This is to be contrasted with the more laborious calculations of Rarita and Present (1937) for the exponential potential, using the variation and equivalent two-body problem techniques ; and the work of Svartholm (1945), using the much more tedious, but admittedly very accurate variation-iteration method. The conclusion reached from the calculations carried out here is given in statement (1), and is thus in agreement with that of Rarita and Present, and Svartholm. It might be remarked, however, that the Yukawa potential yields results for the $\alpha$-particle, which, though agreeing with the latter's conclusion, differ from those of Fröhlich *et al.* (1947) for the longer range of the forces—corresponding to a meson mass of 210–220 $m_e$—which they use. The value obtained here for the binding energy for this particular range is approximately twice as large as that of Fröhlich.

---

* Communicated by the Author.

† See note added in proof.

The total kinetic and potential energies for each nucleus are given explicitly in contrast with Svartholm's calculations, where the nuclear parameters are evaluated to fit the experimentally known binding energies. It is found in the case of the $\alpha$-particle that the kinetic energy for the Yukawa potential is exceptionally high ; the excess binding energy is large ; and, moreover, the nucleus is very concentrated. The exponential potential, on the other hand, gives rise to a much smaller excess binding energy, more reasonable values of the kinetic energy and a not so concentrated nucleus*.

The calculations of Gerjuoy and Schwinger (1942) have indicated, of course, that the introduction of a non-central interaction of the tensor type would considerably reduce the excess binding energy of the $\alpha$-particle. In fact, their investigations with a square well potential have yielded too small binding energies for the triton and the $\alpha$-particle. However, if one considers the exceptionally large binding energy obtained for the Yukawa potential with purely central forces, it is feasible that the introduction of tensor forces might reduce it sufficiently so that the experimental value might be obtained when the normal ranges of the forces used to fit the two-body data are considered. This problem is now being investigated with the wave-functions used in the present calculations.

The wave-functions introduced in this paper are of a form which might be extended for systems of more than four particles, provided the space-part is so modified as to have the correct symmetry properties for the particles in $p$-states.

## § 2. BINDING ENERGY FORMULÆ AND WAVE-FUNCTIONS.

The two-particle central interaction with a mixture of Wigner, Bartlett, Heisenberg and Majorana forces may be written in the form (Rosenfeld, 1948)

$$V_{\text{nucl}}=V(r_{12})\{a_0+a_\sigma\vec{\sigma}^{(1)}\vec{\sigma}^{(2)}+a_\tau\tau^{(1)}\tau^{(2)}+a_{\sigma\tau}\sigma^{(1)}\vec{\sigma}^{(2)}\tau^{(1)}\tau^{(2)}\}$$

or

$$V_{\text{nucl}}=V(r_{12})\{W+BP_\sigma-HP_\tau-MP_\sigma P_\tau\},$$

---

* See note added in proof.

where $V(r_{12})$ is the two-particle triplet potential, $r_{12}$ being the distance between the particles, and the other quantities have their usual meanings. Now the ground states of the nuclei $H^3$, $He^3$ and $He^4$ are S-states, so that an interaction consisting of a mixture of Majorana and Heisenberg forces—so-called exchange forces—yields the same binding energy as an equivalent mixture of Wigner and Bartlett forces. For a wave-function symmetrical in space coordinates the formula for the total energy of the nucleus has the well-known form (Rosenfeld 1948),

$$E^{(3)}=-(\hbar^2/2M)\int\psi\Delta^{(3)}\psi\,dv^{(3)}+(3/2)(1+q)\int V(r_{12})\psi^2\,dv^{(3)}+E_{\mathrm{Coul}} \quad . \quad . \quad . \quad (1)$$

for the three-particle system, and

$$E^{(4)}=-(\hbar^2/2M)\int\phi\Delta^{(4)}\phi\,dv^{(4)}+3(1+q)\int V(r_{12})\phi^2\,dv^{(4)}+E_{\mathrm{Coul}} \quad . \quad . \quad . \quad (2)$$

for the four-particle system. Here $q$ is the ratio of singlet to triplet well depth, $\Delta^{(3)}=\sum_{i=1}^{3}\Delta_i$ and $\Delta^{(4)}=\sum_{i=1}^{4}\Delta_i$, where $\Delta_i$ is the Laplace operator acting on the coordinates of particle whose position vector is $\mathbf{r}_i$ : $\psi$ and $\phi$ are the space parts of the wave-functions for the three-and four-particle systems respectively ; M is the mass of the nucleon. $E_{\mathrm{Coul}}$ denotes the Coulomb energy of the protons in the nucleus and will be treated in the usual way as a perturbation.

The problem of the calculation of the binding energy involves the choice of a good trial wave-function with one or more parameters, subsequent evaluation of the integrals, and minimization with respect to the variation parameters. The Gaussian wave-function has been frequently used in calculations in nuclear problems, because of the great simplification it usually gives in the mathematical analysis. It has, however, an incorrect asymptotic behaviour, and is a very poor approximation to the correct wave-function for a three- or four-particle system, when a Yukawa potential is used. The following new wave-functions with an exponential type of asymptotic behaviour are introduced in the subsequent calculations and result in fairly simple mathematical analysis.

(a) *Three-particle system.*

Let

$$\psi=B^{1/2}\exp\{-\alpha(r_{12}^2+r_{13}^2+r_{23}^2)^{1/2}\}/\{r_{12}^2+r_{13}^2+r_{23}^2\}^n \quad . \quad . \quad . \quad (3)$$

be the wave-function for the three-particle system, where $B^{1/2}$ is the normalization coefficient ; $\alpha$ and $n$ are parameters ; $r_{12}$, $r_{13}$ and $r_{23}$ are the distances between the particles 1 and 2, 1 and 3, 2 and 3 respectively.

The wave-function is of course a function of the relative coordinates of the particles and it may be simplified by a transformation.

Let

$$\boldsymbol{\rho}=-\mathbf{r}_1+(\mathbf{r}_2+\mathbf{r}_3)/2, \qquad \mathbf{r}=(\sqrt{3}/2)(\mathbf{r}_2-\mathbf{r}_3), \qquad \mathbf{R}=(\mathbf{r}_1+\mathbf{r}_2+\mathbf{r}_3)/3, \quad . \quad . \quad . \quad (4)$$

$\mathbf{r}_1$, $\mathbf{r}_2$ and $\mathbf{r}_3$ being the position vectors of the particles 1, 2 and 3 respectively. Relation (3) then assumes the form

$$\psi'=\mathrm{N}_1^{1/2}\exp\{-\sqrt{2}\alpha(\rho^2+r^2)^{1/2}\}/(\rho^2+r^2)^n, \qquad (5)$$

$\mathrm{N}_1^{1/2}$ being the normalization coefficient in the new coordinate system and $\rho=|\boldsymbol{\rho}|$, $r=|\mathbf{r}|$.

In this system of coordinates it is easily shown that the operator $-(\hbar^2/2\mathrm{M})\Delta^{(3)}$ becomes $-(\hbar^2/2m)(\Delta_{\mathbf{r}}+\Delta_{\boldsymbol{\rho}})-(\hbar^2/6\mathrm{M})\Delta_{\mathbf{R}}$, where $\Delta_{\mathbf{r}}$, $\Delta_{\boldsymbol{\rho}}$ and $\Delta_{\mathbf{R}}$ act on the coordinates $\mathbf{r}$, $\boldsymbol{\rho}$ and $\mathbf{R}$ respectively; and $m=2\mathrm{M}/3$. Now $\mathbf{R}$ is the position vector of the centre of mass of the three particles, so that, since $\psi$ or $\psi'$ is a function of the relative coordinates, the expectation value of the kinetic energy of the mass-centre is zero.

Equation (1) may then be written in the form

$$\mathrm{E}^{(3)}=-(\hbar^2/2m)\int\psi'(\Delta_{\mathbf{r}}+\Delta_{\boldsymbol{\rho}})\psi'\,d\mathbf{r}\,d\boldsymbol{\rho}+(3/2)(1+q)\int\mathrm{V}(r_{12})\psi'^2\,d\mathbf{r}\,d\boldsymbol{\rho}+\mathrm{E}_{\mathrm{Coul}}. \qquad (6)$$

The Coulomb energy for two protons, that is, the $\mathrm{He}^3$ nucleus, may be written in the form

$$\mathrm{E}_{\mathrm{Coul}}=e^2\int(1/r_{12})\psi'^2\,d\mathbf{r}\,d\boldsymbol{\rho}, \qquad (7)$$

$e$ being the electronic charge.

(b) *Four-particle system.*

The form of the wave-function taken for this case is similar to that of $\psi$ in equation (3).

Let

$$\phi=\mathrm{C}^{1/2}\exp\{-\alpha(r_{12}^2+r_{13}^2+r_{14}^2+r_{23}^2+r_{24}^2+r_{34}^2)^{1/2}\}/\{r_{12}^2+r_{13}^2+r_{14}^2+r_{23}^2+r_{24}^2+r_{34}^2\}^n, \qquad (8)$$

where $\mathrm{C}^{1/2}$ is the normalization coefficient; $\alpha$ and $n$ are parameters; $r_{12}$, etc. are the distances between the particles 1 and 2, etc. The transformation

$$\left.\begin{array}{ll}\mathbf{u}=(\mathbf{r}_1+\mathbf{r}_2)/2-(\mathbf{r}_3+\mathbf{r}_4)/2, & \mathbf{R}=(\mathbf{r}_1+\mathbf{r}_2+\mathbf{r}_3+\mathbf{r}_4)/4,\\ \mathbf{v}=(\mathbf{r}_1-\mathbf{r}_2)/\sqrt{2}, & \mathbf{w}=(\mathbf{r}_3-\mathbf{r}_4)/\sqrt{2},\end{array}\right\} \qquad (9)$$

where $\mathbf{r}_1$, $\mathbf{r}_2$, $\mathbf{r}_3$ and $\mathbf{r}_4$ are the position vectors of the particles 1, 2, 3 and 4 respectively, applied to (8) gives

$$\phi'=\mathrm{N}_2^{1/2}\exp\{-2\alpha(u^2+v^2+w^2)^{1/2}\}/\{u^2+v^2+w^2\}^n, \qquad (10)$$

$\mathrm{N}_2^{1/2}$ being the normalization coefficient in the new coordinate system, and $u=|\mathbf{u}|$, $v=|\mathbf{v}|$, $w=|\mathbf{w}|$. It is easily shown that equation (2) becomes

$$\mathrm{E}^{(4)}=-(\hbar^2/2\mathrm{M})\int\phi'(\Delta_{\mathbf{u}}+\Delta_{\mathbf{v}}+\Delta_{\mathbf{w}})\phi'\,d\mathbf{u}\,d\mathbf{v}\,d\mathbf{w}+3(1+q)\int\mathrm{V}(r_{12})\phi'^2\,d\mathbf{u}\,d\mathbf{v}\,d\mathbf{w}+\mathrm{E}_{\mathrm{Coul}} \qquad (11)$$

in the new coordinate system, the expectation value of the kinetic energy of the mass-centre vanishing as in the case of the three-particle system.

$\Delta\mathbf{u}$, $\Delta\mathbf{v}$ and $\Delta\mathbf{w}$ are the Laplace operators acting on the coordinates $\mathbf{u}$, $\mathbf{v}$ and $\mathbf{w}$ respectively.

The Coulomb energy for the two protons may be written in the form

$$E_{\mathrm{Coul}}=e^2 \int (1/r_{12})\phi'^2\, d\mathbf{u}\, d\mathbf{v}\, d\mathbf{w}, \qquad (12)$$

$e$ being the electronic charge.

## § 3. EVALUATION OF BINDING ENERGY OF $H^3$ and $He^3$.

The normalization coefficient $N^{1/2}$ for the wave function (5) is easily determined.

$$\int \psi^2\, d\boldsymbol{\rho}\, d\mathbf{r}=N_1(4\pi)^2 \int_0^\infty [\exp\{-\beta(\rho^2+r^2)^{1/2}\}/(\rho^2+r^2)^{2n}]\rho^2 r^2\, d\rho\, dr=1,$$

where $\beta=2\sqrt{2}\alpha$.

Using the transformation $\rho=R\cos\psi$, $r=R\sin\psi$ it is found that

$$N_1=(\alpha^{6-4n}\,.\,2^{9-6n})/\{\pi^3(5-4n)\,!\}. \qquad (13)$$

For the above-mentioned wave-function, the kinetic energy of the nucleons, corresponding to the first term on the right-hand side of equation (6), is given by

$$-(\hbar^2/2m)N_1 \int [\exp\{-\beta(\rho^2+r^2)^{1/2}\}/(\rho^2+r^2)^{2n+1}]$$
$$\times[2\alpha^2(\rho^2+r^2)-\sqrt{2}\alpha(5-4n)(\rho^2+r^2)^{1/2}-n(8-4n)]\, d\boldsymbol{\rho}\, d\mathbf{r}.$$

This is simply evaluated, using the transformation $\rho=R\cos\psi$, $r=R\sin\psi$, so that the kinetic energy is

$$\frac{3}{2}\cdot\frac{(5-n)}{(1-n)(5-4n)}\cdot\frac{\hbar^2}{M}\alpha^2$$

or

$$\frac{(5-n)}{4(1-n)(5-4n)}\cdot\frac{\hbar^2}{M}\kappa^2 c'^2, \qquad (14)$$

where $c'=\sqrt{6}\alpha/\kappa$, $(1/\kappa)$ being the range of the nuclear forces.

When the wave-function (5) is substituted in the expression (7) for the Coulomb energy, then, since from symmetry considerations $r_{12}$ may be replaced by $r_{23}$,

$$E_{\mathrm{Coul}}=\frac{16\sqrt{6}e^2\alpha}{3(5-4n)\pi}=\frac{16e^2\kappa}{3(5-4n)\pi c}, \qquad (15)$$

where $c=\kappa/\sqrt{6}\alpha$.

(a) *Yukawa potential well*: $V(r_{12})=-A\exp(-\kappa r_{12})/(\kappa r_{12})$.

The second term on the right-hand side of equation (6) represents the potential energy of the three-particle system apart from the Coulomb energy. Now, when the wave-function given by (5) is used,

$$\int V(r_{12})\psi'^2\, d\mathbf{r}\, d\boldsymbol{\rho}=-AN_1 \int \exp\{-\beta(\rho^2+r^2)^{1/2}-\kappa r_{12}\}/\{\kappa r_{12}(\rho^2+r^2)^{2n}\}\, d\mathbf{r}\, d\boldsymbol{\rho}.$$

Since from symmetry considerations $r_{12}$ may be replaced by $r_{23}$, that is, $2r/\sqrt{3}$, the integral may be written in the form

$$-(AN_1/\kappa')\int_0^{\pi/2}\cos^2\psi\sin\psi\, d\psi \int_0^\infty R^{4-4n}\exp(-\gamma R)\, dR,$$

where $\gamma=\beta+\kappa'\sin\psi$, $\kappa'=2\kappa/\sqrt{3}$ and the transformation $\rho=R\cos\psi$, $r=R\sin\psi$ has been applied. Hence, by elementary integration, the potential energy has the form

$$-\{(24/\pi)(1+q)Ac'/(5-4n)\}\int_0^{\pi/2}\frac{\cos^2\psi\sin\psi}{(1+c\sin\psi)^{5-4n}}\,d\psi, \quad . \quad . \quad (16)$$

where $c'=1/c=\sqrt{6\alpha/\kappa}$.

Thus, for the $H^3$ nucleus, the total energy is given by

$$E=\frac{(5-n)}{4(1-n)(5-4n)}\cdot\frac{\hbar^2}{M}\kappa^2c'^2-\frac{24(1+q)Ac'}{\pi(5-4n)}\int_0^{\pi/2}\frac{\cos^2\psi\sin\psi}{(1+c\sin\psi)^{5-4n}}\,d\psi. \quad . \quad . \quad . \quad (17)$$

The total energy for the $He^3$ nucleus is obtained by the addition of the Coulomb energy term given in equation (15).

The expression (17) is now minimized with respect to the parameters $c$ and $n$ for different values of the range $(1/\kappa)$, with the corresponding values of A and $q$ fixed by the low-energy $n-p$ scattering and deuteron data. The integral appearing in the expression is easily evaluated for the values $n=0$, 1/4, 1/2 and 3/4. These are given in § 1 of the Appendix. Minimization with respect to $c$ is carried out for each of the values of $n$ mentioned. It should be noted that $n$ must be less than or equal to 3/4 for convergence of the integral representing the kinetic energy.

Table I.

Minima of E for $H^3$ and $He^3$ with respect to $c$ for each value of $n$.

| $n$ | $c$ | K . E (MeV.) | P . E (MeV.) | $H^3/E_{min}$ (MeV.) | $E_{Coul}$ (MeV.) | $He^3/E_{min}$ (MeV.) |
|---|---|---|---|---|---|---|
| 0 | 0·38 | 52·3 | −60·2 | −7·9 | 1·10 | −6·8 |
| 1/4 | 0·46 | 56·5 | −65·0 | −8·5 | 1·13 | −7·4 |
| 1/2 | 0·70 | 46·3 | −53·3 | −7·0 | 0·99 | −6·0 |
| 3/4 | 1·60 | 25·1 | −27·2 | −2·2 | 0·65 | −1·5 |

Table I. gives the minimum values of E for $H^3$ for each value of $n$ considered, for the range $(1/\kappa)=1\cdot17\times10^{-13}$ cm., which corresponds to a meson mass of $326\,m_e$, A and $q$ having the values 67·3 MeV. and 0·69 respectively. The corresponding values of the kinetic and potential energies, the Coulomb energies for the $He^3$ nucleus and the resultant values of the binding energy for the latter nucleus are also tabulated.

The values given in Table I. indicate that the maximum value of $|E|$ of approximately 8·5 MeV. arises for $n\sim1/4$, and $c=0\cdot46$, that is, $1/\alpha=1\cdot318\times10^{-13}$ cm. The value of $(1/\alpha)$ gives an indication of the "size" of the nucleus. The maximum value of $|E|$ for $He^3$ is 7·4 MeV.

The experimental value of the mass-difference of the nuclei $H^3$ and $He^3$, that is, the Coulomb energy of the protons, is accurately known, being $771 \pm 6$ keV. (Tollestrup *et al.* 1949). Comparison of the theoretical value with this gives a check on the accuracy of the binding energy calculations. From Table I., it is seen that the theoretical values of the Coulomb energy are rather high, though the actual values of the binding energies of $H^3$ and $He^3$ are in good agreement with the experimental values of $(8{\cdot}51 \pm 0{\cdot}091)$ MeV. and $(7{\cdot}739 \pm 0{\cdot}1)$ MeV. respectively.

Svartholm, using the variation-iteration method, has calculated the value of the parameter A to fit a triton binding energy of 8·33 MeV. for the ranges $1{\cdot}185 \times 10^{-13}$ cm. and $1{\cdot}835 \times 10^{-13}$ cm. Brown (1939) has also fitted the binding energy of the triton for the latter range, using the variation method with a large number of parameters. Table II. gives the binding energies for these ranges with the new wave-functions, using the values of $q$ and A corresponding to Brown and Svartholm's calculations. Considering the simplicity of the present calculations the results obtained are reasonable.

TABLE II.

Values of the binding energy of $H^3$ with new wave-functions corresponding to different sets of nuclear parameters.

| | $1/\kappa$ ($10^{-13}$ cm.) | A (MeV.) | $q$ | Binding-energy of $H^3$ (MeV.) |
|---|---|---|---|---|
| (Svartholm) | 1·185 | 61·01 | 0·75 | 6·1 |
| | 1·835 | 33·80 | 0·58 | 8·4 |
| (Brown) . . | 1·835 | 32·06 | 0·58 | 6·3 |
| (Assumed) | 1·17 | 67·3 | 0·69 | 8·5 |

(b) *Exponential well*: $V(r_{12}) = -A \exp(-\kappa r_{12})$.

The analysis for this potential is of the same form as that for the Yukawa case. The potential energy reduces to the expression

$$-(24/\pi)(1+q)A\int_0^{\pi/2}\frac{\cos^2\psi\sin^2\psi}{(1+c\sin\psi)^{6-4n}}\,d\psi. \quad . \quad . \quad . \quad . \quad (18)$$

The integral in (18) may be evaluated by elementary methods for $n=0$, 1/4, 1/2, 3/4. [The values for $n=0$ and $n=1/4$ are given in § 2 of the Appendix.] Thus, for the $H^3$ nucleus, the total energy is given by

$$E = \frac{(5-n)}{4(1-n)(5-4n)}\cdot\frac{\hbar^2}{M}\kappa^2c'^2-(24/\pi)(1+q)A\int_0^{\pi/2}\frac{\cos^2\psi\sin^2\psi}{(1+c\sin\psi)^{6-4n}}\,d\psi. \quad . \quad . \quad . \quad (19)$$

The values taken for the nuclear paramerers are: $(1/\kappa)=0{\cdot}865\times10^{-13}$ cm., $A=123{\cdot}3$ MeV., $q=0{\cdot}6$. The minimum value of E in this case occurs at approximately $n=0$, $c=0{\cdot}69$, the kinetic and potential energies having the values 29·1 MeV. and −36·7 MeV. respectively. Thus the minimum value for E of −7·6 MeV. for $H^3$ is reasonably good. The Coulomb term given in the relation (15) has the value 1·02 MeV. at this minimum, so that the binding energy of the $He^3$ nucleus is approximately 6·5 MeV. The value of $(1/\alpha)$, corresponding to $c=0{\cdot}69$, is $1{\cdot}462\times10^{-13}$ cm., indicating the "size" of the nucleus. It is to be noted that there is a considerable difference in the values of the kinetic energies for the Yukawa and exponential potentials at the minimum of E *.

Rarita and Present (1937) have fitted the value of the binding energy of the triton, using the exponential potential and the same values of the nuclear parameters as above, but a much more complicated trial wave-function than that used here has to be introduced.

## § 4. EVALUATION OF THE BINDING ENERGY OF $He^4$.

The normalization coefficient $N_2^{1/2}$ for the wave-function $\phi'$, given by equation (10), is easily determined

$$\int \phi'^2\, d\mathbf{u}\, d\mathbf{v}\, d\mathbf{w} = N_2(4\pi)^3 \int_0^\infty [\exp\{-\beta(u^2+v^2+w^2)^{1/2}\}/(u^2+v^2+w^2)^{2n}]$$
$$\times u^2v^2w^2\, du\, dv\, dw = 1,$$

where $\beta=4\alpha$.

Using the transformation

$$u=R\sin\theta\cos\phi, \qquad v=R\sin\theta\sin\phi, \qquad w=R\cos\theta, \quad . \quad (20)$$

it is found that

$$N_2=(105\,.\,2^{13-8n}\,.\,\alpha^{9-4n})/\{\pi^4(8-4n)\,!\}. \quad . \quad . \quad . \quad . \quad (21)$$

For the above mentioned wave-function, the kinetic energy of the nucleons, corresponding to the first term on the right-hand side of equation (11), is given by

$$-(\hbar^2/2M)\int [\exp\{-\beta(u^2+v^2+w^2)^{1/2}\}/(u^2+v^2+w^2)^{2n+1}]$$
$$\times[4\alpha^2(u^2+v^2+w^2)-2\alpha(8-4n)(u^2+v^2+w^2)^{1/2}-n(14-4n)]\, d\mathbf{u}\, d\mathbf{v}\, d\mathbf{w}.$$

This is simply evaluated, using the transformation (20), so that the kinetic energy is

$$\frac{(28-2n)}{4(4-2n)(7-4n)}\cdot\frac{\hbar^2}{M}\,\kappa^2c^2, \quad . \quad . \quad . \quad . \quad . \quad . \quad (22)$$

where $c=2\sqrt{2\alpha}/\kappa$.

When the wave-function (10) is substituted in the expression (12) for the Coulomb energy, this may be evaluated, using (20), to give

$$E_{\text{Coul}}=\frac{35\sqrt{2}e^2\alpha}{32(2-n)}=\frac{35e^2c\kappa}{64(2-n)}. \quad . \quad . \quad . \quad . \quad . \quad (23)$$

---

* See note added in proof.

(a) *Yukawa potential well*: $V(r_{12}) = -A \exp(-\kappa r_{12})/(\kappa r_{12})$.

The second term on the right-hand side of equation (11) represents the potential energy of the four-particle system apart from the Coulomb energy. Now when the wave-function $\phi'$ given by (10) is used,

$$\int V(r_{12})\phi'^2 \, d\mathbf{u}\, d\mathbf{v}\, d\mathbf{w}$$

$$= -AN_2 \int \exp\{-\beta(u^2+v^2+w^2)^{1/2} - \kappa r_{12}\}/\{\kappa r_{12}(u^2+v^2+w^2)^{2n}\}\, d\mathbf{u}\, d\mathbf{v}\, d\mathbf{w}.$$

Since from symmetry considerations $r_{12}$ may be replaced by $r_{34}$, that is, $\sqrt{2}w$, the integral may, with the help of the transformation (20), be written in the form

$$-(AN_2/\kappa')(4\pi)^3 \int_0^{\pi/2} \sin^2\phi \cos^2\phi \, d\phi \int_0^{\pi/2} \sin^5\theta \cos\theta \, d\theta \int_0^{\infty} R^{7-4n} \exp(-\gamma R)\, dR,$$

where $\kappa' = \sqrt{2}\kappa$ and $\gamma = \beta + \kappa' \cos\theta$. Hence, by elementary integration, the potential energy has the form

$$-\frac{315(1+q)Ac^{9-4n}}{32(2-n)} \int_0^1 \frac{u(1-u^2)^2}{(u+c)^{8-4n}}\, du, \quad . \quad . \quad . \quad . \quad (24)$$

where $u = \cos\theta$ and $c = \beta/\kappa' = (2\sqrt{2\alpha}/\kappa)$.

Thus for the He$^4$ nucleus the total energy is given by

$$E = \frac{(28-2n)}{4(4-2n)(7-4n)} \cdot \frac{\hbar^2}{M} \kappa^2 c^2$$

$$-\frac{315(1+q)Ac^{9-4n}}{32(2-n)} \int_0^1 \frac{u(1-u^2)^2}{(u+c)^{8-4n}}\, du + E_{\text{Coul}}, \quad . \quad . \quad . \quad (25)$$

$E_{\text{Coul}}$ being given by (23).

The minimization is carried out in the same way as in § 3 (*a*) for the H$^3$ nucleus, the Coulomb term being omitted in this stage, and then added later as a perturbation. The values of $n = 0$, 1/4, 1/2, 1, 5/4, 3/2 are considered; convergence of the integral for the kinetic energy imposes the condition that $n \leqslant 3/2$. The values of the integral appearing in the potential energy term in equation (25) are given in § 3 of the Appendix. The results for the values $(1/\kappa) = 1{\cdot}17 \times 10^{-13}$ cm., $A = 67{\cdot}3$ MeV., $q = 0{\cdot}69$ are given in Table III.

TABLE III.

Minima of E for He$^4$ with respect to $c$ for each value of $n$.

| $n$ | $c$ | K . E (MeV.) | P . E (MeV.) | $E_{\text{min}}$ (MeV.) | $E_{\text{Coul}}$ (MeV.) | Binding energy (MeV.) |
|---|---|---|---|---|---|---|
| 0 | 5·0 | 188·9 | −243·5 | −54·6 | 1·97 | 52·6 |
| 1/4 | 4·5 | 200·4 | −255·4 | −55·0 | 1·73 | 53·3 |
| 1/2 | 3·7 | 176·6 | −230·8 | −54·2 | 1·66 | 52·5 |
| 1 | 2·3 | 173·5 | −220·0 | −46·5 | 1·55 | 44·9 |
| 5/4 | 1·5 | 139·0 | −174·0 | −35·0 | 1·33 | 33·7 |
| 3/2 | 0·63 | 75·0 | −88·4 | −13·4 | 0·85 | 12·5 |

The values given in Table III. show that the parameter $n$ for values from 0 to 1/2 does not influence the value of $|E|$ very much. The maximum value of the binding energy is approximately 53·3 MeV. for $n=1/4$, $c=4{\cdot}5$, that is $(1/\alpha)=0{\cdot}735\times10^{-13}$ cm. Thus a very large excess binding energy is obtained, proving the inadequacy of the central Yukawa interaction. The kinetic energy of the nucleons is exceptionally high and the nucleus itself is very concentrated. The Coulomb energy too is rather large.

The minimum values obtained for the binding energy, for the nuclear parameters of Svartholm and Brown, are given in Table IV. In addition, the binding energy is calculated for the parameter $(1/\kappa)=1{\cdot}185\times10^{13}$ cm., $q=0{\cdot}75$, A=56·0, assuming this to be the approximate convergence limit for A for the iteration method. Svartholm gives only the value obtained by the first iteration. It is also shown that the very long range of $1{\cdot}9\times10^{-13}$ cm. has to be taken to obtain a value, which is fairly near the experimental binding energy of 28·2 MeV. It might be mentioned that the value obtained by Fröhlich *et al.* (1947) for a comparable range is only half of the experimental value.

TABLE IV.

Values of the binding energy of He$^4$ with new wave-functions corresponding to different sets of nuclear parameters.

| | $1/\kappa$ ($10^{-13}$ cm.) | $q$ | A | Binding energy (MeV.) |
|---|---|---|---|---|
| (Svartholm) | 1·185 | 0·75 | 61·01 *<br>60·034 † | 43<br>40 |
| ,, | 1·185 | 0·75 | 56 (assumed) | 27 |
| ,, | 1·835 | 0·58 | 33·80 *<br>29·69 ‡ | 39<br>23 |
| (Brown) | 1·835 | 0·58 | 32·06 * | 32 |
| (Assumed) | 1·9 | 0·57 | 29·3 § | 27 |
| (Assumed) | 1·17 | 0·69 | 67·3 § | 53 |

* Depth of well obtained by variation-iteration method to fit binding energy of H$^3$.

† Depth of well obtained in one iteration to fit binding energy of He$^4$.

‡ Depth of well obtained by two iterations to fit binding energy of He$^4$.

§ Depth of well to fit deuteron and low-energy scattering data.

Thus the simple wave-functions introduced in this investigation yield results in close agreement with the calculations of Svartholm for the Yukawa potential.

(b) *Exponential potential well*: $V(r_{12})=-A\exp(-\kappa r_{12})$.

The analysis for this potential is of the same form as that for the Yukawa case. The potential energy reduces to the expression

$$-(315/8)(1+q)Ac^{9-4n}\int_0^1\{u^2(1-u^2)^2/(u+c)^{9-4n}\}\,du. \quad . \quad (26)$$

The integral in (26) is of a similar form to that in (25). Its values for $n=0$, 1/4, 1/2 are given in § 4 of the Appendix. The total energy of the He$^4$ nucleus is then given by

$$E=\frac{(28-2n)}{4(4-2n)(7-4n)}\cdot\frac{\hbar^2}{M}\kappa^2c^2$$
$$-(315/8)(1+q)Ac^{9-4n}\int_0^1\frac{u^2(1-u^2)^2}{(u+c)^{9-4n}}\,du+E_{\text{Coul}}, \quad . \quad . \quad . \quad (27)$$

$E_{\text{Coul}}$ being given by (23).

The values taken for the nuclear parameters are: $(1/\kappa)=0{\cdot}865\times10^{-13}$ cm., $A=123{\cdot}3$ MeV., $q=0{\cdot}6$. The maximum value of the binding energy occurs at approximately $n=0$, $c=2{\cdot}25$, the kinetic, potential, and Coulomb energies having the values 70 MeV., $-102{\cdot}9$ MeV. and 1 MeV. respectively. Thus the maximum binding energy is approximately 31·9 MeV., an excess of 3·7 MeV. over the experimental value of 28·2 MeV. The value of $(1/\alpha)$ corresponding to $c=2{\cdot}25$ is $1{\cdot}087\times10^{-13}$ cm. Thus there is a considerable difference in the effect of the Yukawa and exponential central interactions on the binding energy of the $\alpha$-particle. The latter potential gives a much smaller excess binding energy, a much lower kinetic energy, and does not concentrate the nucleus so much as the former potential*.

The conclusion that the exponential potential leads to too much binding energy for the $\alpha$-particle is in agreement with the calculations of Rarita and Present, though their method results in a slightly larger value for the excess binding energy.

Since the above calculations confirm that central Yukawa and exponential interactions are inadequate for a description of the binding energy of the $\alpha$-particle, consistent with the binding energy of the three-particle system, the deuteron and the low-energy scattering data—the same conclusions have been reached by Svartholm, and Rarita and Present for the Gaussian interaction—the question of non-central forces should be considered. A tensor force is of course necessary to explain the quadrupole moment of the deuteron. Gerjuoy and Schwinger, using a square-well potential with a mixture of central and tensor forces, have come to the conclusion that tensor forces are not very effective in binding the triton and $\alpha$-particle. More recent calculations on the binding energy of the triton (Rarita and Feshbach, 1949, Clapp, 1949, Hu and Hsu, 1950) have shown that it is possible to obtain fairly good agreement with the experimental binding energy with a mixture of central and tensor forces when a Yukawa potential is used. It is still an open question whether such a mixture can account for the binding energy of the $\alpha$-particle when the parameters are chosen to fit the deuteron and low-energy scattering data.

## ACKNOWLEDGMENTS.

The author is indebted to Professor J. C. Gunn for the interest he has shown in these calculations and for useful discussions. He also wishes to thank the Nuffield Foundation for the award of a Fellowship during the tenure of which the work was carried out.

---

* See note added in proof.

## APPENDIX.

The values of the integrals listed in the following sections are used in the text :—

$$\S\,1.\quad \int_0^{\pi/2} \frac{\cos^2\psi \sin\psi}{(1+c\sin\psi)^{5-4n}}\,d\psi.$$

$n=0$ : $(1/24)\{(8+9c^2-2c^4)/(1-c^2)^3-15c\cos^{-1}c/(1-c^2)^{7/2}\}$, $c\leqslant 1$.

$n=1/4$ : $(1/6)\{(2+c^2)/(1-c^2)^2-3c\cos^{-1}c/(1-c^2)^{5/2}\}$, $c\leqslant 1$.

$n=1/2$ : $-(1/2c^3)\{\pi-c/(1-c^2)-(2-3c^2)\cos^{-1}c/(1-c^2)^{3/2}\}$, $c\leqslant 1$.

$n=3/4$ : $(1/c^3)\{\pi-2c-(2-c^2)\cos^{-1}c/(1-c^2)^{1/2}\}$, $c\leqslant 1$.

$(1/c^3)\{\pi-2c-(2-c^2)\log\{c+(c^2-1)^{1/2}\}/(c^2-1)^{1/2}\}$, $c\geqslant 1$.

$$\S\,2.\quad \int_0^{\pi/2} \frac{\cos^2\psi \sin^2\psi}{(1+c\sin\psi)^{6-4n}}\,d\psi.$$

$n=0$ : $(1/120)\{15(1+6c^2)\cos^{-1}c/(1-c^2)^{9/2}-c(81+28c^2-4c^4)/(1-c^2)^4\}$, $c\leqslant 1$.

$n=1/4$ : $(1/24)\{3(1+4c^2)\cos^{-1}c/(1-c^2)^{7/2}-c(13+2c^2)/(1-c^2)^3\}$, $c\leqslant 1$.

$$\S\,3.\quad \int_0^1 u(1-u^2)^2/(u+c)^{8-4n}\,du.$$

$n=0$ : $(35c^3+47c^2+25c+5)/\{210c^6(1+c)^5\}$.

$n=1/4$ : $(5c^2+4c+1)/\{30c^5(1+c)^4\}$.

$n=1/2$ : $\log\{(1+c)/c\}-(15c^2+36c+23)/\{15(1+c)^3\}-(2c^2-1)/(20c^4)$.

$n=1$ : $(10c^2-2)\log\{(1+c)/c\}+5+1/6c^2-10c-4/\{3(1+c)\}$.

$n=5/4$ : $10c^2+1/2c-5c-8/3-(10c^3-6c)\log\{(1+c)/c\}$.

$n=3/2$ : $(5c^4-6c^2+1)\log\{(1+c)/c\}+5c^2/2+13c/3-5c^3-7/4$.

$$\S\,4.\quad \int_0^1 u^2(1-u^2)^2/(u+c)^{9-4n}\,du.$$

$n=0$ : $(64c^3+69c^2+30c+5)/\{840c^6(1+c)^6\}$,

$n=1/4$ : $(8c^2+5c+1)/\{105c^5(1+c)^5\}$,

$n=1/2$ : $\log\{(1+c)/c\}-(4c^2-1)/(60c^4)$
$-(30c^3+103c^2+122c+51)/\{30(1+c)^4\}$.

*Note added in proof.*—Since this paper was written, the author has investigated the effect of changing the range in the case of the exponential potential to the value given by a recent analysis of the low-energy $p-p$ scattering data by Jackson and Blatt (1950). The values for the nuclear parameters are then :

$$(1/\kappa)=0{\cdot}709\times10^{-13}\text{ cm.},\quad A=173{\cdot}0\text{ MeV.},\quad q=0{\cdot}64.$$

The method of calculation of the triplet well depth is given by Blatt and Jackson (1949).

For $H^3$ the maximum value of $|E|$ is approximately 9·5 MeV., corresponding to $n{\sim}0$ and $c=0{\cdot}72$, that is, $1/\alpha=1{\cdot}25\times10^{-13}$ cm. The binding energy of $He^3$ is then 8·5 MeV. Thus an excess binding energy is obtained in this case for the three-particle nuclei. The kinetic energy of $H^3$ is 39·7 MeV. For $He^4$ a binding energy of 47 MeV. is obtained, corresponding to $n{\sim}0$, $c=2{\cdot}32$, that is, $1/\alpha=0{\cdot}864\times10^{-13}$ cm., the Coulomb energy of 1·3 MeV. being taken into acount. Thus the shorter range exponential potential of Jackson and Blatt yields a much greater excess binding energy for the $\alpha$-particle than the range used by Rarita and Present. The excess is in fact comparable to that obtained for the Yukawa potential. The kinetic energy of 106·2 MeV. obtained for the $\alpha$-particle for this case is much more reasonable than the value given by the Yukawa potential.

## REFERENCES.

Blatt, J. M., and Jackson, J. D., 1949, *Phys. Rev.*, **76,** 18.
Brown, F., 1939, *Phys. Rev.*, **56,** 1107.
Clapp, R. E., 1949, *Phys. Rev.*, **76,** 873.
Feshbach, H., and Rarita, W., 1949, *Phys. Rev.*, **75,** 1384.
Fröhlich, H., Huang, K., and Sneddon, I. N., 1947, *Proc. Roy. Soc.* A, **191,** 61.
Gerjuoy, E., and Schwinger, J., 1942, *Phys. Rev.*, **61,** 138.
Hu, T., and Hsu, K., 1950, *Phys. Rev.*, **78,** 633.
Jackson, J. D., and Blatt, J. M., 1950, *Rev. Mod. Phys.*, **22,** 77.
Rarita, W., and Present, R., 1937, *Phys. Rev.*, **51,** 788.
Rosenfeld, L., 1948, *Nuclear Forces.* North-Holland Publishing Company (Amsterdam).
Svartholm, N., 1945, *The Binding Energies of the Lightest Atomic Nuclei.* Thesis (Lund).
Tollestrup, A. V., *et al.*, 1949, *Phys. Rev.*, **75,** 1947.

# XLI. *The Equilibrium of Linear Arrays of Dislocations.*

By J. D. Eshelby, F. C. Frank,
H. H. Wills Physical Laboratory, University of Bristol,
and F. R. N. Nabarro,
Department of Metallurgy, University of Birmingham *.

[Received February 1, 1951.]

## Abstract.

A method is given for finding the equilibrium positions of a set of like dislocations in a common slip-plane under the influence of a given applied stress. Their positions are given by the roots of a certain set of orthogonal polynomials. The case of a set of free dislocations piled up against a fixed dislocation by a constant applied stress is discussed in detail and the resulting stress-distribution is compared with that produced by a crack with freely slipping surfaces.

## §1. Introduction.

The following problem (Frank 1951, Kuhlmann 1951, Nabarro 1951) arises in interpreting the plastic behaviour of solids in terms of dislocations. A set of identical dislocations lie in the same slip-plane. What positions will they take up under the combined action of their mutual repulsions and the force exerted on them by a given applied shear stress, in general a function of position along the plane?

Since the dislocations (assumed to be of infinite length and parallel to one another) repel each other inversely as the distance between them the problem is unchanged if they are replaced by a set of line-charges and the applied stress is replaced by an electric field. This electrostatic problem was used by Stieltjes (1885) (*cf.* also Szegö 1939) to illustrate the properties of the zeros of orthogonal polynomials. In the present paper we show how the properties of the classical orthogonal polynomials may be used to discuss the dislocation problem.

Stieltjes solved the problem by minimizing the potential energy of the charges. We start from the idea of the force acting on a dislocation. The two methods are equivalent.

## §2.

Suppose that there is an infinite straight dislocation parallel to the $z$-axis, having the plane $y=0$ as slip plane, and passing through the point $x=x_i$. Consider the shear stresses $p_{xy}$, $p_{yz}$ in the slip-plane. If the

---

* Communicated by the Authors.

dislocation is of pure screw type $p_{xy}=0$, $p_{yz}\neq 0$. If it is of pure edge type $p_{xy}\neq 0$, $p_{yz}=0$. In either case the non-vanishing stress component which it produces at the point $x$ in the slip-plane is

$$p=\frac{A}{x-x_i}. \qquad (1)$$

For a screw dislocation $A=A_s=\mu b/2\pi$ and for an edge dislocation

$$A=A_e=\mu b/2\pi(1-\sigma)$$

(Burgers 1939). Here $\mu$ is the shear modulus, $\sigma$ is Poisson's ratio and $b$ is the magnitude of the Burgers vector **b** which gives the change of the displacement vector on passing once round the dislocation line. For an edge dislocation in an anisotropic material $A=Kb/2\pi$ where K is a certain function of the elastic constants (Eshelby 1949).

A screw dislocation is acted on by a force $bp_{yz}$ per unit length, where $p_{yz}$ is the total stress acting at its centre, excluding that produced by itself. Similarly an edge dislocation is acted on by a force $bp_{xy}$. If there are $n$ dislocations at the points $x_1, x_2 \ldots x_n$, all of the same type and each one is in equilibrium, the equations

$$\sum_{\substack{i=1\\ i\neq j}}^{n}\frac{A}{x_j-x_i}+P(x_j)=0, \quad j=1, 2, \ldots n \qquad (2)$$

must hold. $P(x)$ is the appropriate component of the applied stress at the point $x$, *i. e.* the $xy$ component for edge and the $yz$ component for screw dislocations.

Equations (1) and (2) apply, more generally, to any set of parallel like dislocations lying in their common slip plane. If $\psi$ is the angle between the line and Burgers vector of each dislocation, we then have

$$A=A_s \cos\psi+A_e \sin\psi,$$

$$P(x)=P_{yz}(x)\cos\psi+P_{xy}(x)\sin\psi,$$

since the screw and edge components interact independently with one another.

In all cases, therefore, the following condition must be satisfied at each dislocation: the component in the direction of **b** of the traction on the plane $y=0$ due to the other dislocations and to the applied stress must vanish.

It will be convenient to choose the unit of stress so that $A=1$. The condition of equilibrium is then

$$\sum_{i\neq j}\frac{1}{x_j-x_i}+P(x_j)=0, \quad j=1, 2 \ldots n. \qquad (3)$$

We may regard the $x_i$ as the zeros of the polynomial

$$f=\prod_{i=1}^{n}(x-x_i). \qquad (4)$$

$f$ has the convenient property that its logarithmic derivative is equal to the stress due to all the dislocations :

$$\frac{f'}{f}=\sum_{i=1}^{n}\frac{1}{x-x_i}.$$

The stress when the $j$th dislocation is missing is

$$\frac{f'}{f}-\frac{1}{x-x_j}. \quad . \quad . \quad . \quad . \quad . \quad . \quad . \quad . \quad . \quad . \quad (5)$$

The value of this expression when $x=x_j$ is

$$\lim_{x\to x_j}\frac{(x-x_j)f'(x)-f(x)}{(x-x_j)f(x)}=\tfrac{1}{2}\frac{f''(x_j)}{f'(x_j)}, \quad . \quad . \quad . \quad . \quad . \quad (6)$$

by double differentiation of numerator and denominator.

The conditions (2) can thus be written

$$\left.\begin{array}{r} f(x_j)=0 \\ \tfrac{1}{2}\dfrac{f''(x_j)}{f'(x_j)}+\mathrm{P}(x_j)=0 \end{array}\right\} j=1, 2 \ldots n. \quad . \quad . \quad . \quad . \quad . \quad (7)$$

Consider the differential equation

$$f''(x)+2\mathrm{P}(x)f'(x)+q(n, x)f(x)=0. \quad . \quad . \quad . \quad . \quad . \quad . \quad (8)$$

Suppose that we can choose $q$ so that this equation has a polynomial solution of the $n$th degree all of whose roots are real and distinct. Then if $q$ does not have a pole at any of the roots the conditions (7) are satisfied and the problem is solved.

In the physical problem we may be interested in cases where certain of the dislocations are "locked" in fixed positions (Cottrell 1948). If a dislocation is locked at $x=x_\alpha$ we imply that it lies in a stress field $p(x)=\text{const}.\delta'(x-x_\alpha)$ where $\delta'$ is the derivative of Dirac's $\delta$-function. The dislocation is in equilibrium at $x=x_\alpha$ where $p(x)=0$. Also, since $p'(x_\alpha)$ is negatively infinite, the equilibrium is stable and an added stress will shift the position of equilibrium only infinitesimally. The other dislocations are unaffected by $p(x)$. It is then convenient to omit $p(x)$ from the expression for the applied stress and to regard one of the dislocations as "locked" at the point $x_\alpha$.

Suppose, then, that in addition to the $n$ "free" dislocations there are locked dislocations at $x_{n+1}$, $x_{n+2} \ldots x_\nu$. The equilibrium positions of the free dislocations are found by regarding the stresses produced by the locked dislocations as forming part of the applied stress, so that (8) becomes

$$f''+2\left\{\mathrm{P}(x)+\sum_{\alpha=n+1}^{\nu}\frac{1}{x-x_\alpha}\right\}f'+q(n, x)f=0. \quad . \quad . \quad . \quad (9)$$

In this case we expect $q$ to have a pole at each $x_\alpha$ in order that $f'/f$ shall not vanish there.

The solution will be of the form (4) and $f'/f$ will give the stress due to the free dislocations alone. If we make the substitution

$$\mathrm{F}(x)=f(x)\prod_{\alpha=n+1}^{\nu}(x-x_\alpha)$$

(9) becomes

$$\mathrm{F}''+2\mathrm{PF}'+\frac{\mathrm{Q}(n,x)}{\prod\limits_{\alpha}(x-x_\alpha)}\mathrm{F}=0, \quad . \quad . \quad . \quad . \quad . \quad . \quad (10)$$

where

$$\frac{\mathrm{Q}(n,x)}{\prod\limits_{\alpha}(x-x_\alpha)}=q(n,x)-2\mathrm{P}(x)\sum_{\alpha}\frac{1}{x-x_\alpha}-\sum_{\alpha}\sum_{\substack{\beta\\ \alpha\neq\beta}}\frac{1}{(x-x_\alpha)(x-x_\beta)}$$

and $\alpha$, $\beta$ take the values $n+1$, $n+2 \ldots \nu$. At the zeros $x_1, x_2 \ldots x_n$ the conditions (7) are satisfied (free dislocations) whilst at the zeros $x_{n+1}$, $x_{n+2}, \ldots x_\nu$ the last term in (10) has a finite value owing to the vanishing of a factor in the denominator, and the second of the conditions (7) (with F replacing $f$) is not satisfied (locked dislocations). F$'$/F is the stress produced by locked and free dislocations.

If a particular problem has been solved in this way it remains to verify that the arrangement of dislocations is stable. The condition for this is that the $x$-derivative of the total stress at the position of a free dislocation (excluding its own stress) shall be negative, *i. e.* that

$$\lim_{x\to x_j}\frac{d}{dx}\left\{\frac{\mathrm{F}'(x)}{\mathrm{F}(x)}-\frac{1}{x-x_j}+\mathrm{P}(x)\right\}<0.$$

After some calculation this reduces to the condition that

$$\mathrm{I}(x)\equiv\mathrm{Q}-\mathrm{P}^2-\mathrm{P}'>0 \quad . \quad . \quad . \quad . \quad . \quad . \quad . \quad . \quad (11)$$

for $x=x_1, x_2 \ldots x_n$. $\mathrm{I}(x)$ is the " invariant " of equation (10) which can be reduced to the form

$$v''+\mathrm{I}(x)v=0 \quad . \quad . \quad . \quad . \quad . \quad . \quad . \quad . \quad . \quad (12)$$

by the substitution

$$v=\mathrm{F}\exp\left(\int\mathrm{P}dx\right). \quad . \quad . \quad . \quad . \quad . \quad . \quad . \quad . \quad (13)$$

$v$ has the same zeros as F with possibly additional ones. A region in which $\mathrm{I}<0$ can usually be dealt with by the following argument. Suppose that $v$ has a zero (which may be at infinity) in the region. Since $v''$ has the same sign as $v$ the curve $v=v(x)$ is convex to the $x$-axis and there can be no other zero in the region. In particular, if $\mathrm{I}<0$ for $x>x'$ and $v\to 0$ as $x\to\infty$ then F can have no zero for $x>x'$.

It is easily seen that $v'/v$ gives the total stress due to free and locked dislocations and the applied stress.

## § 3.

The general method will be illustrated by some cases of physical interest.

(i.) A row of $n$ dislocations under zero applied stress, the outer two being locked at $x=\pm$L. If $\mathrm{L}=1$, (9) becomes

$$f'+2\left\{\frac{1}{x-1}+\frac{1}{x+1}\right\}f'+q(n,x)f=0,$$

or if we take

$$q=\frac{n(n-1)-2}{1-x^2},$$

$$(1-x^2)f''-4xf'+\{n(n-1)-2\}f=0$$

which is satisfied by $f=P'_{n-1}(x)$, the first derivative of the $(n-1)$th Legendre polynomial. Hence

$$f=P'_{n-1}(x/L),\ \ F=(L^2-x^2)f=P'_{n-1}(x/L)\sqrt{(L^2-x^2)}.$$

In ordinary stress units the stress on one of the locked dislocations is

$$\pm AF''(1)/F'(1)=\pm\tfrac{1}{4}n(n-1)A/L.$$

The roots of $f$ up to $n-1=8$ have been given by Kopal (1946).

(ii.) A row of $n$ free dislocations with an applied stress proportional to $x$. Such a uniformly varying stress exists near the centre of a beam supported at the ends and uniformly loaded. We have $P=x(dP/dx)$ with $dP/dx$ constant. The resulting force on a dislocation can be regarded as arising from a potential energy $V=-\frac{1}{2}bx^2\,(dP/dx)$. "Potential troughs" of this type may exist in real crystals owing to the presence of various defects (Mott and Nabarro 1948). If we choose $1/\sqrt{(dP/dx)}$ as the unit of length the equation for $F(=f)$ is

$$F''-2xF'+QF=0.$$

If $Q=2n$, (10) is satisfied by the $n$th Hermite polynomial, $H_n(x)$. The invariant $I=2n+1-x^2$ is positive if $|x|<\sqrt{(2n+1)}$ and negative otherwise. The reduced equation is satisfied by $v=H_n(x)\exp(-\frac{1}{2}x^2)$, so that by the argument following equation (13) all dislocations lie in the region $|x|<\sqrt{(2n+1)}$. (*cf.* also Appendix, § A2).

In ordinary units of length and stress

$$F=H_n\left\{x\sqrt{\left(\frac{dP/dx}{A}\right)}\right\}$$

and all dislocations lie in the region

$$|x|<\sqrt{\left\{\frac{(2n+1)A}{dP/dx}\right\}}.$$

(iii.) A set of $n-1$ free dislocations along the positive $x$-axis in equilibrium under the combined effect of a locked dislocation at the origin and a uniform stress tending to move them in the negative direction. This case is discussed in detail in § 4.

(iv.) Two locked dislocations as in (i.) with an applied stress as in (iii.). This leads to an equation occurring in the theory of the hydrogen molecular ion. There is an extensive literature (Wilson 1928, Teller 1930, Hylleraas 1937) but no general discussion of the polynomial solutions. As we should expect there are $n$ polynomial solutions of order $n$, since we can put 0, 1, 2 . . . $n$ dislocations in the interval $-L<x<L$ and the remainder in the interval $L<x$.

## §4.

For case (iii.) above we have $P(x)$ constant and equal to say $-\tau_0$. Equation (8) becomes

$$f''+2(x^{-1}-\tau_0)f'+qf=0,$$

If we take $1/2\tau_0$ as the unit of length and put $q=(n-1)/x$ this becomes

$$xf''+(2-x)f'+(n-1)f=0 \tag{14}$$

which is satisfied by the first derivative of the $n$th Laguerre polynomial, $L_n'(x)$. Thus in ordinary units of length and stress

$$f=L_n'(2\tau_0 x/A), \quad F=(2\tau_0 x/A)\,L_n'\,(2\tau_0 x/A).$$

The spacing of the dislocations is the same as that of the radial nodes of a hydrogen atom in the *ns* state.

The invariant of (14), $I=nx^{-1}-\frac{1}{4}$ is positive if $x<4n$. The reduced equation is satisfied by $v=xL_n'(x)\exp\left(-\frac{1}{2}x\right)$ so that all zeros of $f$ must occur for $x<4n$. A lower bound for the greatest root is obtained in the Appendix, §A.1. Since

$$L_n'(x)=-\sum_{k=0}^{n-1}\frac{n!\,(-x)^k}{k!\,(k+1)!\,(n-k-1)!} \tag{15}$$

there are no negative roots.

When $x$ is small compared with $n$ we may neglect $\frac{1}{4}$ in comparison with $n/x$ and the reduced equation $v''+Iv=0$ becomes

$$v''+(n/x)v=0$$

with the solution

$$v=\sqrt{x}\,.\,J_1\{\sqrt{(4nx)}\} \tag{16}$$

so that near the origin the position of the $i$th dislocation is given by $x\cong j_i^2/4n$ where $j_i$ is the $i$th zero of the Bessel function $J_1$. The position of the free dislocation nearest to the locked dislocation is $x_1\simeq 3\cdot 67/n$. Since $j_i\cong\pi i$ for large $i$ the number, $i$, of dislocations between the origin and the point $x$ is

$$i\cong(2/\pi)\sqrt{(nx)}, \qquad 1\ll i\ll n.$$

Returning to ordinary units of stress and length in which $x$ becomes $2\tau_0 x/A$ we have the following approximate results for large $n$:

L, the length of the slip plane occupied by dislocations

$$=2nA/\tau_0 \tag{17}$$

the number of dislocations lying between 0 and $x$

$$=\frac{2}{\pi}\sqrt{\left(\frac{2n\tau_0 x}{A}\right)} \tag{18}$$

$d$, the distance between the locked and nearest free dislocation

$$=1\cdot 84\,A/n\tau_0 \tag{19}$$

The difference between the L of equation (17) and the true distance between the locked and furthest free dislocation, L′ say, can be estimated from the inequality

$$1{\cdot}47n^{-2/3}-0{\cdot}55n^{-5/3}<\frac{\mathrm{L}-\mathrm{L}'}{\mathrm{L}}<2{\cdot}56n^{-2/3},$$

obtained by combining the result of § A.1 with an inequality given by Szegö (1939, equation 6.32.6). In what follows we shall refer to L (and not the accurate L′) as the length of the row of dislocations. Equation (18) is true in the sense that if $1 \ll i \ll n$ the ratio of the right-hand side of (18) to the correct $i$ approaches unity as $n$ tends to infinity. Actually (18) is in error by a factor of only $4/\pi$ even if $i=n$ and in error by only one or two units for small $i$ provided $n$ is large. $d$ must be larger than a few atomic distances if our results are to be valid, since the expression (1) is inaccurate very close to a dislocation. (Nabarro 1940).

If we move along the $x$-axis the discontinuity $\Delta$ in the displacement on crossing the slip plane changes by $b$ each time a dislocation is passed. The curve $\Delta=\Delta(x)$ is thus stepped, but according to (17) and (18) it will approximate to the smooth curve

$$\Delta=\frac{2b\tau_0}{\pi\mathrm{A}}\sqrt{(\mathrm{L}x)}, \qquad . \quad . \quad . \quad . \quad . \quad . \quad . \quad (20)$$

provided $n$ is large and we do not go too far from the origin.

From the coefficients of $x^{n-1}$ and $x^{n-2}$ in (16) we find $(2\tau_0/\mathrm{A})\Sigma x_i=n(n-1)$ so that the centre of gravity of the free dislocations is at the point $x=n\mathrm{A}/2\tau_0=\frac{1}{4}\mathrm{L}$ whilst the centre of gravity of the $n$ dislocations is at $x=(n-1)\mathrm{A}/2\tau_0$. The coefficients of $x$ and $x^0$ give $\mathrm{A}\Sigma x_i^{-1}=(n-1)\tau_0$. According to (1) this is the stress at the locked dislocation produced by the free dislocations. The total stress on the locked dislocation is thus $n\tau_0$. This also follows from (14) which gives $f'(0)/f(0)=\frac{1}{2}(n-1)$ which must be multiplied by $2\tau_0$ to convert to ordinary units. Cottrell (1949) has already obtained this result by a virtual work argument.

The behaviour of the stress, $\tau$, beyond the locked dislocation ($x<0$) is also of physical interest (Frank 1951). To discuss it, it is convenient to reverse the sign of $x$ so that the dislocations lie on the negative $x$-axis. The most important region is that in which $x$ is of the order of L, or, in the reduced units in which $2\tau_0/\mathrm{A}=1$, $x\sim n$. In these units the solution (16) with the sign of $x$ changed is

$$v=\text{const.}\ y\,\mathrm{I}_1(y), \quad y=\sqrt{(4nx)}$$

and this is a good approximation when $x\ll 4n$. The total stress is given by $v'/v$, for which we find

$$\frac{v'}{v}=\sqrt{\left(\frac{n}{x}\right)}\cdot\frac{\mathrm{I}_0(y)}{\mathrm{I}_1(y)}, \quad x\ll 4n.$$

From known properties of Bessel functions $I_0/I_1 \rightarrow 1$ as $y \rightarrow \infty$ and $I_0/I_1 \rightarrow 2/y$ as $y \rightarrow 0$ so that $v'/v=\sqrt{(n/x)}$ if $1/4n \ll x \ll 4n$ and $v'/v=1/x$ if $x \ll 1/4n$ or in ordinary units

$$\begin{aligned} \tau/\tau_0&=\sqrt{(\mathrm{L}/x)}, & \tfrac{1}{15}d \ll x \ll \mathrm{L} \\ \tau&=\mathrm{A}/x, & \tfrac{1}{15}d \ll x. \end{aligned} \quad \text{. . . . . . . . (21)}$$

Fig. 1.

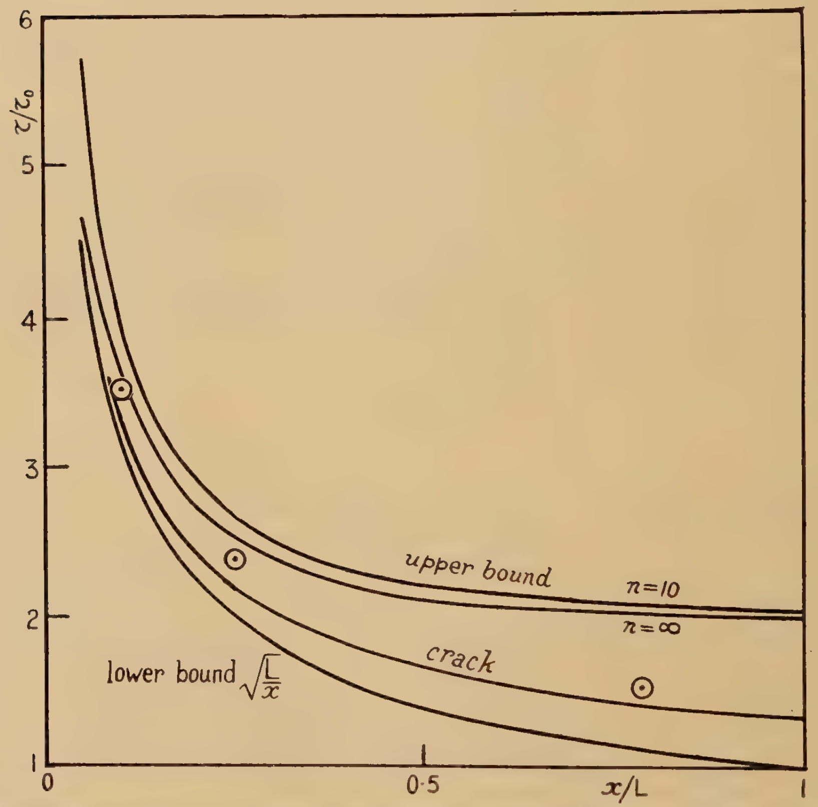

Shear stress in front of a row of held-up dislocations. Upper and lower bounds from equations (22). ○ exact values calculated from the polynomial (15) for $n=10$. For comparison the stress due to a crack of length 4L is given, according to equation (24).

The last equation implies that the effect of the locked dislocation is dominant at points much closer to it than is the nearest free dislocation. It is shown in the Appendix, (§ A3) that

$$\left.\begin{aligned} &\frac{\tau}{\tau_0}=\sqrt{\left(\frac{\mathrm{L}}{x}\right)}\cdot\left[1+\theta\left\{\frac{x}{\mathrm{L}}+\frac{1}{2n}\sqrt{\left(\frac{\mathrm{L}}{x}\right)}\right\}\right], \quad 0<\theta<1 \\ &\text{and also} \qquad \tau>\mathrm{A}/x, \quad \tau>\tau_0. \end{aligned}\right\} \quad . \quad . \quad (22)$$

These relations enable us to set bounds to the departure of $\tau/\tau_0$ from the simple expression $\sqrt{(\mathrm{L}/x)}$ for a given $x$; see figs. 1 and 2.

For large $x$ we have

$$\tau = \tau_0 + n\mathrm{A}/x \quad \text{or} \quad \tau/\tau_0 = 1 + \tfrac{1}{2}\mathrm{L}/x,\ x \ll \mathrm{L}, \qquad . \quad . \quad . \quad (23)$$

as can be seen from the inequality

$$\frac{n\mathrm{A}}{x+\mathrm{L}} < \frac{\mathrm{A}}{x} + \sum_i \frac{\mathrm{A}}{x+|x_i|} < \frac{n\mathrm{A}}{x}$$

which follows from the facts that $0 < |x_i| < \mathrm{L}$. Equation (23) shows that at large distances the stress is the sum of the applied stress and that due to all the dislocations regarded as congregated at the origin.

Fig. 2.

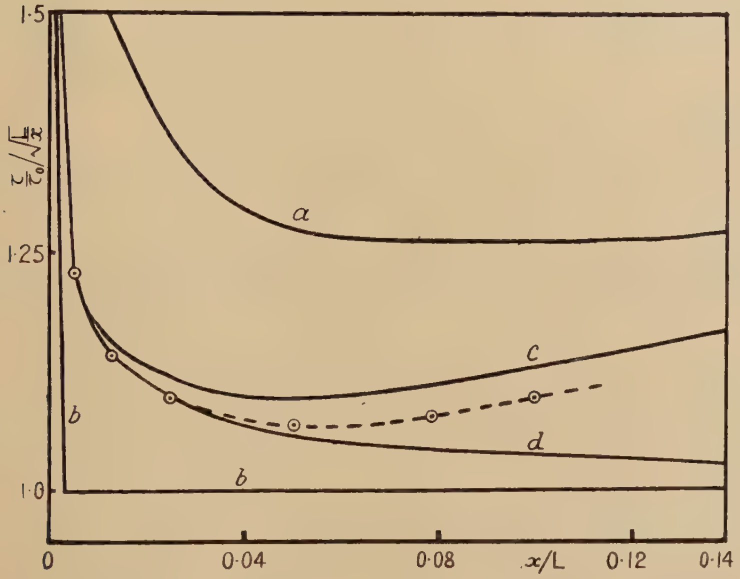

Shear stress in front of a row of ten held-up dislocations. $a$, $b$ upper and lower bounds from equations (22). $c$, $d$ upper and lower bounds from equation ($a$9) (Appendix, § A.3). ⊙, accurate values calculated from the polynomial (15). The stress falls off monotonically with $x$: the convexity arises from plotting $\tau/\tau_0\sqrt{(L/x)}$ instead of $\tau/\tau_0$.

Zener (1948) has compared a slip-band both to a crack and to an array of dislocations and it is interesting to compare the results of this section with those of Starr (1928) for a crack. He finds the following expressions for an infinitely narrow two-dimensional crack of length $l$ extending along the $x$-axis from $x=0$ to $x=-l$ when the body containing it is subjected to a uniform applied shear stress $p_{xy}=\tau_0$. The stress in the plane $y=0$ beyond the tip of the crack is given by the exact formula

$$\frac{\tau}{\tau_0} = \frac{x+\frac{1}{2}l}{\sqrt{\{x(x+l)\}}} = \sqrt{\left(\frac{l}{4x}\right)} \cdot \left(1 + \frac{x}{l} - \frac{1}{2}\frac{x^2}{l^2} + \ldots\right). \qquad . \quad . \quad . \quad (24)$$

If the crack is not infinitely narrow but has a radius of curvature $\rho$ at the end (24) is only correct if $x \gg \rho$. $\tau/\tau_0$ then reaches a maximum in the neighbourhood of $x=\rho$ and falls to zero at $x=0$. We have

$$\tau/\tau_0=1+\tfrac{1}{2}(l/2x)^2, \quad x \gg l \quad . \quad . \quad . \quad . \quad . \quad . \quad . \quad (25)$$

far from the crack.

The discontinuity in the displacement in crossing the $x$-axis, *i. e.* the relative displacement of the two faces of the crack, is given by the exact expression

$$\Delta=\frac{b\tau_0}{\pi \mathrm{A}}\sqrt{\{(l-|x|)|x|\}}, \quad -l<x<0$$

reducing to

$$\Delta=\frac{b\tau_0}{\pi \mathrm{A}}\sqrt{(l|x|)}, \quad x<0, \quad |x| \ll l \quad . \quad . \quad . \quad . \quad . \quad . \quad (26)$$

if we do not go too far from the tip of the crack.

The elastic constants have been expressed in terms of $b$ and A (*cf.* equation (1)) to aid comparison, though of course the problem of the crack does not involve the Burgers vector. A is to be given its value for edge dislocations, $b\mu/2\pi(1-\sigma)$. It can be shown that the last four equations also apply to a crack in an anisotropic medium if we give A the value $b\mathrm{K}/2\pi$. They also cover the case of a crack in an isotropic body in a state of anti-plane strain with $\tau_0$ and $\tau$ representing the $yz$ stress component provided we put $\mathrm{A}=b\mu/2\pi$, the value appropriate to screw dislocations. Consequently these equations can be used to compare a crack under plane strain or anti-plane strain with an array of edge or screw dislocations respectively.

Comparison of (22) and (24) or of (20) and (26) shows that over a certain range of $x$ the row of dislocations of length L simulates a crack of length 4L (*cf.* fig. 1).

It will be noted that near the origin the stress produced by the dislocations and the crack with a finite curvature at the tip diverge in opposite directions from the value $\tau_0\sqrt{(\mathrm{L}/x)}$.

From (23) and (25) it will be seen that for the dislocations $\tau-\tau_0$ falls off as $x^{-1}$ at large distances, but for the crack as $x^{-2}$, that is, in the same way as for a group of positive dislocations near a group of an equal number of negative ones. It is also clear that the array of dislocations simulates only one end of the crack. These facts suggest that a better imitation of a crack would be given by the following sequence of dislocations : a locked positive dislocation, $n$ free positive dislocations, $n$ free negative dislocations, a locked negative dislocation. The free dislocations are prevented from coalescing by the applied stress and the locked dislocations prevent them from spreading and define the length of the equivalent crack (*cf.* Zener 1948, fig. 4). The method of the present paper is not capable of finding their equilibrium positions.

## §5.

The polynomial F also has a physical interpretation for complex values of its argument. Let $Z=x+iy$. Then for a set of screw dislocations the displacement $w$ and stresses at the point $(x, y)$ are given in the isotropic case by

$$\phi+iw=\frac{b}{2\pi}\log F(Z),$$

$$p_{yz}+ip_{xz}=\frac{\mu b}{2\pi}\frac{F'(Z)}{F(Z)}.$$

$\phi$ is the electrostatic potential in the corresponding Stieltjes line-charge problem. These results follow from the fact that for a single screw dislocation at the origin $w=(b/2\pi)\tan^{-1}(y/x)$.

For an array of edge dislocations the results are less simple since problems in plane stress or strain cannot be solved in terms of a single complex variable. We find for the isotropic case

$$(p_{xx}+p_{yy})+2i\mu\varpi/(1-\sigma)=-2iG'$$

$$p_{xy}+\tfrac{1}{2}i(p_{xx}-p_{yy})=G'+iyG''$$

where

$$G(Z)=A\log F(Z),\quad A=\mu b/2\pi(1-\sigma)$$

and $\varpi$ is the rotation. The results follow from the value $\chi=-Ay\log r$ of the Airy function for an edge dislocation at the origin (Koehler 1941).

## ACKNOWLEDGMENTS.

Our thanks are especially due to Professor H. Heilbronn, who first indicated to us the connection between a set of algebraic equations of the form (2) and a differential equation of the form (8) upon which the whole analysis is based. He also obtained the important inequality of §A.1. We wish to thank Dr. C. S. Davis for much assistance and Mr. K. M. Baird for stimulating discussion.

---

# APPENDIX.

## §A.1.

The reduced equation for the problem of §4 is

$$v''+\left(\frac{n}{x}-\frac{1}{4}\right)v=0. \qquad \text{(a1)}$$

Let $X=x_{n-1}$ be the greatest root of $v$. We can arrange that $v>0$ for $x>X$. Choose a constant $\xi>X$. We can write (a1) in the form

$$v''+\lambda^2v=g(x) \qquad \text{(a2)}$$

where

$$\lambda^2=\left(\frac{n}{\xi}-\frac{1}{4}\right),\quad g(x)=n\left(\frac{1}{\xi}-\frac{1}{x}\right)v(x).$$

The solution of the inhomogeneous equation (a2) which satisfies $v(\mathrm{X})=0$ is

$$v(x)=\mathrm{A}\sin\lambda\,(x-\mathrm{X})+\lambda^{-1}\int_{\mathrm{X}}^{x}\sin\lambda\,(\mathrm{X}-x')\,g\,(x')\,dx'$$

where A is an arbitrary constant. Hence

$$v(\mathrm{X}+\pi/\lambda)=\lambda^{-1}\int_{\mathrm{X}}^{\mathrm{X}+\pi/\lambda}\sin\lambda\,(x'-\mathrm{X})\,g\,(x')\,dx'.$$

Since the left-hand side is positive $g(x')$ must be positive for at least part of the range of integration and so

$$\xi<\mathrm{X}+\pi/\lambda.$$

So far $\xi$ is arbitrary. We now try to choose it to give as precise information as possible about X, bearing in mind that $\lambda$ is a function of $\xi$. Put

$$\xi=4n/(1+\phi^2),\quad \lambda=\tfrac{1}{2}\phi.$$

Then

$$\mathrm{X}>\frac{4n}{1+\phi^2}-\frac{2\pi}{\phi}\qquad\text{. . . . . . . .}\qquad\text{(a3)}$$

and *a fortiori*

$$\mathrm{X}>4n(1-\phi^2-\pi/2n\phi).\qquad\text{. . . . . . . .}\qquad\text{(a4)}$$

The right-hand side of (a4) has a minimum when $\phi=(\pi/4n)^{1/3}$ so that

$$\mathrm{X}>4n[1-3(\pi/4)^{2/3}\,n^{-2/3}].$$

A slightly more precise lower limit could be found by minimizing the right-hand side of (a3).

### § A.2.

The same method applied to the Hermite polynomials occurring in § 3 (iii.) gives for the greatest root X

$$\mathrm{X}>\sqrt{(2n+1)}\,[1-\sqrt{(2\pi)}\,(2n+1)^{-3/4}].$$

### § A.3.

With the sign of $x$ changed (a1) becomes

$$v''-\frac{n}{x}v=\tfrac{1}{4}v\qquad\text{. . . . . . . .}\qquad\text{(a5)}$$

which has the exact solution

$$v=(n-1)\,x\,\mathrm{L}_n'\,(-x)\exp\tfrac{1}{2}x\qquad\text{. . . . . . .}\qquad\text{(a6)}$$

with a convenient choice of the arbitrary multiplying factor. If the right-hand side of (a5) were zero it would have the two independent solutions

$$v_1=y\,\mathrm{I}_1\,(y),\quad v_2=y\mathrm{K}_1\,(y),\quad \text{where } y=\sqrt{(4nx)}.$$

It is easily verified that $v$ and $v_1$ agree in value and first derivative at the origin. Solving (a5) as an inhomogeneous equation in the usual way, making use of the relation

$$\mathrm{I}_0\,\mathrm{K}_1+\mathrm{K}_0\,\mathrm{I}_1=1/y, \qquad \text{(a7)}$$

we have

$$v=y\,\mathrm{I}_1(y)+y\{\mathrm{I}_1(y)\mathscr{K}-\mathrm{K}_1(y)\mathscr{I}\}/8n \qquad \text{(a8)}$$

with the abbreviations

$$\mathscr{I}=\int_0^x y'\,\mathrm{I}_1(y')\,v(x')\,dx', \quad \mathscr{K}=\int_0^x y'\mathrm{K}_1(y')\,v(x')\,dx', \quad y'=\sqrt{(4nx')}.$$

The term $y\{\ \}/8n$ vanishes with its first derivative at the origin so that solving the integral equation (a8) would give the exact solution (a6). Differentiating (a8) we have

$$v'=2n\,\mathrm{I}_0+\tfrac{1}{4}\,(\mathrm{I}_0\mathscr{K}+\mathrm{K}_0\mathscr{I}).$$

If we write (a8) in the form

$$v=y\mathrm{I}_1/[1-y\,(\mathrm{I}_1\mathscr{K}+\mathrm{K}_0\mathscr{I})/8nv]$$

we find, using (a7) again,

$$\frac{v'}{v}=\frac{2n\mathrm{I}_0}{y\mathrm{I}_1}\left(1+\frac{\mathscr{I}}{v}\,\frac{1}{8n\mathrm{I}_0}\right).$$

By finding upper and lower limits for $\mathscr{I}/v$ we can give upper and lower limits for $v'/v$. The simplest approximation is the following. Since $v(x)$ is a monotonically increasing function of $x$

$$0<\mathscr{I}/v<\int_0^x y'\,\mathrm{I}_1\,(y')\,dx'=y^2\,\mathrm{I}_2(y)/2n$$

and so, using the relation $y\,\mathrm{I}_2=y\,\mathrm{I}_0-2\mathrm{I}_1$,

$$\frac{\mathrm{I}_0}{\mathrm{I}_1}<\frac{y}{2n}\,\frac{v'}{v}<\frac{\mathrm{I}_0}{\mathrm{I}_1}\left(1+\frac{y^2}{16n^2}\right)-\frac{y}{8n^2}. \qquad \text{(a9)}$$

This estimate could, of course, be improved. Using the recurrence relations for Bessel functions and the fact that, if $m<n$, $\mathrm{I}_m/\mathrm{I}_n$ decreases monotonically to unity as $y$ increases we find the following inequalities:

$$\frac{\mathrm{I}_0}{\mathrm{I}_1}>1, \quad \frac{2}{y}<\frac{\mathrm{I}_0}{\mathrm{I}_1}<\frac{2}{y}+1.$$

With the help of these we can derive from (a9) this weaker relation free from Bessel functions:

$$\max\left(\frac{2}{y},1\right)<\frac{y}{2n}\,\frac{v'}{v}<1+\frac{2}{y}+\frac{y^2}{16n^2}.$$

The notation on the left implies that we are to choose the greater of $2/y$ and 1. Equation (22) in the text follows from the fact that

$$y=4n\sqrt{(x/\mathrm{L})}, \quad yv'/2nv=\tau\sqrt{x}/\tau_0\sqrt{\mathrm{L}}$$

in ordinary units.

## REFERENCES.

BURGERS, J. M., 1939, *Proc. Kon. Ned. Akad. v. Wet.*, **42,** 293.

COTTRELL, A. H., 1948, *Report of a Conference on the Strength of Solids* (London : Physical Society), p. 30 ; 1949, *Progress in Metal Physics* (London : Butterworths Scientific Publications), p. 105.

ESHELBY, J. D., 1949, *Phil. Mag.*, **40,** [7], 903.

FRANK, F. C., 1951, Symposium on Plastic Deformation of Crystalline Solids, May 1950, Carnegie Institute of Technology, Pittsburgh (in the press).

HYLLERAAS, E. A., 1937, *Ann. Inst. Henri Poincaré*, **7,** 121.

KOEHLER, J. S., 1941, *Phys. Rev.*, **60,** 397.

KOPAL, Z., 1946, *Astrophys. J.*, **104,** 61.

KULHMANN, D., 1951, *Proc. Phys. Soc.*, **64,** 140.

MOTT, N. F., and NABARRO, F. R. N., 1948, *Report of a Conference on the Strength of Solids* (London : Physical Society), p. 1.

NABARRO, F. R. N., 1940, *Proc. Phys. Soc.*, **52,** 34 ; 1951, *Some Recent Developments in Rheology* (London : United Trade Press Ltd., for the British Rheologists' Club), p. 38.

STARR, A. T., 1928, *Proc. Camb. Phil. Soc.*, **24,** 489.

STIELTJES, T. J., 1885, *Acta Math.*, **6,** 321.

SZEGÖ, G., 1939, *Orthogonal Polynomials* (Amer. Math. Soc. Colloquium Publications, **23**), p. 136.

TELLER, E., 1930, *Z. Phys.*, **61,** 458.

WILSON, A. H., 1928, *Proc. Roy. Soc.* A, **118,** 617, 635.

ZENER, C., 1948, *Fracturing of Metals* (Symposium, American Society for Metals, Cleveland, Ohio), p. 3.

# XLII. *The Use of Plasticine Models to Simulate the Plastic Flow of Metals.*

By A. P. Green, B.A.,
British Iron and Steel Research Association, Sheffield,
Mechanical Working Division*.

[Received January 11, 1951.]

[Plates XV. & XVI.]

## Summary.

The behaviour of plasticine when permanently deformed is compared with that of an ideal metal, and the necessary conditions for similarity between their flow patterns are examined for flow in two and three dimensions. A brief account of the mechanical properties of plasticine includes a description of stress–strain curves obtained by compressing cylinders between lubricated plates at constant rates of loading. Plane strain experiments, using a plasticine model marked with a grid on a cross-section parallel to the plane of flow, are described, and photographs of the deformed grids are compared with theory. The processes thus examined were: extrusion through square and wedge-shaped dies; indentation of a plane surface by a single wedge and by a row of wedges; and compression of a narrow wedge by a flat die. The profile of a deep narrow block after a small indentation by a flat punch is also compared with theory. All these plane strain plasticine experiments agree well with theory. One experiment using a metal was performed—the compression of a narrow copper wedge by a smooth flat die. This copper wedge deformed in a similar way to the plasticine wedge.

## §1. Introduction.

Many metal working processes can be simulated by plasticine model experiments. The models are cheap and easy to make, and only a small amount of apparatus is needed. In the present paper an attempt is made to examine the mechanical properties that plasticine (or, indeed, any substance) should possess, in order that its manner of deformation should approximate to that of an ideal metal, for flow in two and three dimensions. That plasticine does in fact deform in a similar manner to an ideal metal, under conditions of plane strain, is shown by the close agreement between the model experiments described below and calculations made on the basis of existing theory for an ideal plastic–rigid non-hardening metal. There is no evidence, as yet, that this agreement will extend to flow in three dimensions. However, a model experiment should give a qualitative idea of the flow, provided the hydrostatic component of stress is compressive.

---

* Communicated by R. Hill.

## §2. Properties of Plasticine.

Plasticine is a mixture of an inert mineral oil, probably petroleum jelly, and a mineral filler, mainly calcite. Sometimes an organic dye is added. Its compressive stress–strain curves at three different rates of loading were found by compressing cylindrical specimens, ½-in high and 1-in. diameter, between the parallel plates of a beam test apparatus. During the course of compression the sides of the specimens became slightly concave. This effect was probably due to extrusion of the grease lubricant between the ends of the specimens and the compression plates. In all the stress–strain curves there is a sharp bend, after which the material deforms at an approximately constant stress. Unfortunately, the curves cannot be directly compared, because the temperatures at which the tests were carried out differed by 1–2° C. and the yield stress is very temperature dependent. A rise in temperature from 17° C. to 21° C. caused a decrease in yield stress of about 30 per cent. The curve for the rate of loading 21·15 lb./min.$^{-1}$ at 21° C. is shown in fig. 1. The curves for the two lower rates are similar, except that for strains greater than about 0·1, the small constant slope of the curve is greater. For the rates 21·15, 15·66, and 11·93 lb./min.$^{-1}$, the slopes are, approximately, 3·0, 4·0 and 4·5 lb./sq. in.$^{-1}$ respectively. The rates of loading were chosen to produce rates of strain comparable to those which occurred in the model experiments. If, at any stage of a compression test, loading is stopped and the load is kept constant, deformation continues at a rapidly decreasing rate becoming negligible after a few minutes. For example, at the end of a test where the rate of loading was 21·15 lb.min.$^{-1}$,

Fig. 1.

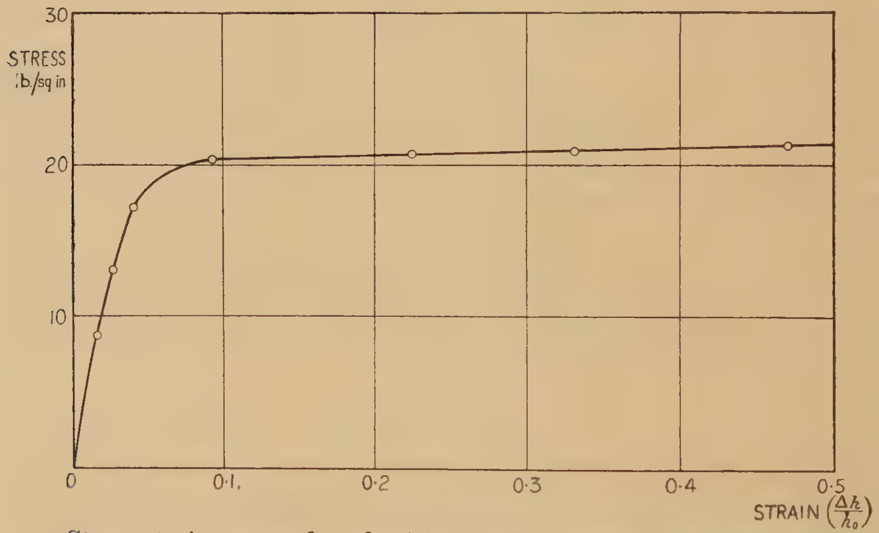

Stress–strain curve for plasticine under uniaxial compression. Rate of loading 21·15 lbs.min.$^{-1}$. Temp. 21° C.

the load was kept constant, and after one minute the strain had increased from 0·51 to 0·53 ; after a further ten minutes it was 0·54 and over the next sixteen hours it increased to 0·55. Provided air bubbles are removed by working the material, its permanent compressibility is negligible. This was checked by weighing cylindrical specimens in water before and after 50 per cent compression. The change in volume was always less than 0·2 per cent.

There appears to be no generally accepted explanation of the stress–strain properties of plasticine. It is possible that friction between the mineral particles embedded in the petroleum jelly prevents continuous flow until a critical shear stress is reached. There may be, in addition, electrostatic forces between the particles, as has been suggested for clay and paints (Houwink 1937).

## §3. COMPARISON OF PLASTICINE AND METAL.

It might appear surprising that close comparison is possible between the deformation of plasticine and that of a metal. It will now be shown why this comparison is possible under conditions of plane strain. Consider plastic flow in plane strain, where plastic strains are large, and the freedom of movement of the material in plastic flow is not constrained completely by material still elastic. Under these conditions of pure shear, plasticine behaves like a non-hardening isotropic metal, provided the flow is slow, so that it can be treated as quasi-static. This is because any element of either material deforms in shear under an approximately constant stress ; both are virtually incompressible ; and their principal axes of stress and strain-increment coincide. The last property must be true of any isotropic body for which the ratios of the plastic strain-increment components depend only on the ratios of the current stress components, and not on the previous stress or strain history. This can be expected on physical grounds, if, after deformation, the new random arrangement of the mineral particles is indistinguishable from the original one, so that there is no " memory " of past deformations. This appears to be true for plasticine judging by the agreement between theory and experiment. The precise degree of similarity between the plasticine and the metal flow patterns depends, of course, on how closely the shapes of the respective shear stress–strain curves correspond.

The equations governing the plane plastic strain of an ideal non-hardening metal were originally derived by Hencky (1923), (stress equations), and Geiringer (1930), (velocity equations). The theoretical flow patterns given in this paper were calculated on the basis of this theory. The flow patterns for plasticine can be expected to differ in the region of small strains from the calculated patterns, because its yield point is not quite sharp, nor, of course, is it rigid before yielding.

It is not known how closely plasticine will correspond to a non-hardening metal in three-dimensional plastic flow, since no experiments have yet been made. If good agreement is to be obtained, the yield criterion for plasticine must approximate closely to that of the metal; for many metals, the Mises criterion is a good approximation. In addition, the relation between Lode's variables for stress and strain-rate must be the same for the two materials. For a Newtonian viscous fluid Lode's variables are equal; this is also a good approximation for many metals (Hill 1950).

## §4. EXPERIMENTAL DETAILS.

Stone-coloured plasticine, containing no dye, was used for most of the experiments. After carefully working the plasticine by hand to eliminate air bubbles, the specimens were cut to shape with a fine wire. Each specimen was made in two halves, $\frac{1}{4}$-in. thick. On the inner face of one half a $\frac{1}{10}$-in. square grid was lightly stamped in ink. French chalk was used to prevent the two halves sticking when placed together. After deformation between parallel lubricated constraints, the two halves could be easily separated and the deformed grid photographed. If it is inconvenient to have the specimen in two halves, either the grid must be ruled on an outer face, or the model may be built up in layers, using two different colours of plasticine (see expt. 5 below). Unfortunately it is difficult to find different colours with exactly the same mechanical properties. Medium grease was used for the lubrication of external surfaces.

## §5. COMPARISON OF THEORY AND EXPERIMENT.

With one exception, the following experiments were carried out under conditions of plane strain, using plasticine models. The exception is the compression of a narrow wedge of annealed copper by a smooth flat die (see expt. 6).

(1) Direct extrusion through a square die with 66·7 per cent reduction (figs. 2 *a* and *b*, Pl. XV.).

(*a*) Full friction at the container walls.

The container was lined with emery paper to ensure that the friction was sufficiently high to cause local yielding of the plasticine at the walls. The distortion of a square grid was calculated, using the slip line field given by Hill (1948 a) for direct extrusion. It is particularly interesting that the observed region of dead plasticine agrees well with that *assumed* in the theory.

(*b*) Smooth container walls and die face.

The slip-line field is an extreme case of the one given by Hill (1948 a) for extrusion through a smooth wedge-shaped die (the die-angle here being 90°). In the theory it is assumed that there is no dead region, but in practice lubrication was not quite perfect, and it was impossible to avoid a small dead region in the corner, which modified the flow pattern. The cusps on the centre line in the theoretical pattern are a result of the tangential velocity discontinuities across the entry and exit slip lines. In practice, since the yield point of plasticine is not sharp, there is a region of rapid shear instead of a velocity discontinuity, and the cusps and sharp corners in the flow lines are rounded off. The experimental and theoretical grids are out of step, because the actual moment of comparison was not the same.

(2) Direct extrusion through a smooth wedge-shaped die; semi-angle of die 15°; 34 per cent reduction (fig. 3, Pl. XV.).

The slip-line field for this problem (Hill 1948 a) is the same as that found for the plane strain problem of sheet drawing. The latter problem is dealt with in a paper by Hill and Tupper (1948), and the theoretical distortion of a square grid is taken from that paper. The theoretical region of uniform motion is well demonstrated in the experimental pattern. The squares become parallelograms, in this special configuration, due to a single line of shear at entry; the preservation of the parallelograms indicates uniform flow. The boundary of the region of large plastic strains, defined by the sharp bends in the longitudinal flow lines, agrees well with theory. There is again a rounding off of cusps and sharp corners. The slope of the straight sections of the deformed transverse lines is greater than in theory, probably due to friction at the die face.

Fig. 8.

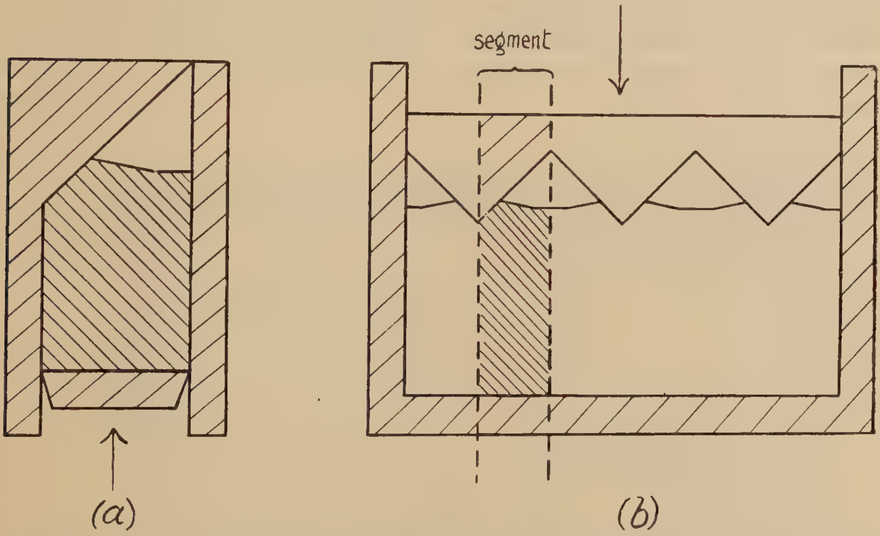

(*a*) Diagram of the experimental arrangement for wedge indentation and coining.
(*b*) Segment of the coining process.

(3) Indentation of a plane surface by a smooth wedge of semi-angle 50° (fig. 4, Pl. XV.).

The distortion of a square grid was calculated according to the theory given by Hill, Lee and Tupper (1947), who computed one for a wedge of semi-angle 30°. The wider semi-angle of 50° was chosen for this experiment because the region of non-uniform motion is larger, and a clearer comparison can be made with the theory. It is difficult in practice to obtain good lubrication using a full wedge. Instead, therefore, a rectangular block, constrained between two parallel lubricated guides was compressed against an oblique face (fig. 8 *a*). This face represented half a wedge, and one of the guides replaced the line of symmetry through the apex of the wedge. It is assumed that the slip-line field and velocity solution are the same as for one half of the field of a full wedge, so long as there still remains a part of the original surface undeformed. The stresses in the plastically deforming region differ only by the addition of a hydrostatic pressure due to the lateral constraint of the guides. The oblique face was removed and re-lubricated intermittently, but there still remained an appreciable amount of friction due to newly sheared plasticine being continually presented to the face, both at the tip of the half wedges and the apex of the plasticine lip. Calculations by Hill (1950, unpublished) show that the effect of friction is to lessen the slope of the lip which, however, remains straight if the friction is uniform. By comparing measurements on the experimental block with the theory, the mean coefficient of friction was deduced to be approximately 0·3. This high value appears reasonable in view of the breakdown of lubrication which occurs for the reason already explained. The curvature of the surface near the apex of the lip is, no doubt, partly due to uneven friction, and partly to strain hardening.

(4) Indentation of a plane surface by a row of smooth wedges of semi-angle 45° (fig. 5, Pl. XVI.).

## EXPLANATION OF THE PLATES.

### Plate XV.

Fig. 2.

Direct extrusion of plasticine through a square die with 66·7 per cent reduction. (*a*) Perfect friction ; (*b*) Smooth.

Fig. 3.

Direct extrusion of plasticine through a smooth wedge-shaped die with 34 per cent reduction ; total die angle 30°.

Fig. 4.

Indentation of a plane plasticine surface by a smooth 100° wedge.

### Plate XVI.

Fig. 5.

Three stages in a plasticine coining process using smooth 90° wedges : Ratios of depths of indentation to width of specimen. (*a*) 0·3, (*b*) 0·42, (*c*) 0·5.

Fig. 6.

Compression of a 40° plasticine wedge by a smooth flat die.

Fig. 7.

Compression of a 34° *annealed copper* wedge by a smooth flat die.
(*a*) Vertical section.
(*b*) View from above showing compressed surface.

Fig. 2.

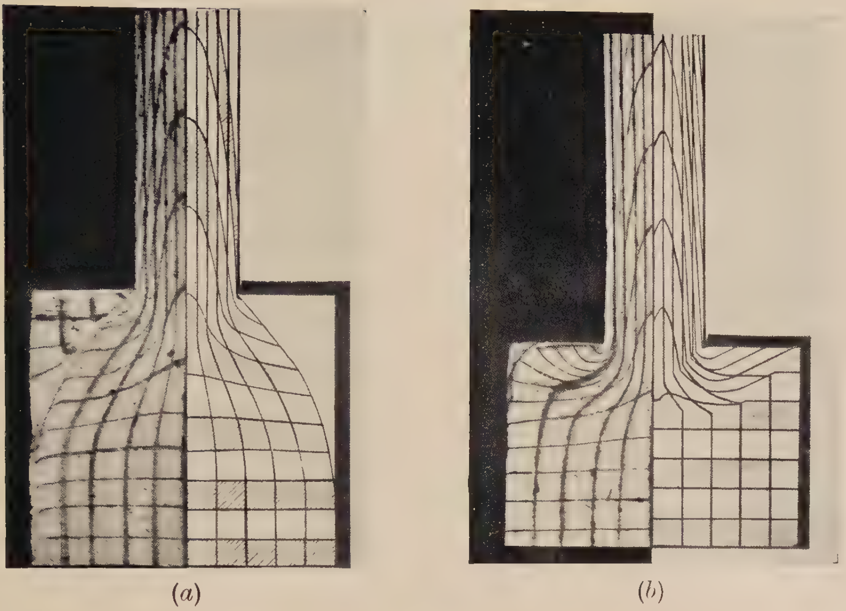

(*a*) (*b*)

Fig. 3.

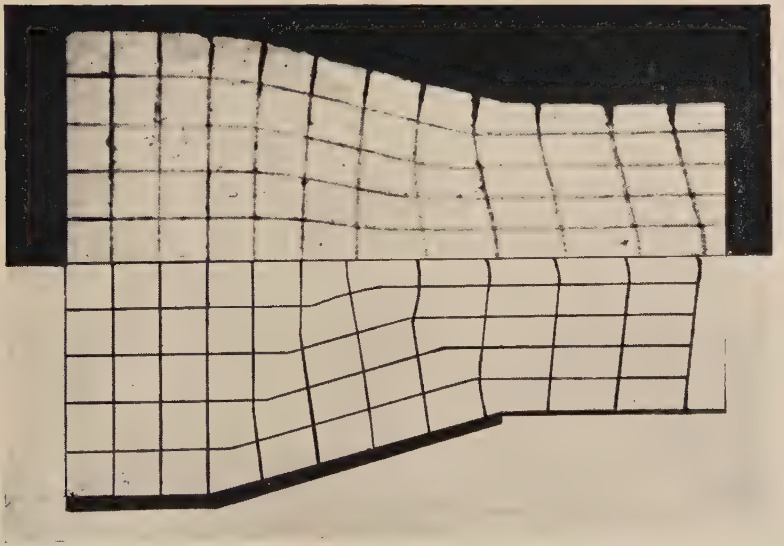

Fig. 4.

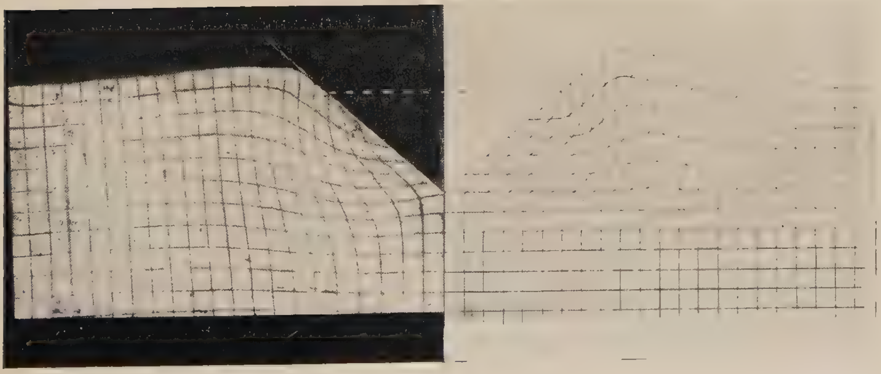

Fig. 5.

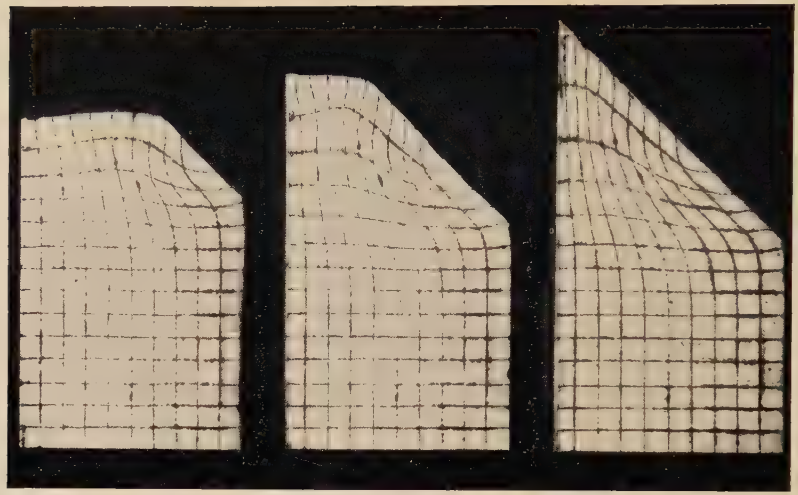

Fig. 6.

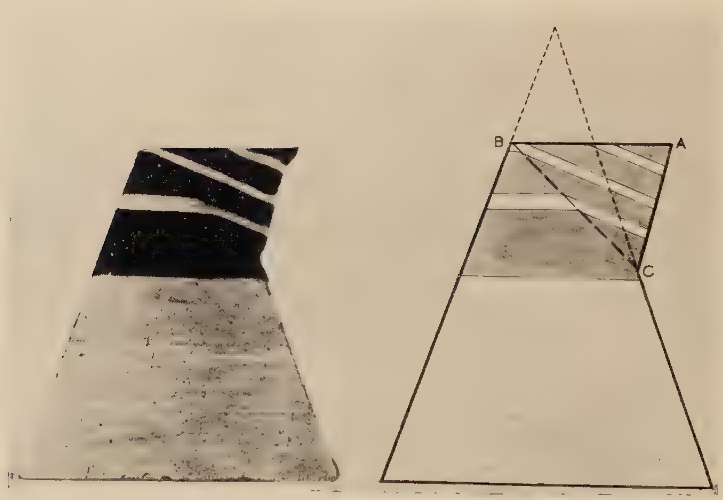

Fig. 7.

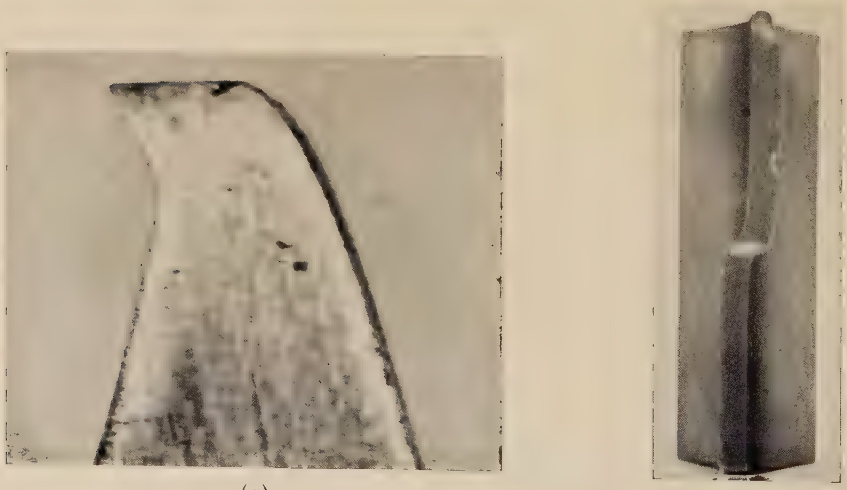

(*a*) (*b*)

This may be regarded as a process of coining. A block is constrained on all faces, except the surface which is to be indented. The flow pattern can be split up into exactly similar segments between the planes of symmetry through the angles of the wedges (fig. 8 *b*). Each of these segments is identical with that for half-wedge indentation, described in the previous section, and the experiment can, therefore, be carried out in a similar manner. In this case, however, compression was continued, until the specimen was completely "coined". After the region of deformation has reached the line of symmetry between adjacent wedges, (*i. e.* the outer guide), the configuration is no longer geometrically similar. The slip-line field is then continually changing and no theoretical solution has yet been found. It is interesting to see that there is little deformation below the tip of the wedge.

(5) Compression of a 40° wedge by a smooth flat die (fig. 6, Pl. XVI.).

The model was made of layers of two different colours. The mode of deformation shown in fig. 6 (Pl. XVI.) is one of the ways in which a narrow wedge can deform. The observed deformation suggested the following theory. It appears that a simple shear takes place along a single moving slip-line, BC, which makes an angle of 45° with the smooth die. Any element of the wedge remains stationary until reached by the moving slip-line. It then shears instantaneously, and continues to move as part of the rigid body ABC, parallel to BC. If angle ACB were less than 45°, the material in ABC would be unable to support the calculated forces on BC. This restricts the range of validity of the solution to wedge angles less than 45°. The experimental pattern agrees well with this theory. The bends in the deformed layers are sharp and lie on a straight line which makes an angle of 43° with the die face.

Other experiments were attempted with wider angle wedges but it was difficult to obtain consistent results because of varying friction conditions at the die face. Two possible symmetrical solutions have been suggested by Hill (1948 b). In one of these a steadily increasing wedge-shaped region of material is carried down with the die. This type of solution tends to occur when lubrication is poor, since it involves no relative motion between the die and the plasticine surface in contact with it. It is valid for wedge angles greater than 28° 4′. When lubrication is good the other type of solution, which is valid for wedge-angles greater than 53° 12′, is sometimes observed. The wedge gradually divides down the centre; newly sheared plasticine is continually presented to the die face from the centre and is then displaced outwards towards the sides. Sometimes a wedge will change its mode of deformation as frictional conditions alter.

(6) Compression of a 34° *annealed copper* wedge by a smooth flat die (figs. 7 *a* and *b*, Pl. XVI.).

The wedge was not constrained at its ends, but towards the centre conditions approximated to plane strain, since the ratios of depth of compression to the dimensions of the wedge were small. Initially, the wedge was 0·75 in. high and 1·36 in. long. It was compressed through 0·1 in., in six stages, between polished plates made of sintered hard metal, which were lubricated intermittently with calcium oleate. There was no deformation at the base, but the length of the top of the wedge increased by 0·06 in. After compression the wedge was sectioned vertically (*i. e.* along a plane perpendicular to its length), 0·35 in. from one end (fig. 7 *a*, Pl. XVI.). It can be seen that its mode of deformation was similar to that shown in fig. 6 Although work-hardening broadened the single slip line, BC, into a region of rapid shear, the final shape of the section, except for the rounded corners, agrees well with the theory for an ideal metal. Initially, some vertical sections of the wedge commenced to shear to one side and some to the other, while some sections even deformed symmetrically. Viewed from above, the compressed surface zig-zagged along its length. As compression continued, the longer unsymmetrical sections began to carry the other sections with them. Finally, half the wedge was shearing to one side and half to the other (fig. 7 *b*, Pl. XVI.).

Fig. 9.

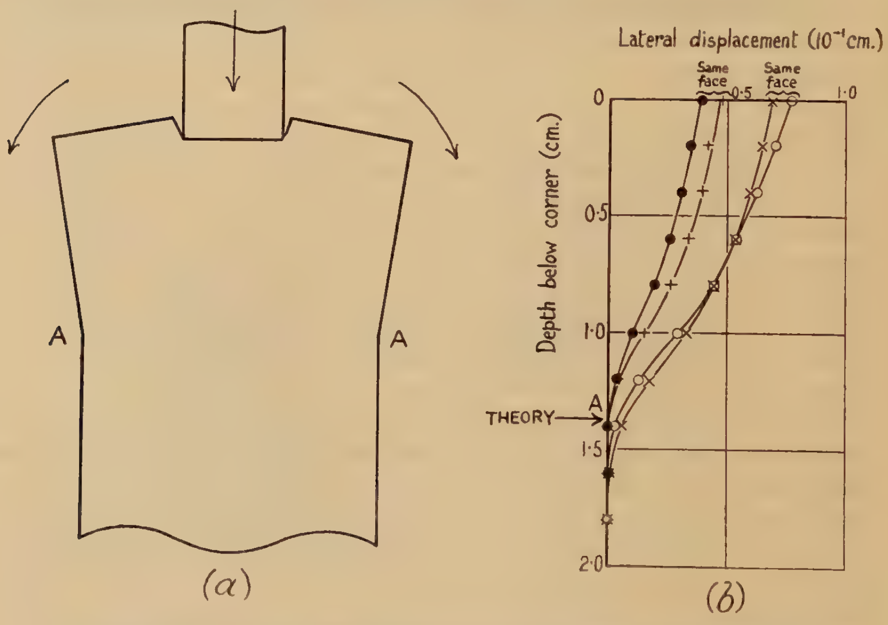

Indentation of a narrow plasticine block by a smooth flat punch.
(*a*) Diagram showing nature of initial deformation (exaggerated);
(*b*) Profile of block after indentation.

(7) Indentation of a deep narrow block by a smooth flat punch*.

---

* The theory has been worked out by R. Hill (1950) and I quote, by kind permission, from his as yet unpublished results.

With a sufficiently narrow block, the plastic region spreads out to the sides as the load is increased, and the initial deformation of the corners is a rotation outwards (fig. 9 *a*). The rotation on each side takes place along a curved slip line which meets the side of the block at a point, A, whose position can be calculated. A plasticine block, $\frac{3}{4}$-in. wide, was indented to a depth of $\frac{1}{25}$-in. by a flat lubricated punch $\frac{1}{4}$-in. wide. After indentation the shapes of the lateral faces of the block were plotted with a travelling microscope. The occurrence of a rigid-body rotation and the position of A agreed well with theory (fig. 9 *b*).

## § 6. CONCLUSION.

Under conditions of plane strain, agreement with theory has been shown to be encouragingly good. It is planned to extend these experiments to other processes, and also to measure the applied loads. This should provide an additional test of the similarity between plasticine and an ideal metal. Similar experiments using a metal such as pre-strained copper are desirable for further comparison with theory and with plasticine. An experiment in which lead blocks were indented by steel wedges coated with vaseline is described in the paper on wedge indentation (Hill, Lee and Tupper 1947). When the theory is not known, a plasticine experiment may assist in finding a solution (for example, see expt. 5).

## ACKNOWLEDGMENTS.

The author is greatly indebted to Dr. R. Hill for his help and counsel during this work. He would also like to thank his colleagues Mr. F. Carr for the photography and Mr. G. Douglass for the calculation of the theoretical flow patterns shown in figs. 2 *a* and 4. He thanks the Director of the British Iron and Steel Research Association for permission to publish this paper.

## REFERENCES.

GEIRINGER, H., 1930, *Proceedings of the Third International Congress for Applied Mechanics* (Stockholm), **2.**

HENCKY, H., 1923, *Zeits. f. Math. Mech.*, **3,** 241.

HILL, R., 1948 a, *J. Iron & Steel Inst.*, **158,** 182 ; 1948 b, *Proceedings of the Seventh International Congress for Applied Mechanics* (London).

HILL, R., LEE, E. H., and TUPPER, S. J., 1947, *Proc. Roy. Soc.* A, **188,** 273.

HILL, R., and TUPPER, S. J., 1948, *J. Iron & Steel Inst.*, **159,** 359.

HILL, R., 1950, *The Mathematical Theory of Plasticity*, pp. 44–5. (Oxford : Clarendon Press.)

HOUWINK, R., 1937, *Elasticity, Plasticity and Structure of Matter.* (Cambridge : Cambridge University Press.)

# XLIII. *Collective Electron Ferromagnetism: Rectangular Energy Bands.*

By E. P. Wohlfarth, Ph.D.,
Department of Mathematics, Imperial College, London*.

[Received January 18, 1951.]

## Summary.

Calculations similar to those of Stoner (1938, 1939) are carried out for an energy band for which the energy density of states is constant. These have a bearing on calculations of the actual band form for nickel (Fletcher and Wohlfarth 1951). After brief reference to previous work and a statement of the basic assumptions of the treatment, relations are derived giving the dependence on temperature and the interchange interaction energy of the spontaneous magnetization below and the susceptibility above the Curie point. Various explicit limiting relations are deduced. The numerical results of the calculations are given in Table I. and fig. 1 (§2). Formulæ are also derived which give the internal energy and specific heat over the whole temperature range. Relations are given for the most important experimentally observable thermal characteristics, such as the specific heat discontinuity at the Curie point. The results are shown in figs. 2 and 3 (§3). Experimental results which are briefly discussed (§4) include those on the magnetic properties of nickel and its alloys and the thermal properties of nickel, including the energy and specific heat characteristics, the temperature variation of specific heat and the magneto-caloric effect. The high temperature specific heat of paramagnetics is also discussed. In an Appendix certain results for an energy band of more general form are given.

## §1. Introduction.

The collective electron treatment of ferromagnetism was originally developed by Stoner (1938 a, 1939, 1948, 1951) for an energy band of standard form, for which the energy density of states is proportional to the square root of the energy. In the present paper similar calculations are carried out for an energy band for which the density of states is constant. Consideration of this problem arose mainly as a result of calculations, which are still proceeding, aiming at a determination of the actual band form for nickel. Preliminary results of these calculations (Fletcher and Wohlfarth 1951) indicate that the actual band form near the top of the band is almost certainly intermediate between that assumed by Stoner and that considered here. A comparison of the two sets of theoretical results serves to show to what extent discrepancies between theory and experiment are due to the assumption of a particular band form and to what extent they result from other assumptions of the treatment. As compared with the parabolic band, the band with constant density of states has the practical advantage that the main formulæ may be obtained in closed algebraical form; for the parabolic band extensive numerical computation is often required.

---

* Communicated by the Author.

Rectangular bands have been considered previously by Néel (1938) and Watanabe (1948). Néel obtains expressions for spontaneous magnetization and susceptibility equivalent to relations (2.7) and (2.9) of the present paper. Watanabe considers susceptibility in some detail, but attempts to represent his results by a Curie–Weiss law, which has no immediate significance in the treatment. This type of representation underlies his analysis of the experimental results for iron, cobalt and nickel, and little significance can be attached to the estimated values of the specifying parameters for these metals. Watanabe also discusses the experimental results for some nickel alloys, but does not seem to have appreciated the primary effect of alloying on the magnetic properties (*cf.* §4). It is believed, however, that Watanabe's procedure in attributing some of the details of the observed susceptibility curves to band overlap effects is essentially correct. In the same paper the temperature dependence of specific heat is investigated and the calculated curve for nickel is similar in shape to that given here (fig. 2).

In the present paper calculations of spontaneous magnetization and susceptibility, appropriate to the basic assumptions (§2), are followed by calculations of the internal energy and specific heat (§3). Use is made of the recently published table of the Fermi–Dirac function of order 1 (Rhodes 1950). The bearing of the theoretical results on experimental data is discussed in §4. In an Appendix certain results are derived for an energy band of more general form.

## §2. MAGNETIC PROPERTIES.

The calculations are based on the following assumptions: (i.) The energy band contains N particles, in actual ferromagnetics holes in the 3*d* band. At absolute zero and in the absence of any interchange interaction the holes occupy the band in balanced pairs over an energy range between the top of the band, $\epsilon_b$, and the top of the Fermi distribution, $\epsilon_b-\epsilon_0$. The energy density of states for particles of either spin, $\nu(\epsilon)$, is constant and is given by

$$\nu(\epsilon)=\mathrm{N}/2\epsilon_0. \qquad \qquad (2.1)$$

(ii.) The interchange interaction effects give rise to a term in the total energy of amount

$$\mathrm{J}(\zeta)=-\tfrac{1}{2}\mathrm{N}k\theta'\zeta^2, \qquad \qquad (2.2)$$

where $\zeta$ is the relative magnetization, related to the magnetic moment, M, by $\zeta=\mathrm{M}/\mathrm{N}\mu$, and $\theta'$ is a constant parameter.

*Fundamental relations.* With the above assumptions a development of the statistical treatment (Stoner 1938 a) leads to the following expressions for $\zeta$ as a function of temperature, T, and applied field, H:

$$\left.\begin{aligned}\zeta&=\tfrac{1}{2}\frac{k\mathrm{T}}{\epsilon_0}\{\mathrm{F}_0(\eta+\beta+\beta')-\mathrm{F}_0(\eta-\beta-\beta')\},\\ 1&=\tfrac{1}{2}\frac{k\mathrm{T}}{\epsilon_0}\{\mathrm{F}_0(\eta+\beta+\beta')+\mathrm{F}_0(\eta-\beta-\beta')\}.\end{aligned}\right\} \quad . \quad . \quad . \quad (2.3)$$

Here $\eta$ is related to the chemical potential, $\xi$, by $\eta=\xi/k\mathrm{T}$ and $\beta=k\theta'\zeta/k\mathrm{T}$, $\beta'=\mu\mathrm{H}/k\mathrm{T}$. The function $\mathrm{F}_0$ is the Fermi–Dirac integral of zero order which may be evaluated exactly,

$$\mathrm{F}_0(\eta)=\int_0^\infty\frac{dx}{\exp(x-\eta)+1}=\ln(1+e^\eta). \quad . \quad . \quad . \quad . \quad (2.4)$$

In the absence of an applied field manipulation of (2.3) and (2.4) gives an implicit relation for spontaneous magnetization in the form

$$\frac{k\theta'}{\epsilon_0}=\frac{\tau}{2\zeta}\ln\left\{\frac{\exp[(1+\zeta)/\tau]-1}{\exp[(1-\zeta)/\tau]-1}\right\}, \quad . \quad . \quad . \quad . \quad . \quad . \quad (2.5)$$

where $\tau=k\mathrm{T}/\epsilon_0$. Two useful alternative relations may be obtained:

$$\frac{k\theta'}{\epsilon_0}-\tfrac{1}{2}=\frac{\tau}{\zeta}\tanh^{-1}\{\tanh(\zeta/2\tau)/\tanh(1/2\tau)\}, \quad . \quad . \quad (2.6)$$

$$\frac{k\theta'}{\epsilon_0}-1=\frac{\tau}{\zeta}\sinh^{-1}\{\exp(-1/\tau)\sinh\beta\}, \quad . \quad . \quad . \quad . \quad (2.7)$$

where $\beta=(k\theta'/\epsilon_0)\,\zeta/\tau$. The Curie temperature, $\theta$, is given by

$$\left.\begin{aligned}\frac{\epsilon_0}{k\theta}&=-\ln\left(1-\frac{\epsilon_0}{k\theta'}\right),\\ \text{or inversely}\qquad \frac{\epsilon_0}{k\theta'}&=[1-\exp(-\epsilon_0/k\theta)].\end{aligned}\right\} \quad . \quad . \quad . \quad . \quad . \quad . \quad . \quad (2.8)$$

The inverse of the susceptibility above the Curie point, $\chi$, is given by (2.3) and (2.4) as

$$\frac{1}{\zeta}\frac{\mu\mathrm{H}}{\epsilon_0}=\frac{1}{\chi}\frac{\mathrm{N}\mu^2}{\epsilon_0}=[1-\exp(-1/\tau)]^{-1}-k\theta'/\epsilon_0, \quad . \quad . \quad . \quad (2.9)$$

if $\mu\mathrm{H}/k\mathrm{T}$ and $\zeta$ are small compared with 1.

*Limiting relations.* (i.) *The limit $k\theta/\epsilon_0\to\infty$.* Relation (2.8) shows that in this limit $\theta'\to\theta$ and hence, from (2.6), $\zeta=\tanh(\zeta\theta/\mathrm{T})$, the classical Weiss relation for spontaneous magnetization. Relation (2.9) shows that in the same limit $\chi=\mathrm{N}\mu^2/k(\mathrm{T}-\theta)$, the Curie–Weiss law.

(ii.) *Condition for ferromagnetism. Relative magnetization at absolute zero.* Relation (2.8) shows the condition for ferromagnetism (finite spontaneous magnetization at absolute zero) to be $k\theta'/\epsilon_0>1$ and (2.5) shows that as soon as ferromagnetism occurs at all the relative magnetization at absolute zero,

$\zeta_0$, is unity. As shown in the Appendix (relation (A.8)), however, in a band of general form there is usually a range of values of $k\theta'/\epsilon_0$ over which, although $\zeta_0$ is finite, it may be less than 1. For parabolic bands, for example, this range was shown by Stoner (1938 a, relation (5.10)) to be $\frac{2}{3}<k\theta'/\epsilon_0<2^{-1/3}$, the lower limit giving the condition for ferromagnetism in that case. In this respect, therefore, the rectangular band form with strictly constant density of states is a very special case.

(iii.) *Approach to saturation*, $kT/\epsilon_0 \rightarrow 0$. In this limit $\zeta \rightarrow \zeta_0 = 1$ and relation (2.5) gives the law of approach to saturation as

$$\zeta = 1 - \frac{kT}{\epsilon_0} \exp\left\{ -\frac{2\epsilon_0}{kT}\left(\frac{k\theta'}{\epsilon_0} - 1\right)\right\}, \quad . \quad . \quad . \quad . \quad (2.10)$$

analogous to Stoner's relation (1938 a, relation (5.21)) for parabolic bands in the range of values of $k\theta'/\epsilon_0$ for which $\zeta_0 = 1$. For parabolic bands, however, the law of approach takes the form $(\zeta/\zeta_0)^2 = 1 - \alpha(\zeta_0)(T/\theta)^2$ when $\zeta_0 < 1$, where $\alpha$ is in general close to 1 (Stoner 1938 a, relation (5.26))

(iv.) *Magnetization near the Curie point*, $T/\theta \rightarrow 1$. Relation (2.6) may be used to show that in the neighbourhood of the Curie point

$$\zeta^2 = 6k\theta/\epsilon_0 \tanh (\epsilon_0/2k\theta)(1 - T/\theta),$$

which, on transforming (2.8) into $\coth (\epsilon_0/2k\theta') = 2k\theta'/\epsilon_0 - 1$, gives

$$\zeta^2 = \frac{6k\theta/\epsilon_0}{2k\theta'/\epsilon_0 - 1}(1 - T/\theta). \quad . \quad . \quad . \quad . \quad . \quad . \quad . \quad (2.11)$$

Relation (2.11) gives correctly the classical dependence of magnetization on temperature near the Curie point, $\zeta^2 = 3(1 - T/\theta)$ for $k\theta/\epsilon_0 \rightarrow \infty$, but shows that the slope of the $\zeta^2$, $T/\theta$ curve decreases as $k\theta/\epsilon_0$ decreases. In the limit $k\theta/\epsilon_0 \rightarrow 0$, $k\theta'/\epsilon_0 \rightarrow 1$, (2.11) becomes $\zeta^2 = 6k\theta/\epsilon_0\ (1 - T/\theta)$.

*Computations*. Relation (2.5) was used to compute values of $\zeta$ for $T/\theta = 0{\cdot}0\ (0{\cdot}1)\ 0{\cdot}9\ (0{\cdot}05)\ 1{\cdot}0$ and for $k\theta'/\epsilon_0 = 1{\cdot}01$, $1{\cdot}04$, and $1{\cdot}10$, using a balancing method of solution. Since $\zeta_0 = 1$, $\zeta$ equals the usual reduced specific magnetization, $\sigma/\sigma_0$. The range of values of $k\theta'/\epsilon_0$ covered is indicated by the susceptibility results to include practically all ferromagnetic metals and alloys. The susceptibility above the Curie point was calculated using relation (2.9) for $T/\theta = 1{\cdot}0\ (0{\cdot}2)\ 3{\cdot}0$ and the above 3 values of $k\theta'/\epsilon_0$, in the form

$$\frac{1}{\zeta}\frac{\mu H}{\epsilon_0}\frac{\epsilon_0}{k\theta} = \frac{1}{\zeta}\frac{\mu H}{k\theta} = \frac{\mu\sigma_0}{k\theta}\frac{1}{\chi},$$

which gives the classical curve as the straight line $(\mu\sigma_0/k\theta)\ 1/\chi = T/\theta - 1$. The final results are given in Table I. and fig. 1.

Fig. 1 also includes the values calculated by Stoner (1938 a) for parabolic bands with $k\theta'/\epsilon_0 = 2^{-1/3}$. The most marked difference between the results for $\zeta$ calculated for rectangular and for parabolic bands is that for the former the $\zeta$, $T/\theta$ curves move downwards as $k\theta'/\epsilon_0$ decreases. For the latter (*cf.* Stoner 1938 a, fig. 5) the curves giving $\zeta/\zeta_0$ move downwards as

$k\theta'/\epsilon_0$ decreases to the lower limiting value ($2^{-1/3}$) for $\zeta_0=1$, but they actually move very slightly upwards as $k\theta'/\epsilon_0$ decreases further to the lower critical value $\frac{2}{3}$, mainly as a result of the simultaneous decrease of $\zeta_0$.

The susceptibility curves, on the other hand, have similar characteristics for both types of band form. The reduced curves move downwards as $k\theta/\epsilon_0$ decreases, coinciding with the $T/\theta$ axis as $k\theta/\epsilon_0 \to 0$ (*cf.* also Wohlfarth 1949 a, fig. 9).

TABLE I. Spontaneous magnetization and susceptibility.

| $k\theta'/\epsilon_0$ | 1·01 | 1·04 | 1·10 | $\infty$ |
|---|---|---|---|---|
| $k\theta/\epsilon_0$ | 0·2167 | 0·3069 | 0·4170 | $\infty$ |
| $T/\theta$ | | Relative magnetization. | | |
| 0·0 | 1·0000 | 1·0000 | 1·0000 | 1·0000 |
| 0·1 | 0·9889 | 0·9976 | 0·9996 | 1·0000 |
| 0·2 | 0·9553 | 0·9799 | 0·9919 | 0·9999 |
| 0·3 | 0·9083 | 0·9468 | 0·9702 | 0·9974 |
| 0·4 | 0·8505 | 0·9003 | 0·9341 | 0·9856 |
| 0·5 | 0·7826 | 0·8410 | 0·8834 | 0·9575 |
| 0·6 | 0·7041 | 0·7679 | 0·8161 | 0·9073 |
| 0·7 | 0·6122 | 0·6780 | 0·7286 | 0·8286 |
| 0·8 | 0·5015 | 0·5638 | 0·6123 | 0·7104 |
| 0·9 | 0·3556 | 0·4058 | 0·4448 | 0·5254 |
| 0·95 | 0·2517 | 0·2897 | 0·3189 | 0·3795 |
| 1·0 | 0·0000 | 0·0000 | 0·0000 | 0·0000 |
| | | Reduced inverse susceptibility. | | |
| 1·2 | 0·0546 | 0·1006 | 0·1363 | 0·2000 |
| 1·4 | 0·1312 | 0·2219 | 0·2879 | 0·4000 |
| 1·6 | 0·2271 | 0·3587 | 0·4501 | 0·6000 |
| 1·8 | 0·3388 | 0·5071 | 0·6199 | 0·8000 |
| 2·0 | 0·4638 | 0·6646 | 0·7952 | 1·0000 |
| 2·2 | 0·5995 | 0·8287 | 0·9748 | 1·2000 |
| 2·4 | 0·7439 | 0·9983 | 1·1577 | 1·4000 |
| 2·6 | 0·8955 | 1·1560 | 1·3429 | 1·6000 |
| 2·8 | 1·0533 | 1·3496 | 1·5303 | 1·8000 |
| 3·0 | 1·2157 | 1·5299 | 1·7193 | 2·0000 |

$T/\theta$, reduced temperature. For $T/\theta<1$ the figures give $\zeta$, the relative magnetization. For $T/\theta>1$ they give $(\mu\sigma_0/k\theta)(1/\chi)$, the reduced inverse mass susceptibility. The $\zeta$ values for $k\theta/\epsilon_0=\infty$ are taken from Stoner (1938 a, Table I.); the susceptibility values in this limit are given by

$$(\mu\sigma_0/k\theta)(1/\chi)=T/\theta-1.$$

## §3. THERMAL PROPERTIES.

*Fundamental relations.* With the basic assumptions as in §2 and Stoner's nomenclature (1939) the expressions for the reduced electronic and "molecular field" energies in the absence of an external field become

$$\frac{E_E}{N\epsilon_0}=\frac{1}{2}\left(\frac{kT}{\epsilon_0}\right)^2\{F_1(\eta+\beta)+F_1(\eta-\beta)\}, \quad \ldots \quad (3.1)$$

$$\frac{E_M}{N\epsilon_0}=-\frac{1}{2}\frac{k\theta'}{\epsilon_0}\zeta^2, \quad \ldots \quad (3.2)$$

Fig 1

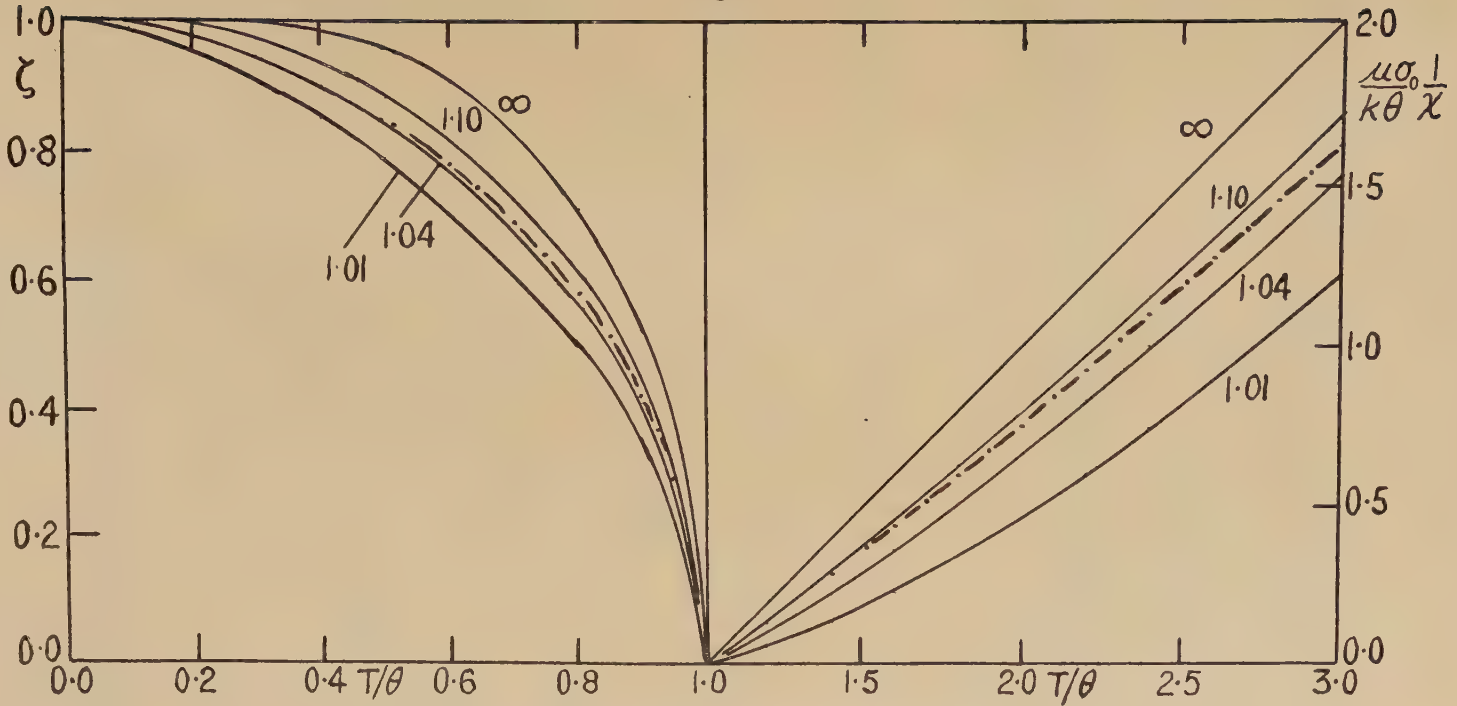

Spontaneous magnetization and susceptibility.

ζ, relative magnetization; $(\mu\sigma_0/k\theta)(1/\chi)$, reduced inverse susceptibility; T/θ, reduced temperature. Values of $k\theta'/\epsilon_0$ as shown. The broken curves are for parabolic bands with $k\theta'/\epsilon_0=2^{-1/3}$ (Stoner 1938a, fig. 5). The curves marked ∞ are given by the classical relations.

and the total internal energy is given by the sum $E = E_E + E_M$. Here

$$F_1(\eta) = \int_0^\infty x\,dx/[\exp(x-\eta)+1],$$

the Fermi–Dirac function of order 1 (Rhodes 1950), and $\eta$ and $\beta$ were defined in §2. The reduced specific heat, $C/Nk$, may be calculated, with Stoner, as the sum of three contributory terms

$$\begin{aligned} C_1/Nk &= \{\partial(E_E/N\epsilon_0)/\partial\tau\}_\zeta, \\ C_2/Nk &= \{\partial(E_E/N\epsilon_0)/\partial\zeta\}_\tau\, d\zeta/d\tau, \\ C_M/Nk &= \{d(E_M/N\epsilon_0)/d\zeta\}\, d\zeta/d\tau, \end{aligned}$$

where $\tau = kT/\epsilon_0$. These may be calculated directly from (3.1) and (3.2) if use is made of the following auxiliary relations, derived from (2.3), (2.4) and the general relation $F'_s(\eta) = sF_{s-1}(\eta)$ (Rhodes 1950),

$$\frac{dF_1(\eta\pm\beta)}{d(\eta\pm\beta)} = F_0(\eta\pm\beta) = \ln[1+\exp(\eta\pm\beta)] = (1\pm\zeta)/\tau. \quad . \quad (3.3)$$

It is found that

$$\left.\begin{aligned} \frac{C_1}{Nk} &= \frac{2}{\tau}\frac{E_E}{N\epsilon_0} - \frac{1}{2\tau}\{(1+\zeta)^2X_+ + (1-\zeta)^2X_-\}, \\ \frac{C_2}{Nk} &= \tfrac{1}{2}\{(1+\zeta)X_+ - (1-\zeta)X_-\}\frac{d\zeta}{d\tau}, \\ \frac{C_M}{Nk} &= -\frac{k\theta'}{\epsilon_0}\zeta\frac{d\zeta}{d\tau}, \\ \text{where} \quad X_\pm &= \{1-\exp[-(1\pm\zeta)/\tau]\}^{-1}. \end{aligned}\right\} \quad . \quad . \quad . \quad (3.4)$$

The functions $X_\pm$ may be expressed in more convenient form using (2.5) and (2.7), giving

$$X_\pm = \frac{\sinh n\zeta/\tau}{\sinh \zeta/\tau}\exp[\mp(n-1)\zeta/\tau], \quad . \quad . \quad . \quad . \quad (3.5)$$

where $n = k\theta'/\epsilon_0$. The relations for the contributory specific heat terms then become

$$\left.\begin{aligned} \frac{C_1}{Nk} &= \frac{1}{\tau}\left[\frac{2E_E}{N\epsilon_0} - \frac{\sinh n\zeta/\tau}{\sinh\zeta/\tau}\{(1+\zeta^2)\cosh(n-1)\zeta/\tau - 2\zeta\sinh(n-1)\zeta/\tau\}\right], \\ \frac{C_2}{Nk} &= \{\zeta\cosh(n-1)\zeta/\tau - \sinh(n-1)\zeta/\tau\}\frac{\sinh n\zeta/\tau}{\sinh\zeta/\tau}\frac{d\zeta}{d\tau}, \\ \frac{C_M}{Nk} &= -n\zeta\frac{d\zeta}{d\tau}. \end{aligned}\right\} \quad . \quad . \quad . \quad (3.6)$$

The value of $\eta$, required for the evaluation of $E_E/N\epsilon_0$ and $C_1/Nk$, may be calculated from the relation, derived from (3.3) and (3.5),

$$\eta = \frac{1}{\tau} - \ln\frac{\sinh n\zeta/\tau}{\sinh\zeta/\tau}, \quad . \quad . \quad . \quad . \quad . \quad . \quad (3.7)$$

and the temperature derivative $d\zeta/d\tau$ from (2.7), giving

$$\frac{d\zeta}{d\tau}=\frac{\zeta}{\tau}+\frac{1}{\tau}\left\{(n-1)\coth\frac{(n-1)\zeta}{\tau}-n\coth\frac{n\zeta}{\tau}\right\}^{-1}. \quad . \quad . \quad (3.8)$$

*Energy and specific heat characteristics. Limiting values.* Relations giving the internal energy and specific heat at low temperatures and at the Curie point as functions of the specifying parameter $k\theta/\epsilon_0$ are useful in briefly summarizing the thermal properties of a wide range of ferromagnetics. The relations may be used immediately in an analysis of experimental results (§ 4). With Stoner (1939) calculations are made of the internal energy change between absolute zero and the Curie point and the specific heat at low temperatures and just below and just above the Curie point. The relations are obtainable in algebraical form by direct manipulation of the expressions derived above. In the derivation use is made of the limiting relations for $F_1(\eta)$, viz.

$$F_1(\eta)=\tfrac{1}{2}\eta^2+\tfrac{1}{6}\pi^2-O(e^{-\eta}), \quad \eta\rightarrow\infty,$$
$$F_1(\eta)=e^{\eta}-O(e^{2\eta}), \quad \eta\rightarrow-\infty .$$

(i.) *Internal energy change between* 0°K *and the Curie point.*

It follows from (3.1), (3.2) and (3.7) that

$$\frac{E_\theta-E_0}{Nk\theta}=\frac{k\theta}{\epsilon_0}F_1\left(\frac{\epsilon_0}{k\theta}-\ln\frac{k\theta'}{\epsilon_0}\right)-\frac{\epsilon_0}{k\theta}\left(1-\frac{1}{2}\frac{k\theta'}{\epsilon_0}\right). \quad . \quad . \quad . \quad (3.9)$$

(ii.) *Specific heat in the limit* $kT/\epsilon_0\rightarrow 0$.

In this limit $C_2$ and $C_M$ tend to zero since $d\zeta/d\tau\rightarrow 0$ (*cf.* (2.10)), so that $C=C_1$. Also from (2.10), (3.3) and (3.7)

$$\eta+\beta=\frac{2}{\tau}, \quad \eta-\beta=-\frac{2}{\tau}\left(\frac{k\theta'}{\epsilon_0}-1\right),$$

where $\tau=kT/\epsilon_0$. Hence from (3.1)

$$\frac{E_E}{N\epsilon_0}=1+\tfrac{1}{12}\pi^2\tau^2,$$

so that

$$\frac{C}{Nk}=\tfrac{1}{6}\pi^2\tau,$$

*i. e.*

$$\left(\frac{C/Nk}{T/\theta}\right)_{T/\theta\rightarrow 0}=\tfrac{1}{6}\pi^2\frac{k\theta}{\epsilon_0}. \quad . \quad . \quad . \quad . \quad . \quad . \quad . \quad (3.10)$$

(iii.) *Specific heat just below Curie point.*

The three contributory terms become from (2.11), (3.1), (3.6) and ((3.7)

$$\left.\begin{aligned}\left(\frac{C_1}{Nk}\right)_{\theta\to 0}&=2\left(\frac{k\theta}{\epsilon_0}\right)F_1\left(\frac{\epsilon_0}{k\theta}-\ln\frac{k\theta'}{\epsilon_0}\right)-\frac{\theta'}{\theta},\\ \left(\frac{C_2}{Nk}\right)_{\theta\to 0}&=3\frac{\theta'}{\theta}\,\frac{k\theta'/\epsilon_0-1}{2k\theta'/\epsilon_0-1}-3\,\frac{k\theta'/\epsilon_0}{2k\theta'/\epsilon_0-1},\\ \left(\frac{C_M}{Nk}\right)_{\theta\to 0}&=3\,\frac{k\theta'/\epsilon_0}{2k\theta'/\epsilon_0-1}.\end{aligned}\right\} \quad . \quad . \quad . \quad (3.11)$$

(iv.) *Specific heat just above Curie point. Specific heat discontinuity.* It is easily seen that $(\mathrm{C}/\mathrm{N}k)_{\theta+0}=(\mathrm{C}_1/\mathrm{N}k)_{\theta-0}$, given in (3.11), and hence the specific heat discontinuity at the Curie point becomes

$$\Delta\mathrm{C}/\mathrm{N}k=(\mathrm{C}/\mathrm{N}k)_{\theta-0}-(\mathrm{C}/\mathrm{N}k)_{\theta+0}=\frac{3\theta'}{\theta}\,\frac{k\theta'/\epsilon_0-1}{2k\theta'/\epsilon_0-1}. \quad . \quad . \quad (3.12)$$

(v.) *Temperature variation of specific heat of paramagnetics.*

An immediate application of the relation for $(\mathrm{C}_1/\mathrm{N}k)_{\theta-0}$ in (3.11) is to the calculation of the electronic specific heat of paramagnetics. This may be derived from (3.11) by replacing $k\theta/\epsilon_0$ by $\tau=k\mathrm{T}/\epsilon_0$ and consequently $k\theta'/\epsilon_0$ by $\{1-\exp(-1/\tau)\}^{-1}$ (*cf.* (2.8)). The resulting expression is

$$\left(\frac{\mathrm{C}}{\mathrm{N}k}\right)_p=2\tau\mathrm{F}_1\,\{\ln[\exp(1/\tau)-1]\}-\{\tau[1-\exp(-1/\tau)]\}^{-1}. \quad . \quad (3.13)$$

An alternative derivation of (3.13) is by direct differentiation of the expression for the internal energy of paramagnetics

$$\left(\frac{\mathrm{E}}{\mathrm{N}\epsilon_0}\right)_p=\tau^2\mathrm{F}_1\,\{\ln[\exp(1/\tau)-1]\},$$

which may be derived from (3.1) and (3.3) by putting $\beta=0$.

Relation (3.13) shows that in the limit $\tau\rightarrow 0$

$$\left(\frac{\mathrm{C}}{\mathrm{N}k}\right)_p=\tfrac{1}{3}\pi^2\tau, \quad . \quad . \quad . \quad . \quad . \quad . \quad . \quad . \quad (3.14)$$

twice as large as the low temperature specific heat of ferromagnetics (*cf.* (3.10)). This change arises from the fact that in a paramagnetic the states near the top of the Fermi distribution are doubly occupied at low temperatures, while in a ferromagnetic, with saturation always complete in the case of rectangular bands, they are singly occupied. For parabolic bands saturation may not be complete at 0°K. if $k\theta'/\epsilon_0$ is small enough and the corresponding increase of specific heat as $k\theta'/\epsilon_0$ decreases is more gradual (*cf.* Stoner 1939, relation (3.15); also Appendix).

(vi.) *The limit* $k\theta/\epsilon_0\rightarrow\infty$.

The expression for internal energy in this limit may be derived from (3.1), (3.2) and (3.3), giving

so that

$$\left.\begin{aligned}\mathrm{E}/\mathrm{N}&=k\mathrm{T}-\tfrac{1}{2}k\theta\zeta^2,\\ \mathrm{C}/\mathrm{N}k&=1-\tfrac{1}{2}d\zeta^2/d(\mathrm{T}/\theta),\end{aligned}\right\} \quad . \quad . \quad . \quad . \quad . \quad . \quad (3.15)$$

since here $\theta'\rightarrow\theta$. Relations (3.15) for rectangular bands may be compared with the corresponding limiting relations for parabolic bands (Stoner 1939, relations (3.1), (3.2))

$$\left.\begin{aligned}\mathrm{E}/\mathrm{N}&=\tfrac{3}{2}k\mathrm{T}-\tfrac{1}{2}k\theta\zeta^2,\\ \mathrm{C}/\mathrm{N}k&=\tfrac{3}{2}-\tfrac{1}{2}d\zeta^2/d(\mathrm{T}/\theta).\end{aligned}\right\}$$

The second term in the expression for C/N$k$, the classical "magnetic" specific heat, is the same for both types of band form. The first term, however, the electronic specific heat, is different in the two cases. This dependence on band form also appears in the limiting values of the various energy and specific heat characteristics derived above. For rectangular bands, in the limit $k\theta/\epsilon_0 \rightarrow \infty$,

$$(E_\theta - E_0)/Nk\theta = 1{\cdot}5, \quad (C_1/Nk)_{\theta-0} = (C/Nk)_{\theta+0} = (C/Nk)_p = 1,$$
$$(C_2/Nk)_{\theta-0} = 0, \quad (C_M/Nk)_{\theta-0} = 1{\cdot}5, \quad (C/Nk)_{\theta-0} = 2{\cdot}5, \quad (\Delta C/Nk) = 1{\cdot}5;$$

the corresponding limiting values for parabolic bands are 2, 1·5, 0, 1·5, 3, 1·5. A similar dependence on band form is immediately apparent in the respective expressions for the electronic specific heat at low temperatures (*cf.* (3.10), (3.14) and Stoner 1939, relation (4.15); also Appendix).

Fig. 2.

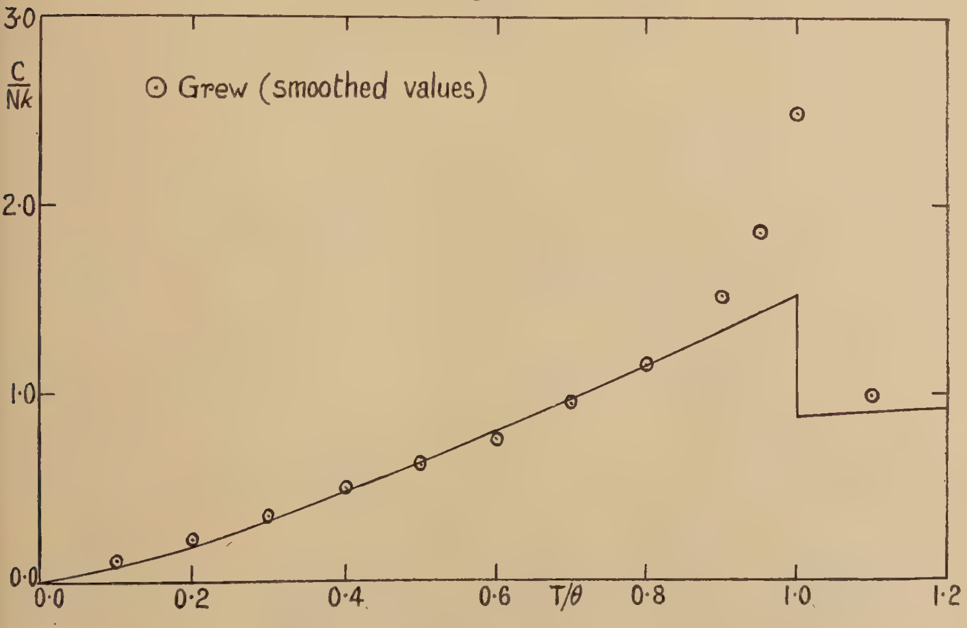

Temperature variation of specific heat.

C/N$k$, reduced specific heat, T/$\theta$, reduced temperature. Calculated values are for $k\theta'/\epsilon_0 = 1{\cdot}10$. Experimental values are for nickel, due to Grew (1934; *cf.* also Stoner 1936, and § 4).

*Computations.* The internal energy and specific heat expressions derived above were evaluated numerically for $T/\theta = 0{\cdot}0\ (0{\cdot}1)\ 0{\cdot}9\ (0{\cdot}05)\ 1{\cdot}0$ and for $k\theta'/\epsilon_0 = 1{\cdot}10$, using the corresponding values of $\zeta$ given in Table I. The particular value of $k\theta'/\epsilon_0$ chosen is indicated by the susceptibility results to be close to the actual value for nickel (*cf.* § 4). The calculated variation of C/N$k$ with T/$\theta$ is shown in fig. 2, together with experimental values for nickel discussed in § 4.

The curve may be compared with Stoner's (1939, fig. 2), from which it differs only slightly in shape. Watanabe (1948) also gives a calculated specific heat curve for nickel, using a value of $k\theta'/\epsilon_0$ larger than the one of fig. 2 owing to an incorrect analysis of the susceptibility results (*cf.* §4). He gives, moreover, no indication in his paper that values of $\zeta$ as dependent on $T/\theta$, which are clearly necessary, have been calculated. Watanabe's final curve, however obtained, agrees quite closely in shape with Stoner's and the present curve.

Fig. 3.

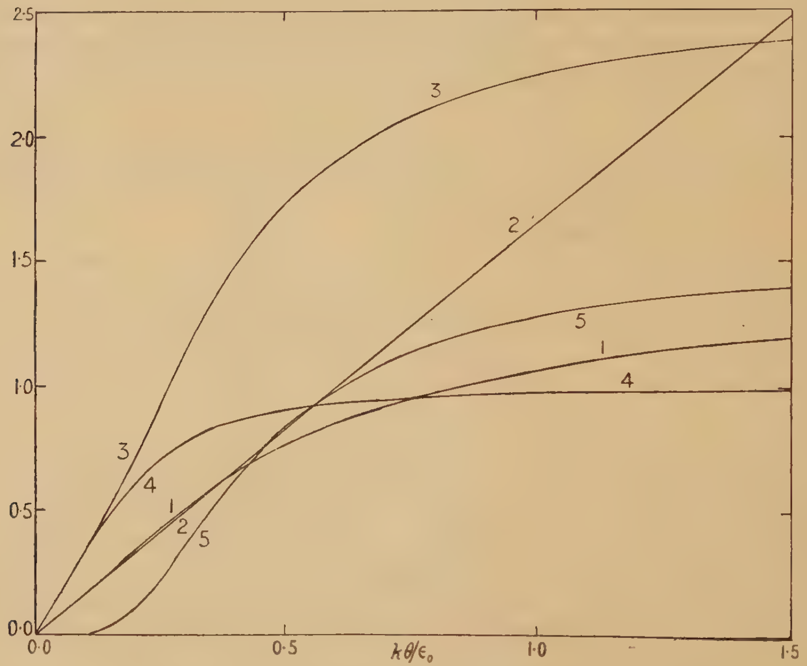

Energy and specific heat characteristics.

1, $(E_\theta-E_0)/Nk\theta$, reduced internal energy change between absolute zero and the Curie point, $\theta$; 2, $\{(C/Nk)/(T/\theta)\}_{T/\theta\to 0}$, ratio of reduced specific heat to reduced temperature in the limit $T/\theta\to 0$; 3, $(C/Nk)_{\theta-0}$, reduced specific heat just below the Curie point; 4, $(C/Nk)_{\theta+0}$, reduced specific heat just above the Curie point; 5, $\Delta C/Nk$, reduced specific heat discontinuity at the Curie point. For limiting values as $k\theta/\epsilon_0\to\infty$, see text.

Computations have also been made of the various energy and specific heat characteristics given by the relations (3.9), (3.10), (3.11), (3.12) which were evaluated numerically for $k\theta/\epsilon_0=0{\cdot}0\ (0{\cdot}05)\ 0{\cdot}5\ (0{\cdot}1)\ 1{\cdot}5$. The results are shown in fig. 3.

The curves may be compared with those derived by Stoner (1939, figs. 3, 4 and 5) for parabolic bands. The most marked differences appear in the limiting values as $k\theta/\epsilon_0\to\infty$, already noted, and in the low temperature specific heat curve (*l.c.* fig. 5, curve 2).

## §4. DISCUSSION OF SOME EXPERIMENTAL RESULTS.

In previous papers (for summaries see Stoner 1948, 1951) results of experimental investigations into the magnetic and thermal behaviour of ferromagnetic metals and alloys were fully discussed on the basis of the collective electron treatment with the assumption of a particular, parabolic, band form. In this section it will suffice, therefore, to consider very briefly certain of the experimental data in the light of the theoretical results obtained above with the assumption of a rectangular band form. As before, it is mainly nickel and its alloys which are to be considered.

(i.) *Susceptibility above the Curie point.* It has been shown (Wohlfarth 1949 a) that for nickel the experimental reduced susceptibility curve lies very close to the curve of fig. 1 for a parabolic band with $k\theta'/\epsilon_0=2^{-1/3}$ if this is corrected for band overlap effects. Inspection of fig. 1 thus indicates that with rectangular bands the appropriate value of $k\theta'/\epsilon_0$ for nickel is about 1·10, and hence from (2.8) $k\theta/\epsilon_0 \doteqdot 0{\cdot}42$. For iron and cobalt the analysis is, for several reasons, less conclusive, but Stoner's discussion (1938 b) shows that the reduced susceptibility curves for these metals lie very close to that for nickel. Although it is questionable whether for these two metals the assumption of either a parabolic or a rectangular band form over the whole of the relevant energy range is justified, an estimate for $k\theta/\epsilon_0$ of about 0·4 may be accepted provisionally for all three metals. It may be noted, incidentally, that the value of $k\theta/\epsilon_0$ corresponding to $k\theta'/\epsilon_0=2^{-1/3}$ for parabolic bands is also close to 0·4. Watanabe (1948), on the other hand, gives the following as estimates for iron, cobalt and nickel respectively: $k\theta/\epsilon_0=0{\cdot}45,\ 0{\cdot}37,\ 0{\cdot}50$, basing his estimates on a Curie-Weiss representation of the susceptibility results. With $k\theta/\epsilon_0=0{\cdot}4$ the values of $\epsilon_0/k$ are 2·6, 3·5 and $1{\cdot}6\times10^3$ °K. for iron, cobalt and nickel respectively, the nickel value being close to that estimated previously.

The analysis of the susceptibility results given previously for nickel alloys shows that in general alloying is accompanied by a shift of the reduced $1/\chi$, T curves towards the T axis as the alloying content increases. For both types of band form (*cf.* fig. 1) this decrease indicates primarily a decrease of $k\theta/\epsilon_0$ on alloying, not, as Watanabe believes, an increase in importance of band overlap effects (*cf.* also Wohlfarth 1949 a).

It may be concluded that the analysis of the susceptibility results is essentially similar for both types of band form.

(ii.) *Spontaneous magnetization.* It has already been shown (Wohlfarth 1949 b) that the experimental curve relating $\sigma/\sigma_0$ and $T/\theta$ for nickel lies considerably above that calculated for parabolic bands (with $k\theta'/\epsilon_0=2^{-1/3}$, as given by the susceptibility results). The observed curve lies in fact, very close to the classical curve ($k\theta'/\epsilon_0\rightarrow\infty$). Inspection of fig. 1 shows a similar discrepancy although slightly less serious, between the observed curve (close to the classical curve) and that calculated for a rectangular band (with $k\theta'/\epsilon_0=1{\cdot}10$). The main reason for the discrepancy is believed to be the temperature variation of the effective $\theta'$ below the Curie point, owing to the fundamental relation (2.2) being an oversimplified representation of the interchange interaction energy. This effect, called for brevity the " $\theta'$ effect " below, is apparently of greater importance in determining the shape of magnetization, temperature curves than is the band form.

Only two complete sets of curves for ferromagnetic alloys are available, for Ni–Cu and Ni–Co. These have been analyzed by Wohlfarth (1949 c). For Ni–Co the reduced curves were shown to coincide over the whole concentration range (*l.c.* fig. 6), in agreement with the coincidence of the reduced susceptibility curves (*l.c.* fig. 3). For Ni–Cu the reduced experimental magnetization curves shift towards the temperature axis as the copper concentration increases (*l.c.* fig. 7). For parabolic bands, as already noted, the reduced theoretical curves for different $\zeta_0$ values coincide very nearly if $k\theta'/\epsilon_0 \leqslant 2^{-1/3}$. The interpretation of the observed shift for Ni–Cu was here based on the decrease of $\zeta_0$ with increasing copper concentration and the consequent increasing accuracy of (2.2) in representing the interchange interaction energy. For rectangular bands the theoretical curves themselves shift as $k\theta'/\epsilon_0$ decreases (*cf.* fig. 1), but $\zeta_0$ remains equal to unity. The interpretation of the experimental shift is thus more straightforward, but it is perhaps easy to see that fundamentally it is similar to that already put forward for parabolic bands.

(iii.) *Energy and specific heat characteristics.* The values of the five characteristics given in fig. 3, with $k\theta/\epsilon_0=0{\cdot}42$, the estimated value for nickel, Stoner's values for parabolic bands ($k\theta'/\epsilon_0=2^{-1/3}$) and experimental values for nickel due to Grew (1934) and Keesom and Clark (1935), analysed by Stoner (1936), are shown in Table II.

TABLE II. Calculated and observed energy and specific heat characteristics for nickel. For symbolism see caption to fig. 3.

| | $\frac{\mathrm{E}_\theta-\mathrm{E}_0}{\mathrm{N}k\theta}$ | $\left(\frac{\mathrm{C/N}k}{\mathrm{T}/\theta}\right)_{\mathrm{T}/\theta\to0}$ | $\left(\frac{\mathrm{C}}{\mathrm{N}k}\right)_{\theta-0}$ | $\left(\frac{\mathrm{C}}{\mathrm{N}k}\right)_{\theta+0}$ | $\frac{\Delta\mathrm{C}}{\mathrm{N}k}$ |
|---|---|---|---|---|---|
| Rectangular band ($k\theta/\epsilon_0=0{\cdot}42$) | 0·67 | 0·69 | 1·52 | 0·87 | 0·65 |
| Parabolic band ($k\theta'/\epsilon_0=2^{-1/3}$) | 0·86 | 1·26 | 1·76 | 1·19 | 0·57 |
| Experimental (nickel) | 0·8 | 0·91 | 2·5 | 1·0 | 1·5 |

It is seen (*a*) that the theoretical values, for the two types of band form, for $(\mathrm{E}_\theta-\mathrm{E}_0)/\mathrm{N}k\theta$ and $(\mathrm{C/N}k)_{\theta+0}$ agree quite closely with each other and bracket the experimental value in either case, (*b*) that the theoretical values for $\{(\mathrm{C/N}k)/(\mathrm{T}/\theta)\}_{\mathrm{T}/\theta\to0}$ differ by nearly 100 per cent but that they again bracket the experimental value, (*c*) that the theoretical values for $(\mathrm{C/N}k)_{\theta-0}$ and $\Delta\mathrm{C/N}k$ are quite close to each other, but are considerably smaller than the observed values. The discrepancies in (*c*) are doubtless due to the " $\theta'$ effect " mentioned above, which brings about discrepancies between observed and calculated magnetization, temperature curves. The effect of assuming a particular band form is shown in Table II. to be important only in the case of low temperature specific heat. Here, as in (*a*), the experimental results for nickel seem to show that close agreement between theory and observation should be obtainable if the assumed band form is intermediate between parabolic and rectangular form, bearing out the conclusion of Fletcher and Wohlfarth's calculation for the metal (1951). It may be noted, on the other hand, that the values of $\{(C/Nk)/(T/\theta)\}_{T/\theta\to 0}$ for cobalt and iron are much smaller than that for nickel, 0·49 and 0·28 respectively, so that these metals must have a much more complicated band form than that considered satisfactory for nickel.

(iv.) *Temperature variation of specific heat.* Grew's results for nickel (1934; *cf.* Stoner 1936) are shown in fig. 2 together with calculated values for a rectangular band form ($k\theta'/\epsilon_0=1{\cdot}10$). It is seen that the agreement between the two curves is very close up to $T/\theta=0{\cdot}8$, but that for $0{\cdot}8<T/\theta<1$ the observed values lie markedly above the theoretical curve. The disagreement close to the Curie point is, as already stated, believed to be due to the "$\theta'$ effect". Although this has been shown to introduce discrepancies between observed and calculated magnetization, temperature curves over the whole $T/\theta$ range, the magnetization and its temperature derivative enter in the expressions for specific heat in such a complicated way (*cf.* relations (3.6)) that here the discrepancies seem to cancel over most of the lower temperature range.

(v.) *Magneto-caloric effect.* As stated by Stoner (1951) calculations on the magneto-caloric effect on the basis of the collective electron treatment are now in progress at Leeds. It will suffice, therefore, to indicate by an example how such calculations could be carried out in a particularly simple way for a rectangular energy band. The example chosen concerns the magneto-caloric effect in the temperature range below the Curie point where the applied field is negligible compared with the "molecular field". The relevant experimental results for nickel have been considered by Stoner (1936).

If classical statistics were applicable the effective molecular field coefficient, $\nu$, could be derived immediately from the observed adiabatic change of temperature with magnetization, since in negligible fields ($H\ll\nu I$)

$$\nu=-\frac{1}{I}\left(\frac{\partial E}{\partial I}\right)_T=\frac{\rho C_I}{I}\left(\frac{\partial T}{\partial I}\right)_S, \quad . \quad . \quad . \quad . \quad . \quad . \quad (4.1)$$

where $C_I$ is the specific heat at constant magnetization I and $\rho$ the density. The classical relation for internal energy, E, is just that derived above (relation (3.15)), giving the well known relation between $\nu$ and the Curie temperature $\theta$,

$$\nu=\frac{Nk\theta}{I_0^2}, \quad . \quad . \quad . \quad . \quad . \quad . \quad . \quad . \quad . \quad (4.2)$$

where $\zeta=I/I_0$. With Fermi–Dirac statistics applicable, however, the correct relation for internal energy is $E=E_E+E_M$, given by (3.1) and (3.2).

Hence the *apparent* molecular field coefficient, derivable from the magnetocaloric data, becomes

$$\nu'=\frac{\mathrm{N}k\theta'}{\mathrm{I}_0^2}-\frac{1}{\mathrm{I}_0^2}\frac{1}{\zeta}\left(\frac{\partial \mathrm{E}_\mathrm{E}}{\partial \zeta}\right)_\mathrm{T}.$$

The second term is closely related to the specific heat term $C_2$ given in (3.6) and it is readily found that

$$\left.\begin{aligned}\nu'&=\frac{\mathrm{N}k\theta'}{\mathrm{I}_0^2}\phi(\mathrm{T}/\theta,\, k\theta'/\epsilon_0),\\ \text{where}\quad \phi&=1-\{\zeta\cosh(n-1)\zeta/\tau-\sinh(n-1)\zeta/\tau\}\frac{\sinh n\zeta/\tau}{n\zeta\sinh\zeta/\tau},\end{aligned}\right\}\qquad(4.3)$$

and where $n=k\theta'/\epsilon_0$, $\tau=k\mathrm{T}/\epsilon_0=(k\theta/\epsilon_0)(\mathrm{T}/\theta)$ and $\zeta$ is a function of $k\theta'/\epsilon_0$ and $\mathrm{T}/\theta$ (*cf.* relation (2.5)). It follows from (4.2) and (4.3) that the ratio $r$ of the apparent molecular field coefficient, $\nu'$, to that derived from classical statistics, $\nu$, is given by

$$r=\nu'/\nu=(\theta'/\theta)\phi(\mathrm{T}/\theta,\ k\theta'/\epsilon_0),\qquad . \ . \ . \ . \ . \ . \quad (4.4)$$

a function of temperature. If the approximate value of $k\theta'/\epsilon_0$ for nickel, 1·10, is inserted into (4.3) and (4.4) it is found that $r$ increases very nearly linearly with $\mathrm{T}/\theta$ from

$$r_0=(\theta'/\theta)\phi(0,\ k\theta'/\epsilon_0)=(\epsilon_0/k\theta)(k\theta'/\epsilon_0-1)\qquad =0{\cdot}24\ \text{ to}$$

$$r_1=(\theta'/\theta)\phi(1,\ k\theta'/\epsilon_0)=(\theta'/\theta)(\epsilon_0/k\theta)(k\theta'/\epsilon_0-1)=0{\cdot}63$$

as the temperature increases from 0°K to $\theta$. Stoner's analysis (1936) of the results for nickel indicates a temperature increase of the apparent molecular field coefficient below the Curie point of this order of magnitude, although close to the Curie point $\nu'$ is strongly field dependent (*l.c.* p. 180).

(vi.) *High temperature specific heat of paramagnetics.* Relation (3.13) shows that for rectangular bands the electronic specific heat of paramagnetics tends to the value N$k$ at high temperatures ($k\mathrm{T}/\epsilon_0>1$). The corresponding limiting value for parabolic bands is 1·5N$k$. This dependence on band form has a bearing on the experimental finding that the high temperature electronic specific heat of palladium is considerably smaller than that of nickel above the Curie point. The observed values are about 1 and 2 cal. mol.$^{-1}$ deg.$^{-1}$ respectively, whereas the number of holes per atom, proportional to N, is roughly the same for both metals, about 0·6. This anomaly has been variously mentioned (*e.g.* by Mott 1949), but does not seem to have been interpreted by an explicit consideration of differences in the band form for the two metals. It must be pointed out, however, that other effects, such as the anharmonicity of the lattice vibrations and band overlap effects, make a quantitative discussion of high temperature electronic specific heats of much less direct significance than discussions of thermal and magnetic properties at lower temperatures.

# APPENDIX.

## *Results for a more general band form.*

The discussion of the preceding sections indicates that some of the results of the treatment do not depend very markedly on the band form, parabolic or rectangular, but that others are, in fact, quite sensitive to it. In this Appendix a very brief discussion is given of such results as are easily obtainable for energy bands of more general form.

If the energy dependence of the density of states, $\nu(\epsilon)$, were only available in numerical form, all but a very few results would have to be derived by a long process of numerical integration. It is easily seen, however, that in the limit $k\theta/\epsilon_0 \rightarrow \infty$ the magnetic properties, spontaneous magnetization and susceptibility, are independent of the band form and are given by the relations based on classical statistics. The thermal properties, however, depend on the band form even in the classical limit, as shown in § 3, and it does not seem possible to derive any general results in this case. For a band for which the density of states is given by the simple relation

$$\nu(\epsilon)=a\epsilon^m, \qquad \text{(A.1)}$$

the expressions for internal energy and specific heat in the limit $k\theta/\epsilon_0 \rightarrow \infty$, corresponding to (3.15), are

$$\left.\begin{aligned} \mathrm{E/N}&=(m+1)k\mathrm{T}-\tfrac{1}{2}k\theta\zeta^2, \\ \mathrm{C/N}k&=(m+1)-\tfrac{1}{2}d\zeta^2/d(\mathrm{T}/\theta). \end{aligned}\right\} \qquad \text{(A.2)}$$

In the low temperature limit the internal energy and specific heat are easily calculable for an energy band of general form, such as that which has been obtained for nickel. If $\epsilon_{01}$ and $\epsilon_{02}$ denote the energy widths of the unoccupied states for the two spin directions at 0° K. and $\epsilon_0$ the corresponding width for zero spontaneous magnetization, then

$$\frac{\mathrm{N}}{2}=(1+\zeta_0)^{-1}\int_0^{\epsilon_{01}}\nu(\epsilon)\,d\epsilon=(1-\zeta_0)^{-1}\int_0^{\epsilon_{02}}\nu(\epsilon)\,d\epsilon=\int_0^{\epsilon_0}\nu(\epsilon)\,d\epsilon, \qquad \text{(A.3)}$$

giving $\epsilon_{01}$, $\epsilon_{02}$ as functions of $\zeta_0$, the relative magnetization. The internal energy is therefore an implicit function of $\zeta_0$,

$$\mathrm{E}=\mathrm{E}(\zeta_0)=\int_0^{\epsilon_{01}}\epsilon\nu(\epsilon)\,d\epsilon+\int_0^{\epsilon_{02}}\epsilon\nu(\epsilon)\,d\epsilon-\tfrac{1}{2}\mathrm{N}k\theta'\zeta_0^2, \qquad \text{(A.4)}$$

and the condition for E to be a minimum gives the relation between $\zeta_0$ and $k\theta'/\epsilon_0$, as well as the values of $\epsilon_{01}$ and $\epsilon_{02}$. The low temperature specific heat is then given by

$$\mathrm{C}=\tfrac{1}{3}\pi^2k^2\mathrm{T}\{\nu(\epsilon_{01})+\nu(\epsilon_{02})\}. \qquad \text{(A.5)}$$

If $\nu(\epsilon)$ is given by (A.1) it is easily found that

$$\frac{\mathrm{E}}{\mathrm{N}\epsilon_0}=\frac{1}{2}\left(\frac{m+1}{m+2}\right)\{(1+\zeta_0)^{m+2/m+1}+(1-\zeta_0)^{m+2/m+1}\}-\frac{1}{2}\frac{k\theta'}{\epsilon_0}\zeta_0^2, \quad . \quad \text{(A.6)}$$

and

$$\frac{\mathrm{C}}{\mathrm{N}k}=\frac{m+1}{6}\pi^2\frac{k\mathrm{T}}{\epsilon_0}\{(1+\zeta_0)^{m/m+1}+(1-\zeta_0)^{m/m+1}\}. \quad . \quad . \quad . \quad . \quad . \quad . \quad \text{(A.7)}$$

The relative magnetization at absolute zero is found from (A.6) and is given by

$$\frac{k\theta'}{\epsilon_0}=\frac{1}{2\zeta_0}\{(1+\zeta_0)^{1/m+1}-(1-\zeta_0)^{1/m+1}\}; \quad . \quad . \quad . \quad \text{(A.8)}$$

hence the condition for ferromagnetism is $k\theta'/\epsilon_0>1/(m+1)$ and the range of incomplete saturation at absolute zero $(0<\zeta_0<1)$ is given by

$$\frac{1}{m+1}<\frac{k\theta'}{\epsilon_0}<2^{-m/(m+1)}. \quad . \quad . \quad . \quad . \quad . \quad . \quad . \quad \text{(A.9)}$$

The relations given above for rectangular and parabolic bands may be derived at once by putting $m=0, \frac{1}{2}$.

## REFERENCES.

Fletcher, G. C., and Wohlfarth, E. P., 1951, *Phil. Mag.*, **42,** 106.

Grew, K. E., 1934, *Proc. Roy. Soc.* A, **145,** 509.

Keesom, W. H., and Clark, C. W., 1935, *Physica*, **2,** 513.

Mott, N. F., 1949, *Proc. Phys. Soc.* A, **62,** 416.

Néel, L., 1938, *C.R. Acad. Sci., Paris*, **206,** 1471.

Rhodes, P., 1950, *Proc. Roy. Soc.* A, **204,** 396.

Stoner, E. C., 1936, *Phil. Trans. Roy. Soc.* A, **235,** 165 ; 1938 a, *Proc. Roy. Soc.* A, **165,** 372 ; 1938 b, *Proc. Leeds Phil. Soc.*, **3,** 457 ; 1939, *Proc. Roy. Soc.* A, **169,** 339 ; 1948, *Phys. Soc. Rep. Progr. Phys.*, **11,** 43 ; 1951, *Proc. Grenoble Conference, J. Phys. Radium* (in the press).

Watanabe, H., 1948, *J. Phys. Soc., Japan*, **3,** 12, 317.

Wohlfarth, E. P., 1949 a, *Proc. Roy. Soc.* A, **195,** 434 ; 1949 b, *Phil. Mag.*, **40,** 703 ; 1949 c, *Ibid.*, **40,** 1095.

# XLIV. *The Virial Theorem in Quantum Mechanics.*

By T. L. Cottrell and S. Paterson,
I.C.I. Ltd., Nobel Division, Research Department, Stevenston, Ayrshire†.

[Received January 16, 1951.]

## Summary.

A derivation is given of a form of the virial theorem in quantum mechanics suitable for the discussion of a system of particles in a box.

If T and V are the kinetic and potential energies of a system, and $\mathbf{r}_i$ is the position vector of the $i$th particle, the virial theorem in classical mechanics states that

$$-2\overline{\mathrm{T}}=-\overline{\sum_i \mathbf{r}_i\,.\,\nabla_i \mathrm{V}}, \qquad \text{. . . . . . . (1)}$$

where the bars denote time averages, and the R.H.S. is known as the virial. This result has been used in the discussion of equations of state (*cf.* Jeans 1925). In the discussion of the thermal equation of state derived from quantum dynamical principles, de Boer (1949) has used the virial theorem, a procedure which is only justifiable if it can be shown that it holds in quantum mechanics. In view of the recent controversy concerning quantum mechanical equations of state (*cf.* Green 1949, Uhlenbeck and Riddell 1950) it seemed particularly desirable to examine the validity of this assumption.

de Boer justifies the use of the theorem in quantum mechanics by referring to Slater (1933), who concluded that it is valid if the time averages of classical theory are replaced by quantum mechanical averages. A similar conclusion had been reached by Finkelstein (1928). It appears, however, that these proofs apply only to systems where there are no infinite discontinuities of potential, and are thus not applicable to a system in an enclosure where the potential is infinite at the walls. As it is under just these conditions that the theorem is applied in the discussion of equations of state, a further proof is required. The subject has been touched upon again in more recent publications, though only incidentally, and these contributions will be discussed in relation to our treatment.

After some manipulation of the Schrödinger equation, Slater obtains the result

$$\sum_i -\frac{\hbar^2}{2m_i}\sum_j x_j\left(\psi^*\frac{\partial^3\psi}{\partial x_i^2\partial x_j}-\frac{\partial\psi}{\partial x_j}\frac{\partial^2\psi^*}{\partial x_i^2}\right)+\psi^*\left(\sum_j x_j\frac{\partial V}{\partial x_j}\right)\psi=0, \qquad . \quad (2)$$

---

† Communicated by James Taylor.

where the symbols have their obvious significance. To integrate this, use is made of the identity

$$\sum_j x_j \left(\psi^* \frac{\partial^3\psi}{\partial x_i^2 \partial x_j} - \frac{\partial\psi}{\partial x_j}\,\frac{\partial^2\psi^*}{\partial x_i^2}\right) = -2\psi^* \frac{\partial^2\psi}{\partial x_i^2} + \frac{\partial}{\partial x_i}\left[\psi^{*2}\frac{\partial}{\partial x_i}\,\frac{\sum_j x_j \dfrac{\partial\psi}{\partial x_j}}{\psi^*}\right]. \qquad . \quad . \quad . \quad (3)$$

The second term on the R.H.S. is set equal to zero after integration with respect to $x_i$, because $\psi^{*2}$ is zero at the limits. It may be seen on performing the differentiation inside the brackets, however, that the term

$$\left[-\sum_j x_j \frac{\partial\psi}{\partial x_j}\cdot\frac{\partial\psi^*}{\partial x_i}\right]_{l_1}^{l_2}, \qquad . \quad . \quad . \quad . \quad . \quad . \quad . \quad . \quad (4)$$

where $l_1$ to $l_2$ is the range of integration, remains, and that this is zero only if $\partial\psi^*/\partial x_i$ vanishes. In free space where the range of integration is $-\infty$ to $+\infty$, the derivative of the wave function vanishes at the limits, but this does not happen when we are concerned with a system inside a box. Here $\psi$ is typically a sine function with a non-vanishing derivative at the limits. This term must be concerned with the virial of the external forces acting on the system by virtue of the walls, and we shall now show that, if $a$ is a parameter defining the scale of the box, the neglected term is equal to $a(\partial E/\partial a)$, giving the final result

$$2\overline{T} = -a\frac{\partial E}{\partial a} + \overline{\sum_i \mathbf{r}_i \,.\, \nabla_i V}, \qquad . \quad . \quad . \quad . \quad . \quad . \quad . \quad . \quad (5)$$

which is the form in which the theorem has, in fact, generally been used.

If

$$H = T + V = -\sum_i \frac{\hbar^2}{2m_i}\nabla_i^2 + V(\mathbf{r}_i), \qquad . \quad . \quad . \quad . \quad . \quad . \quad (6)$$

and the wave equation $H\psi = E\psi$ and its complex conjugate hold, it is easy to show, by differentiating with respect to $a$, *keeping* $\mathbf{r}_i$ *constant*, that

$$\frac{\partial E}{\partial a} = -\sum_i \frac{\hbar^2}{2m_i}\int\left(\psi^*\nabla_i^2\frac{\partial\psi}{\partial a} - \frac{\partial\psi}{\partial a}\nabla_i^2\psi^*\right)d\tau. \qquad . \quad . \quad . \quad (7)$$

In the above, as in all following equations, the volume integral is over the volume of the box for each particle. This volume integral may be transformed into a surface integral using Green's theorem, the surface being that corresponding to the volume through which the $\mathbf{r}_i$ integration is carried. This allows one of the terms to be dropped because $\psi^*$ is zero when any position-vector $\mathbf{r}_i$ terminates on the surface $\mathbf{S}_i$. We obtain

$$\frac{\partial E}{\partial a} = \sum_i \frac{\hbar^2}{2m_i}\int\left[\int \frac{\partial\psi}{\partial a}(\nabla_i\psi^*) \,.\, d\mathbf{S}_i\right]d\tau'_i, \qquad . \quad . \quad . \quad . \quad . \quad (8)$$

where $d\tau$ has been replaced by $d\mathbf{r}_i \,.\, d\tau_i'$ in the usual convention.

Similarly, starting with the wave equation and proceeding in the same manner as Slater, we obtain

$$-\psi\psi^*\mathbf{r}_j \,.\, \nabla_j V = \psi^*\mathbf{r}_j \,.\, \nabla_j\left(\sum_i -\frac{\hbar^2}{2m_i}\nabla_i^2\psi\right) - \left(\sum_i -\frac{\hbar^2}{2m_i}\nabla_i^2\psi^*\right)\mathbf{r}_j \,.\, \nabla_j\psi \quad . \quad . \quad . \quad (9)$$

which is equation (2) expressed in vector notation. It can easily be shown by expansion that

$$\sum_j \mathbf{r}_j \,.\, \nabla_j\left(\sum_i -\frac{\hbar^2}{2m_i}\nabla_i^2\psi\right) \equiv \sum_i -\frac{\hbar^2}{2m_i}\nabla_i^2\left(\sum_j \mathbf{r}_j \,.\, \nabla_j\psi\right) - 2\sum_i -\frac{\hbar^2}{2m_i}\nabla_i^2\psi. \quad . \quad . \quad . \quad (10)$$

On substituting in (9) we obtain, after integration throughout the available configuration space,

$$\begin{aligned}
-2\overline{\mathrm{T}} + \overline{\sum_j \mathbf{r}_j \,.\, \nabla_j V} \\
&= -\sum_i -\frac{\hbar^2}{2m_i}\int[\psi^*\nabla_i^2(\sum_j \mathbf{r}_j \,.\, \nabla_j\psi) - (\sum_j \mathbf{r}_j \,.\, \nabla_j\psi)\nabla_i^2\psi^*]\,d\tau \\
&= \sum_i -\frac{\hbar^2}{2m_i}\int[\textstyle\int(\sum_j \mathbf{r}_j \,.\, \nabla_j\psi)\nabla_i\psi^* \,.\, d\mathbf{S}_i]\,d\tau_i'. \quad . \quad . \quad . \quad . \quad . \quad . \quad . \quad . \quad (11)
\end{aligned}$$

If $a$ defines the scale of the box then it may be shown (see Appendix) that $\sum_j \mathbf{r}_j \,.\, \nabla_j\psi = -a(\partial\psi/\partial a)$. Comparing this result with equation (8) we conclude that

$$2\overline{\mathrm{T}} - \overline{\sum_j \mathbf{r}_j \,.\, \nabla_j V} + a\frac{\partial \mathrm{E}}{\partial a} = 0, \quad . \quad . \quad . \quad . \quad . \quad . \quad . \quad (12)$$

which is the form in which the virial theorem is usually used.

Since this work was carried out, it has come to our notice that Price (1950) has derived an expression for the stress tensor at the boundary in a fluid using a similar transformation to a surface integral. By applying Fröhlich's method of boundary perturbations, he obtained a result which can, by combining his equations (25) and (39), be put into the usual form of the virial theorem.

It is true that if the virial in Slater's discussion is regarded as the sum of the virial of the external and internal forces, the result is formally correct, but because of the infinite discontinuity at the walls, the integration of equation (2) throughout infinite space cannot properly be carried out, as has been pointed out by Uhlenbeck and Riddell (1950). These authors attempted to get round this difficulty by considering a smooth though nearly step-like potential at the wall of the box. This does not define the box properly, as pointed out by Green (1950), but it is possible to use Uhlenbeck and Riddell's analytical method together with an infinite potential wall, to give the correct result. Their method, which has also been applied by Zwanzig (1950) in a similar connection, used a device due to Green (1949) to differentiate the Hamiltonian, but as there seems to be some confusion about the Hermitian character of one of the terms involved, and also because this seems to be a more elegant, if less superficially convincing method, we apply it here.

In Cartesian coordinates the Hamiltonian is

$$\mathrm{H}=\mathrm{T}+\mathrm{V}=-\sum_i \frac{\hbar^2}{2m_i}\left(\frac{\partial^2}{\partial x_i^2}+\frac{\partial^2}{\partial y_i^2}+\frac{\partial^2}{\partial z_i^2}\right)+\mathrm{V}(x_1 \ldots . z_n). \quad . \quad . \quad (13)$$

We introduce new variables $\xi_i, \eta_i, \zeta_i$ defined by $x_i=a\xi_i$, $y_i=a\eta_i$, $z_i=a\zeta_i$, and differentiate the Hamiltonian with respect to $a$, *keeping* $\xi, \eta, \zeta$ *constant.* Thus

$$\frac{\partial \mathrm{H}}{\partial a}=\sum_i 2\frac{\hbar^2}{2m_i a^3}\left(\frac{\partial^2}{\partial \xi_i^2}+\frac{\partial^2}{\partial \eta_i^2}+\frac{\partial^2}{\partial \zeta_i^2}\right)+\frac{\partial \mathrm{V}}{\partial a}, \quad . \quad . \quad . \quad . \quad (14)$$

and so

$$a\frac{\partial \mathrm{H}}{\partial a}=-2\mathrm{T}+\sum_i \mathbf{r}_i \,.\, \nabla_i \mathrm{V}, \quad . \quad . \quad . \quad . \quad . \quad . \quad . \quad (15)$$

$$\therefore \quad a\int \psi^* \frac{\partial \mathrm{H}}{\partial a}\psi \, d\tau=-2\overline{\mathrm{T}}+\overline{\sum_i \mathbf{r}_i \,.\, \nabla_i \mathrm{V}}. \quad . \quad . \quad . \quad . \quad (16)$$

By differentiating the Schrödinger equation, and integrating the result, we have

$$\frac{\partial \mathrm{E}}{\partial a}=\int \psi^* \frac{\partial \mathrm{H}}{\partial a}\psi \, d\tau+\int \psi^*(\mathrm{H}-\mathrm{E})\frac{\partial \psi}{\partial a} d\tau. \quad . \quad . \quad . \quad . \quad (17)$$

Since $(\partial\psi/\partial a)_{\xi,\eta,\zeta}=0$ at the wall (see Appendix), the second term on the R.H.S. is Hermitian, and so disappears, giving a result which may be combined with (16) to give the virial theorem (12). Green (1950) has stated that when the potential at the wall is infinite, this term is not Hermitian because $\partial\psi/\partial a$ is not zero at the surface. This seems to be due to a confusion about what is kept constant in the partial differentiations. In the present treatment we are concerned with $(\partial\psi/\partial a)_{\xi,\eta,\zeta}$, which is zero at the wall. $(\partial\psi/\partial a)_{x,y,z}$, on the other hand, which we used in the previous treatment, is finite at the wall.

## APPENDIX.

Let the equation of the box in rectangular Cartesians be

$$\mathrm{S}(\xi, \eta, \zeta)=0, \quad . \quad . \quad . \quad . \quad . \quad . \quad . \quad . \quad . \quad . \quad (18)$$

where $\xi=x/a$, etc. We can also write

$$\psi(x_i, y_i, z_i, a)\equiv \Psi(\xi_i, \eta_i, \zeta_i, a), \text{ say.} \quad . \quad . \quad . \quad . \quad . \quad . \quad . \quad . \quad (19)$$

Then provided $\xi_i, \eta_i, \zeta_i$ satisfy (18) for any single $i$, *i. e.* provided the $i$th particle is on the surface, $\Psi$ is identically zero.

$$\therefore \quad \left(\frac{\partial \Psi}{\partial a}\right)_{\xi, \eta, \zeta} \equiv 0 \qquad \text{when} \qquad \mathrm{S}(\xi_i, \eta_i, \zeta_i)=0. \quad . \quad . \quad (20)$$

But

$$a\frac{\partial \Psi}{\partial a} = \sum_i \left(x_i \frac{\partial \psi}{\partial x_i} + y_i \frac{\partial \psi}{\partial y_i} + z_i \frac{\partial \psi}{\partial z_i}\right) + a\frac{\partial \psi}{\partial a} \equiv \sum_i \mathbf{r}_i \,.\, \nabla_i \psi + a\left(\frac{\partial \psi}{\partial a}\right)_{x, y, z} \quad . \quad . \quad . \quad (21)$$

The R.H.S. of (21) is, therefore, also zero.

## References.

de Boer, J., 1949, *Physica*, **15,** 843.
Finkelstein, B. N., 1928, *Z. f. Physik*, **50,** 293.
Green, H. S., 1949, *Physica*, **15,** 882 ; 1950, *J. Chem. Physics*, **18,** 1123.
Jeans, J. H., 1925, *The Dynamical Theory of Gases*, Cambridge, 4th Edition, Ch. VI.
Price, P. J., 1950, *Phil. Mag.*, **41,** 948.
Slater, J., 1933, *J. Chem. Physics*, **1,** 687.
Uhlenbeck, G. E., and Riddell, R. J., 1950, *J. Chem. Physics*, **18,** 1066.
Zwanzig, R. W., 1950, *J. Chem. Physics*, **18,** 1412.

# XLV. *The Processing of Thick Photographic Emulsions.*

By A. D. Dainton, A. R. Gattiker, and W. O. Lock,
H. H. Wills Physical Laboratory, University of Bristol*.

[Received February 27, 1951.]

[Plate XVII.]

## Summary.

An attempt has been made to determine satisfactory processing conditions for Ilford G5 electron-sensitive emulsions up to 600 $\mu$ in thickness. The penetration and temperature characteristics of metol-hydroquinone, para-aminophenol, and p-diaminophenol developers have been investigated. The observations show that a p-diaminophenol developer gives satisfactory results and a suitable procedure for processing is described. In addition the problems of fixing, washing and drying, have been studied.

## Introduction.

Photographic emulsions have been used as detectors of charged particles ever since Reinganum, in 1911, discovered that an alpha-particle was capable of producing tracks which were observable under a microscope. The early emulsions did not possess great sensitivity; consequently accurate measurements of the properties of nuclear particles could not be made. In 1946, however, Ilford Ltd. in Great Britain produced " Nuclear Research " emulsions containing about eight times the normal amount of silver bromide per unit volume (Powell *et al.* 1946). These emulsions were capable of recording the tracks of particles with a specific ionization of five or more times the minimum value. Their thickness was usually 50–100 $\mu$ and no particular difficulties were encountered during processing. Owing to the high concentration of silver bromide, however, it was found advantageous to agitate the fixing solution and to change it fairly frequently (Powell and Occhialini 1947).

When emulsions of 150 $\mu$ thickness or greater were produced, the application of the processing methods previously employed resulted in a large variation of development with depth. This was found to be due to the fact that the developer took a considerable time to penetrate the emulsion. This difficulty was overcome by Dilworth, Occhialini and Payne (1948) by the method of " temperature development " in which the developer is allowed to penetrate the emulsion at a low temperature, and is subsequently warmed to allow the main development to occur. Details have been given by Wilson and Vaneslow (1949), while the results of an extensive investigation have been published by Dilworth, Occhialini and Vermaesen (1950).

An alternative approach has been suggested by Blau and De Felice (1948). They first soak the emulsion in a developing solution made up without alkali. When permeation is complete the plate is transferred to developer containing excess alkali. This is known as the " two bath " method. For the successful application of this method to thick emulsions, it is necessary that the speed of travel of a pH change through gelatin from the surface should be much greater than the rate of diffusion of the developer as a whole. This condition is not satisfied (Waller 1951). The " temperature development " method has therefore come into general use, and forms the subject of the work to be described in this paper.

---

* Communicated by Professor C. F. Powell, F.R.S.

In 1948 Kodak Ltd. produced an emulsion, 200 $\mu$ in thickness, capable of recording the tracks of particles at minimum ionization (Berriman 1948). Similar emulsions are now manufactured by Ilford Ltd. The production of such emulsions represented an important technical advance and has made possible a considerable extension of the field of research in nuclear physics. The analysis of the tracks of charged particles by a study of their multiple scattering and grain density requires tracks of great length in the emulsion. With the early thin emulsions, the number of tracks of sufficient length was, for simple reasons of geometry, relatively small, and it became desirable to employ emulsions of greater thickness. The first successful steps in this direction were taken by Dilworth *et al.* (1948).

For the successful application of the scattering method, distortion of the emulsion must be reduced to a minimum, for at the present time errors due to this cause commonly determine the maximum energy of a particle of given track length which can be measured, and contribute to the errors of any given measurement. These considerations emphasize the importance of processing emulsions of relatively great thickness with a minimum of distortion.

In this paper we give an account of the processing methods which have been found satisfactory for Ilford G5 emulsions up to 600 $\mu$ in thickness. These methods are not necessarily the best or the only ones available but they may be employed in dealing with large numbers of plates. It must be emphasized that each batch of plates is slightly different from any other, and the optimum processing conditions must be found by trial and error.

## § 1. THE DEVELOPING AGENT.

### *General Considerations.*

Following Dilworth *et al.* (1950) we may specify several conditions which an ideal developer should satisfy. For the " temperature development " method a satisfactory developer should :—

(i.) be capable of penetrating the emulsion reasonably quickly.

(ii.) possess a moderate or high-temperature coefficient.

(iii.) produce negligible background fog and stain in the emulsion.

(iv.) be stable at temperatures up to 30° C.

(v.) have a pH as close as possible to that of the emulsion.

Each of these factors will be considered in turn. The developers chosen for investigation were : D19b (metol-hydroquinone), Azol (para-aminophenol), Amidol (p-diaminophenol) and Amidol-bisulphite. Details of the constitution of the solutions are given in Table I.

### *The Characteristics of the Developers.*

(i.) *Penetration characteristics.*

There has been little published work on the penetration times of various developers in " electron-sensitive " emulsions. Payne (1949) has shown that for thin emulsions the rate of diffusion of any developing agent increases with decreasing pH of the solution ; and that pre-soaking the emulsion in water reduces the developer penetration time by as much as 40 per cent ; see also Dilworth *et al.* (1948).

Table I.

The Developing Solutions Investigated

| Name | D19b | Azol | Normal amidol | Amidol bisulphite |
|---|---|---|---|---|
| Developing agent | Metol-hydroquinone | Para-aminophenol | p-diaminophenol | p-diaminophenol |
| Formula used | Metol 2·2 g.<br>Hydroquinone 8·8 g.<br>Anhydrous sodium sulphite 72·0 g.<br>Sodium carbonate 48·0 g.<br>Potassium bromide 4·0 g.<br>Distilled water to 2000 mls.<br>The above stock solution diluted 1 : 1 with distilled water | Johnson's Azol solution 16 mls.<br>1 per cent potassium bromide 88 mls.<br>Distilled water (add) 384 mls. | Amidol 3·0 g.<br>Anhydrous sodium sulphite 12·0 g.<br>Distilled water (add) 1000 mls. | Amidol 3·0 g.<br>Anhydrous sodium sulphite 6·7 g.<br>Sodium bisulphite liquor (S.G. 1·34)* 1·4 mls.<br>Distilled water (add) 930 mls. |
| pH | 10·0 | 11·5 | 7·2 | 6·7 |

* The sodium bisulphite liquor is a commercial preparation supplied by British Drug Houses Ltd.

The method adopted for the determination of the penetration times of various developers in Ilford G5 emulsions was the following. Plates coated with emulsion of different thicknesses up to 1000 $\mu$ were cut into pieces of dimensions $\frac{3}{4}$ in. × $\frac{3}{4}$ in. The back of each plate was exposed to the image of a characteristic pattern, produced by a photographic enlarger. As the light impinged on the emulsion from the back of the plate, a latent image was produced in the emulsion at the glass-emulsion interface. The exposure time was such that a clearly defined image was produced at the bottom surface of an emulsion 5 μ thick, when developed in the D19b developer at 20° C. for one to two seconds. Even at 5° C. the corresponding period is only about 70 seconds. The same exposure was given to all the emulsions, of various thickness, by means of an accurate photographic timer, the voltage supply to the light source and "timer" being accurately controlled.

To ensure that the photographic latent image was confined to the glass-emulsion interface, the light from the enlarger was passed through a Wratten No. 35 filter before striking the plate. Such a filter transmits red and blue light but not the intermediate wavelengths. The silver halide is sensitive only to the blue light which is strongly absorbed, and the latent image formed is confined to a layer approximately 3 μ thick at the glass-emulsion interface. Thus, no trace of the geometrical pattern appeared on the surface of the emulsion 5 μ thick exposed in this way. The first appearance of the pattern at the bottom of an emulsion is therefore a good indication of the time the developer has taken to penetrate the full thickness of the emulsion in sufficient strength to develop the exposed grains of silver halide. For the purpose of the present experiment, we may define the penetration time as the period the developer takes to penetrate to the bottom of the emulsion and develop the image of the geometric pattern. It may be emphasized that the penetration time so defined is not appreciably affected by the variation with temperature of the time taken to develop the image once the developer is present at a given concentration ; for all temperatures this time is relatively very short.

Details of the emulsion thicknesses used are given in Table II.

TABLE II.

Emulsion Thicknesses Used.

| Nominal Thickness | Actual Thickness |
|---|---|
| 50 μ | 45 μ |
| 100 μ | 105 μ |
| 200 μ | 230 μ |
| 300 μ | 260 μ |
| 400 μ | 400 μ |
| 600 μ | 675 μ |
| 800 μ | 720 μ |
| 1000 μ | 1050 μ |

The measurements were first carried out at 20° C. with the different developing solutions. One complete set of plates was first pre-soaked in distilled water for three hours, whilst a second set was not pre-soaked. The results obtained are given in Table III. and in fig. 1.

Table III.

Penetration Times of the Different Developing Solutions at 20° C., in Pre-soaked and non Pre-soaked Emulsions.

| Developer | Soaking | Penetration Time in Minutes for Different Thicknesses | | | | | | |
|---|---|---|---|---|---|---|---|---|
| | | 105 μ | 230 μ | 260 μ | 400 μ | 675 μ | 720 μ | 1050 μ |
| Azol | Pre-soaked | 4½ | 17 | 22 | 38 | 96 | 96 | 210 |
| | Non Pre-soaked | 6 | 21 | 27 | 50 | 138 | 123 | 330 |
| D19b | Pre-soaked | 3½ | 9½ | 14½ | 21 | 50 | 64 | 140 |
| | Non Pre-soaked | 5 | 12 | 20 | 37 | 110 | 125 | 270 |
| Normal amidol | Pre-soaked | 1½ | 6 | 8½ | 12 | 26 | 26 | 58 |
| | Non Pre-soaked | 3½ | 9½ | 11½ | 22 | 49 | 52 | 120 |
| Amidol bisulphite | Pre-soaked | 2 | 6½ | 8 | 12 | 25 | 25 | 55 |
| | Non Pre-soaked | 2 | 8½ | 10 | 20½ | 53 | 46 | 110 |

All pre-soaked emulsions soaked in distilled water for three hours irrespective of thickness.

Fig. 1.

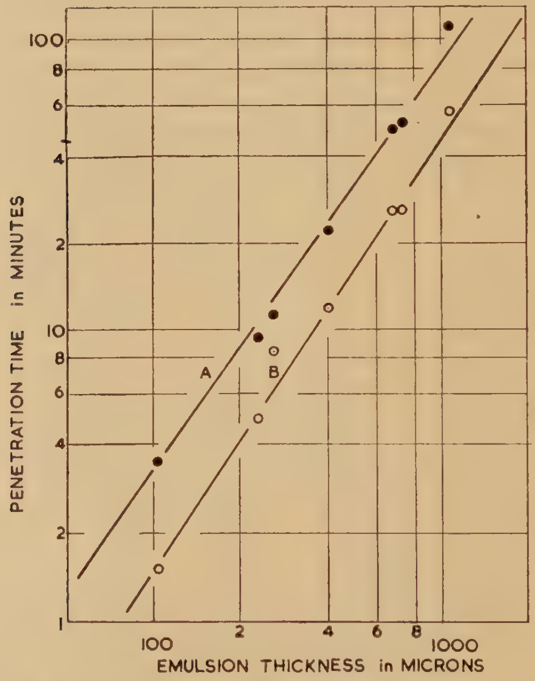

Penetration time of the developer as a function of emulsion thickness for normal amidol at 20° C.; curve A for emulsion without pre-soaking; curve B emulsion pre-soaked in distilled water at 20° C. for three hours.

These show that pre-soaking the emulsion in water considerably reduces the penetration time of the developer. The ratio of average penetration times, without and with pre-soaking, for the various developers is :—

| | |
|---|---|
| Azol | 1·34 ± 0·05 |
| D19b | 1·70 ± 0·13 |
| Normal amidol | 1·86 ± 0·12 |
| Amidol bisulphite | 1·65 ± 0·14 |

It will be seen that the amidol and amidol bisulphite developers are equivalent in penetrating power, and they penetrate the emulsion more rapidly than D19b or Azol.

Fig. 2.

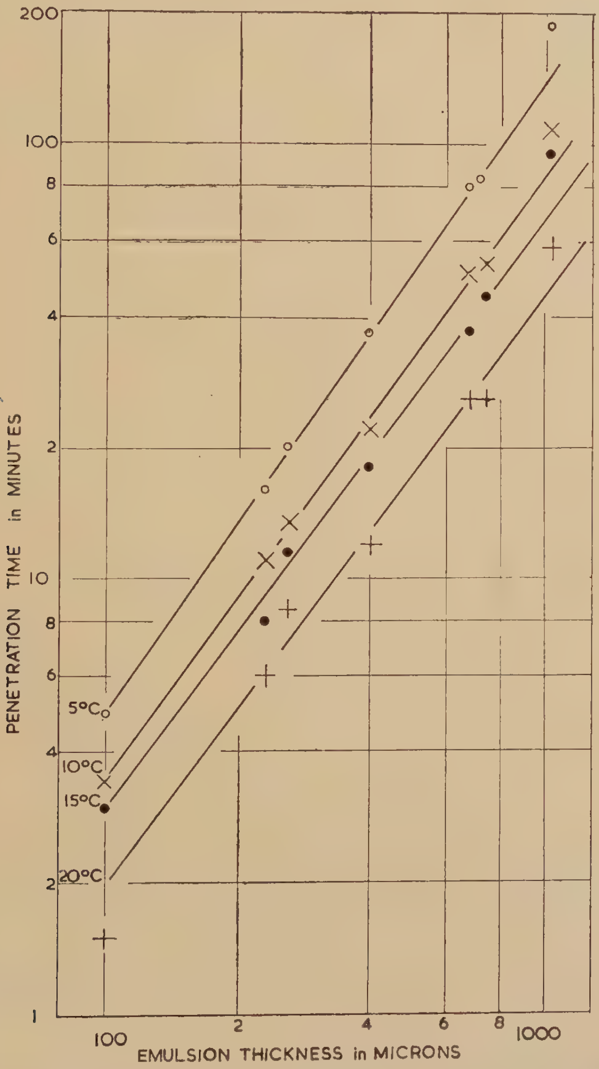

Penetration time of the developer as a function of emulsion thickness for normal amidol at 5° C., 10° C., 15° C., and 20° C. All emulsions pre-soaked in distilled water for three hours at the appropriate temperature.

In view of these results, the penetration measurements at 15° C., 10° C., and 5° C. were carried out, using only the first three developing solutions specified in Table I., and always pre-soaking the emulsions in distilled water for three hours at the appropriate temperature, whatever the thickness of the emulsion. The results obtained are displayed in Table IV. and plotted graphically in figs. 2 and 3. The penetration time, T, may be expressed in terms of the thickness of the emulsion, $t$, by a relation of the form

$$T=k\,.\,t^{x},$$

where $x$ is of the order of 1·4, and $k$ is a constant for a given developer at a given temperature.

Fig. 3.

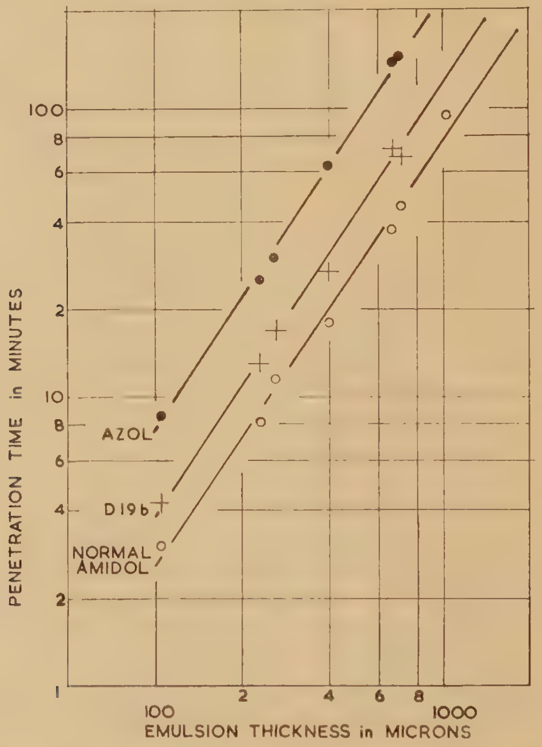

Penetration time of the developer as a function of emulsion thickness for normal amidol, D19b and Azol developing solutions at 15° C. All emulsions pre-soaked in distilled water for three hours at 15° C.

It must be emphasized that T is the penetration time as defined above and not necessarily the time required for satisfactory processing. The latter periods are given in Table VIII.

(ii.) *Temperature characteristics.*

It was also desirable to determine the temperature characteristics of the different developers in the G5 emulsion. Strips of dimensions

$\frac{3}{8}$ in. × $\frac{3}{4}$ in. were cut from 2 in. × 2 in. plates with emulsion 5 $\mu$ thick. These were exposed to light passed through a step wedge (15 steps of density range 0–2) held in a photographic enlarger, the image of this step wedge being formed on the glass-emulsion interface of the plate. The exposure was accurately controlled as in the previous experiment and was such that the image of the middle portion of the wedge was satisfactorily developed using the D19b developer at 20° C. for 10 minutes.

For any one developer at any one temperature, five emulsion strips were used. These were immersed in the developer in question for various times, depending on the normal time used for that developer. For example, the D19b developer is usually used for 20 minutes at 20° C.; thus strip no. 1 was removed from the developer and put to fix after 1½ minutes, no. 2 after 3 minutes, no. 3 after 7 minutes, no. 4 after 15 minutes, and no. 5 after 30 minutes. At a lower temperature, these times were increased, *e. g.* at 5° C. using the same developer the times were twice those used at 20° C.

### Table IV.

Penetration Times, in Pre-soaked Emulsions, of the Various Developing Agents at 5° C., 10° C., 15° C., and 20° C.

| Developer | | Penetration Time in Minutes | | | | | | |
|---|---|---|---|---|---|---|---|---|
| | | 105 $\mu$ | 230 $\mu$ | 260 $\mu$ | 400 $\mu$ | 675 $\mu$ | 720 $\mu$ | 1050 $\mu$ |
| Azol | 5° C. | 11 | 45 | 50 | 100 | 270 | 300 | 300 |
| | 10° C. | 8½ | 27 | 34 | 70 | 185 | 208 | 210 |
| | 15° C. | 8½ | 25 | 30 | 63 | 145 | 150 | 210 |
| | 20° C. | 4½ | 17 | 22 | 38 | 96 | 96 | 210 |
| D19b | 5° C. | 6 | 21 | 27 | 58 | 165 | 172 | 270 |
| | 10° C. | 5 | 16½ | 19 | 37 | 108 | 114 | 210 |
| | 15° C. | 4 | 13 | 17 | 27 | 72 | 68 | 220 |
| | 20° C. | 3½ | 9½ | 14½ | 21 | 50 | 64 | 140 |
| Normal amidol | 5° C. | 5 | 16 | 20 | 37 | 80 | 84 | 190 |
| | 10° C. | 3½ | 11 | 13½ | 22 | 51 | 53½ | 110 |
| | 15° C. | 3 | 8 | 11½ | 18 | 37½ | 45 | 95 |
| | 20° C. | 1½ | 6 | 8½ | 12 | 26 | 26 | 58 |

The figures for 20° C. are given again for comparison purposes.

The above procedure was carried out at 5° C., 10° C., and 20° C. for each of the four developers under consideration. When all the plates had been processed and dried the density of each step in each wedge was determined using an Ilford densitometer and recorder.

The usual method of determining temperature coefficients was found to be inapplicable in this experiment owing to the extreme contrast of the plates. Instead, the times to produce equal densities on the same step (no. 6 in this case) of each wedge were used as a basis of comparison between developers. Equivalent readings were not available in the case of Azol, which was found to be incapable of giving images of sufficiently high density. The results are given in Tables V. and VI. and are presented

TABLE V.

Corrected Density Readings, D, as a Function of Development Time, T, for the Different Developers. for Step 6 on the Step Wedge.

| Developer | | Temperature | | | | | | | | | | | | | | | | | | | |
|---|---|---|---|---|---|---|---|---|---|---|---|---|---|---|---|---|---|---|---|---|---|
| | | 5° C. | | | | | 10° C. | | | | | 15° C. | | | | | 20° C. | | | | |
| Azol | T | 25 | 60 | 140 | — | — | 10 | 22 | 40 | 90 | 160 | 8 | 18 | 35 | 75 | 140 | 7 | 15 | 30 | 60 | 120 |
| | D | 0·1 | 0·24 | 0·17 | — | — | 0·07 | 0·08 | 0·20 | 0·23 | 0·25 | 0·11 | 0·18 | 0·27 | 0·37 | 0·42 | 0·2 | 0·3 | 0·33 | 0·56 | 0·64 |
| D19b | T | — | — | — | — | — | 2 | 4½ | — | 22 | 45 | 1½ | 4 | 9 | 18 | 38 | 1½ | 3 | 7 | 15 | 30 |
| | D | — | — | — | — | — | 0·25 | 0·48 | — | 0·85 | 1·43 | 0·37 | 0·67 | 1·19 | 1·55 | >2·3 | 0·81 | 0·91 | 1·37 | ~2·5 | >2·3 |
| Normal | T | 4 | 10 | 20 | 40 | 80 | 3 | 7½ | 15 | 30 | 60 | — | — | — | — | — | 2 | 5 | 10 | 20 | 40 |
| Amidol | D | 0·2 | 0·34 | 0·65 | 0·92 | 1·6 | 0·31 | 0·57 | 1·05 | 1·37 | ~2·3 | — | — | — | — | — | 0·78 | 1·27 | 1·55 | ~2·4 | >2·2 |
| Amidol | T | — | — | — | — | — | 3 | 7½ | 15 | 30 | 60 | 2½ | 6 | 12½ | 25 | 51 | 2 | 6 | 10 | 20 | 40 |
| Bisulphite | D | — | — | — | — | — | 0·19 | — | 0·72 | 1·02 | 1·5 | 0·3 | 0·52 | 0·88 | 1·15 | 1·95 | 0·42 | 0·63 | 1·15 | 1·83 | >2·2 |

TABLE VI.

Development Time for Unit Density as a Function of Temperature.

| Developer | | Time for Density 1 in Minutes | Figures Normalized to Density 3½ at 20° C. |
|---|---|---|---|
| D19b | 5° C. | — | — |
| | 10° C. | 30 | 30 |
| | 15° C. | 8 | 8 |
| | 20° C. | 3½ | 3½ |
| Normal amidol | 5° C. | 45 | 45 |
| | 10° C. | 18 | 18 |
| | 15° C. | — | — |
| | 20° C. | 3½ | 3½ |
| Amidol bisulphite | 5° C. | — | — |
| | 10° C. | 30 | 10½ |
| | 15° C. | 18 | 6 |
| | 20° C. | 10 | 3½ |
| Azol | 15° C. | 400 | 3½ |
| | 20° C. | 1200 | 10½ |

Fig. 4.

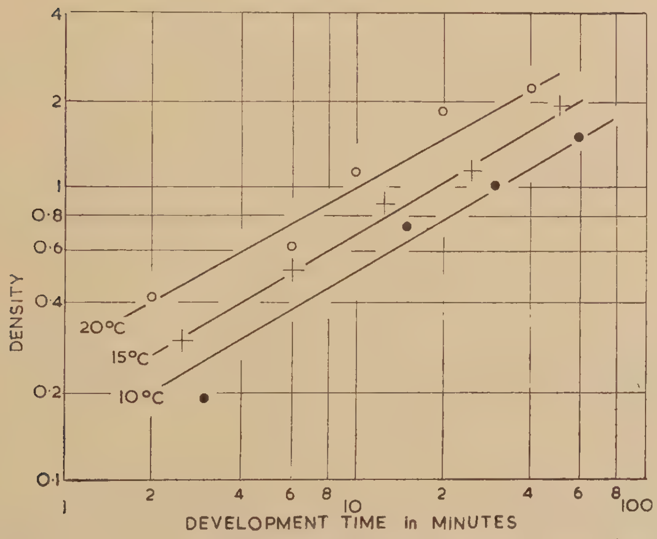

Density of step 6 of the step wedge as a function of development time for amidol bisulphite developer at various temperatures.

graphically in figs. 4 and 5. It may be seen that the rate of action of all the developers changes rapidly with temperature. The measurements suggest that D19b is more sensitive than the amidol developers. Azol, although very sensitive to temperature, has very low activity.

(iii.) *Background formation and staining properties of developers.*

Background grains not associated with recognizable tracks are due, in part, to particles traversing the emulsion at a large angle of dip, and to fog grains arising from (*a*) chemical action during the preparation of the emulsion, and (*b*) the action of the developing agent.

A measure of the number of background grains per unit area was obtained by counting the number of such grains in focus under specified optical conditions. The microscope used was a Cooke M4000 with ×95 objective and ×15 eyepieces. Some results for emulsions exposed and processed under different conditions are given in Table VII. A background of as much as 80 grains per 10,000 $\mu^2$ can be tolerated in emulsions in which the grain density in the track of a particle with minimum specific ionization is of the order of 15 grains per 50 $\mu$.

Fig. 5.

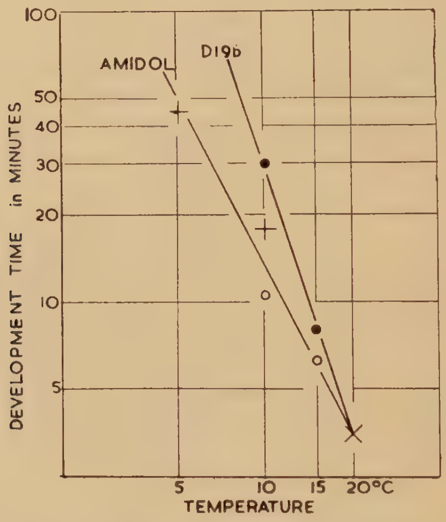

Time for unit density of step 6 against temperature, for amidol type and D19 b developing solutions. The figures are normalized at 20° C.

TABLE VII.

| Exposure | Developer | Stop Bath | Background Grains/10,000 $\mu^2$ 5 $\mu$ from surface | | Percentage of Light Transmitted |
|---|---|---|---|---|---|
| | | | | 5 $\mu$ from glass | |
| 1. G5 400 $\mu$ 1½ hrs. at 68,000 ft. | Azol | 5 per cent sodium bisulphite | 35 ± 2 | Too misty | 27 |
| 2. G5 400 $\mu$ 5½ hrs. at 64,000 ft. | Normal amidol | pH3 HCl | 95 ± 5 | 74 ± 3 | 17 |
| 3. G5 400 $\mu$ 5½ hrs. at 64,000 ft. | Amidol bisulphite | 2 per cent acetic acid | 34 ± 2 | 33 ± 2 | 40 |
| 4. G5 500 $\mu$ Glass 2 mm. 6 hrs. at 75,000 ft. | Amidol bisulphite | ½ per cent acetic acid | 59 ± 3 | 61 ± 3 | 25 |

The degree of stain in an emulsion is difficult to define quantitatively. We may estimate the combined effect of background and stain by means of an Ilford densitometer which measures the percentage of light transmitted by the photographic plate. The figures given in Table VII. show that the stain is not necessarily related to the background grain density. It may also be seen that the use of amidol bisulphite developer results in plates of good optical quality.

### (iv.) *Stability of the developer as a function of temperature.*

Following Dilworth *et al.* (1950), who drew attention to the possibility of employing developing solutions at higher temperatures than those commonly used, we have found that very satisfactory results are obtained when a temperature of the order of 27° C. is used in the hot stage of the temperature cycle. For such work it is necessary that the developer should remain stable at these temperatures, and all the developers given in Table I. are satisfactory in this respect.

### (v.) pH *considerations.*

It has been shown that when Ilford Nuclear Research emulsions are immersed in a solution the swelling of the emulsion decreases as the pH of the solution is reduced. In fact, the emulsion will even shrink when placed in dilute acid (Waller 1951). These considerations make it desirable that the developer employed should be slightly acid, for the less the swelling of the emulsion, the smaller the distortion introduced at this stage of the processing.

## CONCLUSIONS.

From a consideration of the factors discussed above, it appeared to us that amidol promised to give the most satisfactory results. It was therefore adopted as a standard developer for emulsions up to 300 $\mu$ in thickness. For thicker emulsions it was found that normal amidol produced a slight variation of development with depth. We have succeeded in reducing this variation by adding sodium bisulphite to the developing solution (Balagny 1912). Balagny employed normal photographic emulsions and his recommended value for the pH of the developer was not found to be suitable for thick electron sensitive emulsions. Using the amidol bisulphite developing solution given earlier, with a pH of about 4, we have found it possible to develop the lower regions of an emulsion without developing the surface layers. The pH of the solution which gives satisfactory development throughout the entire thickness of the emulsion is 6·7.

Experiments were also carried out in an attempt to reduce the formation of fog in the emulsion by reducing the concentration of amidol, but tracks of particles of minimum ionization were not recorded for concentrations less than 3 gm./litre.

## § 2. The Development Process.

We may now consider the details of the development procedure. The results given in the previous section suggest that: (*a*) the emulsion should be pre-soaked in water before being placed in the developing solution; and (*b*) that the developer used should be amidol in some form.

In our procedure the plate is therefore first immersed in distilled water at room temperature. The water is then cooled to 5° C. and maintained at this temperature for a time which depends on the thickness of the emulsion. It is then transferred to the developing solution, which is also at 5° C., and remains in this solution until the developer has completely permeated the emulsion. During this time little development will have taken place.

For the main development process two alternative methods may be employed. The developer and plate together may be warmed to about 18° C., and the temperature maintained at this value for the time required to give satisfactory development. Alternatively, following Dilworth *et al.* (1950), the plate may be separated from the developing solution, any excess solution being removed by means of filter paper, and the plate then placed glass downwards on a dry surface. This surface is then brought to a temperature between 25 and 30° C., and maintained at a constant value for the requisite time. In this method one thus relies upon the developer already present in the body of the emulsion and avoids over-development at the top of the emulsion due to the entry of fresh developer. This is known as the " hot-plate " method.

In our experience the second method gives the more satisfactory results. To obtain tracks of particles with minimum ionization, the actual value of the temperature of the " hot plate " does not appear to be critical. If, however, it is important to preserve uniformity of development among plates from different batches it is necessary to introduce an accurate system of temperature control. Care must also be taken to ensure good thermal contact between the plates and the " hot plate ".

If amidol is used as the developing solution, the surface of the emulsion, after processing, is usually covered with a deposit of silver. This may sometimes, although not always, be swabbed off with cotton wool soaked in methylated spirits, when the emulsion is thoroughly dry. For some experiments, such as those with artificially accelerated particles, it is important to know the exact point where a particle entered the surface. Any surface silver deposit is therefore to be avoided if possible. It has been suggested by Dilworth *et al.* (1950) that developing the plates in an inert atmosphere may lead to a diminution in the amount of the surface deposit. Alternatively, for emulsions less than 400 $\mu$ in thickness, azol may be employed, using the first of the development methods described above, since it commonly leaves little or no surface deposit.

The next problem is to stop the development at the correct moment. The general procedure is to transfer the plates to a " stop bath " which is at a temperature near to that of the " hot plate "; the temperature of the solution is then lowered to about 5° C. and kept at that value until all development has ceased. The solution and plates may then be warmed to the temperature of the fixing solution, and after a short wash in water, transferred to it. Thus development is stopped both by the application of a stopping agent and by the use of low temperature. We have tried several stopping agents including distilled water, a 1 per cent potassium bromide solution, a 5 per cent sodium bisulphite solution, $\frac{1}{2}$ per cent solution of hydrochloric acid and solutions of acetic acid. The best results were obtained with the acetic acid. The concentration did not appear to be critical, and we find that a $\frac{1}{2}$ per cent solution is satisfactory.

In all the processes mentioned above, the plates are kept horizontal. This is especially important when dealing with very thick emulsions.

## § 3. Fixation.

The critical importance of avoiding distortion has already been stressed. The main causes of distortion are the stresses introduced when the emulsion suffers volume changes including those during manufacture. These changes may be caused by mechanical agitation, temperature variations, pH changes, and the removal of the unsensitized silver halide from the emulsion. Since most of the silver halide, which constitutes a large fraction of the unprocessed emulsion, is removed during processing, it is probable that most of the distortion is introduced during fixation, washing and drying. After the fixing solution has been washed out and the plate allowed to dry, the emulsion has less than half its original thickness.

The plate is fixed with sodium thiosulphate—"hypo". Camerini and Franzinetti (1947), working with thin emulsions, found that a concentration of 40 grams of hypo to 100 mls. of water gives the most satisfactory results. We have confirmed this result for emulsions 400 $\mu$ thick.

Owing to the large amount of silver halide in electron-sensitive emulsions the fixing process takes a relatively long time. It is well known that ammonium thiosulphate acts rapidly as a fixing agent. The addition of a small amount of ammonium chloride to the hypo solution also shortens the total fixing time. We have found, however, that a fixing solution of this nature tends to remove some of the developed grains near the surface of the emulsion, especially in the case of thick emulsions where the total fixing time may be of the order of two or three days. This has also been observed by Wilson and Vaneslow (1949). Because of this effect we do not favour the use of ammonium chloride.

On the other hand, we have found it advantageous to add sodium bisulphite to the hypo solution ; this leads to a reduction of the stain in the finally processed emulsion (Mees 1942). The fixing solution which has been adopted as standard in this laboratory is :—

| | |
|---|---|
| Sodium thiosulphate | 400 grams. |
| Sodium bisulphite | 30 grams. |
| Water to add | 1,000 mls, |

The pH of this solution is 5·0,

### *Agitation.*

It has been found by several workers that gentle agitation of the fixing solution leads to a reduction in the total fixing time (Powell and Occhialini 1947; Wilson and Vaneslow 1949). It is essential that the plates are kept horizontal and that the agitation, if any, is very gentle. This is especially important for emulsions thicker than 400 $\mu$. If, for example, a 500 $\mu$ emulsion is held vertically during the fixing process, the emulsion tends to " creep ", and it is frequently observed that tracks near to the bottom are discontinuous. An example of this nature which we call 'chopping' is shown in Pl. XVII. *a*. Similar effects sometimes occur in emulsions processed horizontally (Herz 1950) and have been seen in emulsions 200 $\mu$ thick.

We have found that suitable agitation is provided by a slow steady flow of the fixing solution over the surface of the plates. Satisfactory results may also be obtained by placing the plates in a static fixing bath, provided the bath is changed fairly frequently. A fixing bath is considered to be exhausted when the concentration of silver in it rises above between five and seven grams per litre.

### *Fixation time.*

The period for complete fixation is usually taken as one and a half times that for the emulsion to clear, that is, when the last trace of opaque silver halide has disappeared from the bottom of the emulsion. For a 400 $\mu$ emulsion, the total fixation time is of the order of 24 hours, while for a 1,000 $\mu$ emulsion it may be as long as 100 hours.

## § 4. WASHING AND DRYING.

### *Washing.*

When all the surplus silver halide has been removed from the emulsion, the fixing solution must be washed out. Thin emulsions may be washed in a stream of tap water. When this method is employed with emulsions 600 $\mu$ thick, however, the emulsion frequently distorts, and " bubbles " may be formed on the surface.

We have therefore found it necessary to commence washing with water at a low temperature (5–10° C.). The plates are placed in a large dish of fixing solution and the cold water is allowed to trickle in slowly at first. As the concentration of the fixing solution is reduced, the rate of flow of the water and its temperature may be increased. The washing process may take as long as two or three days, and it is only considered complete when the washing solution gives no indication of the presence of hypo as judged by the potassium permanganate test.

### *Drying.*

Following a suggestion of Mr. C. Waller, we next soak the plates in a solution of glycerine for approximately an hour. This prevents the emulsion from stripping off the glass after it has dried. A 1 per cent solution has been found to be satisfactory for this purpose. We have found some indication that the use of a 5 per cent solution tends to reduce the distortion, although the processed emulsion is then rather soft.

After removal from the glycerine solution, the plates are placed side by side in the form of a square or a rectangle in an enclosed box. If they are of a small size it is of some advantage to place a " guard ring " of wet emulsion around the plates to be dried (Dilworth 1950). It is more convenient, however, to use large plates, say 8 in. × 8 in. and then cut them to 6 in. × 6 in. after they have dried. The distortion effects at the edges are thus almost completely eliminated.

A preliminary investigation has shown that distortion is reduced if the drying of the plates is not unduly prolonged. A batch of plates was allowed to dry for seven days at a relative humidity of 90 per cent, and then for a further seven days during which the relative humidity was gradually lowered to about 55 per cent. The distortion in these plates was a little greater than that in emulsions of equal thickness which had been dried over a period of three days. Drying by gently blowing air over the plates is undesirable and introduces severe C-shaped distortion. Warming the plates by means of a 25 watt electric light bulb at a distance of a few feet appears to give satisfactory results.

## § 5. CONCLUSIONS.

### *Distortion.*

The effect of distortion on the measurement of the scattering of a track has been briefly discussed by Fowler (1950), while Cosyns and Vanderhaeghe (1950) have described a method of estimating its magnitude. It is, of course, most severe at the edges of a plate ; examples of both C- and S-shaped distortion at the edge of a 400 $\mu$ plate are shown in Pl. I. *b* and *c*. The elimination of these edge effects has been discussed in the previous section.

The distortion in the centre of a large emulsion is usually of the C-type and its effect on the scattering of a track may then be estimated. On the other hand, it may occasionally take the form of irregular and local " chopping " for which no correction can be made.

### *General considerations.*

The results given above have been summarised in Tables VIII. and IX. which detail satisfactory processing methods for G5 emulsions of various thicknesses.

The methods given in Table VIII. have been used in the processing of Ilford C2, D1, and E1 emulsions 200 $\mu$ thick (Danysz 1950 ; Muirhead 1950), Ilford C2 emulsions 600 $\mu$ thick (Smith 1950) and Kodak NT4 emulsion 200 $\mu$ thick (King 1950). Satisfactory results were obtained in all cases.

In collaboration with Mr. M. G. K. Menon, and Mr. G. T. Zorn, the investigations described are being extended to still greater emulsion thicknesses, and to the diluted emulsions recently produced by Ilford Ltd. (Dodd and Waller 1950).

### TABLE VIII.

Amidol Type Developer.

| | Emulsion Thickness. | | | | |
|---|---|---|---|---|---|
| | $100\,\mu$ | $200\,\mu$ | $400\,\mu$ | $600\,\mu$ | $1000\,\mu$ |
| Soak in distilled water | 15 mins. | 25 mins. | 90 mins. | 120 mins. | 240 mins. |
| Developer at 5° C. | 15 ,, | 25 ,, | 90 ,, | 120 ,, | 300 ,, |
| " Hot plate " 27° C. | 25 ,, | 25 ,, | 30 ,, | 30 ,, | 35 ,, |
| Stop bath | 10 ,, | 20 ,, | 90 ,, | 120 ,, | 180 ,, |
| Fixing | 2 hours | 5 hours | 24 hours | 70 hours | 100 hours |
| Washing | 4 ,, | 12 ,, | 60 ,, | 72 ,, | 120 ,, |
| Drying | 6 ,, | 12 ,, | 60 ,, | 100 ,, | 120 ,, |

### TABLE IX.

Azol Developer.

| | Emulsion Thickness | | |
|---|---|---|---|
| | $100\,\mu$ | $200\,\mu$ | $400\,\mu$ |
| Soak in distilled water | 15 mins. | 25 mins. | 90 mins. |
| Developer at 5° C. | 30 ,, | 90 ,, | 120 ,, |
| Warm stage 18° C. | 105 ,, | 105 ,, | 105 ,, |
| Stop bath | 30 ,, | 45 ,, | 90 ,, |
| Fixing | 2 hours | 5 hours | 24 hours |
| Washing | 4 ,, | 12 ,, | 60 ,, |
| Drying | 6 ,, | 12 ,, | 60 ,, |

The stop bath may be 5 per cent sodium bisulphite or $\frac{1}{2}$ per cent acetic acid.

## ACKNOWLEDGMENTS.

This work was originally undertaken in collaboration with Mr. H. Muirhead, now at the University of Glasgow, and we are indebted to him for introducing us to the problem and for his advice and criticism.

We have pleasure in thanking Professor C. F. Powell, F.R.S., for his continued interest and encouragement; Mr. C. Waller and Mr. M. A. Vincent of Ilford Ltd., who have supplied us with the emulsions of many different sizes and thicknesses, and who have given us the benefit of their experience with electron-sensitive emulsions; Dr. R. H. Herz of Kodak Ltd., who has supplied us with test samples of NT4 emulsions; Miss C. C. Dilworth and Professor G. P. S. Occhialini of the University of Brussels for helpful advice; Miss Mary Blundell of the University of Manchester, who kindly gave us the formula for the Azol developer; and Mr. A. J. Herz of Imperial College, London, for discussions.

Finally we would like to express our appreciation to those members of the laboratory research team who have helped in various ways at all hours, particularly Mr. J. H. Davies, Mr. D. W. Kent, Mr. D. T. King, Mr. M. G. K. Menon and Mr. G. T. Zorn; and to Dr. H. K. Heitler, Mr. H. Ellacott and Mr. M. A. Roberts, for considerable technical assistance.

This work has been carried out as part of a programme of research supported by the D.S.I.R., and two of us (A.D.D. and W.D.L.) are indebted to this body for maintenance grants.

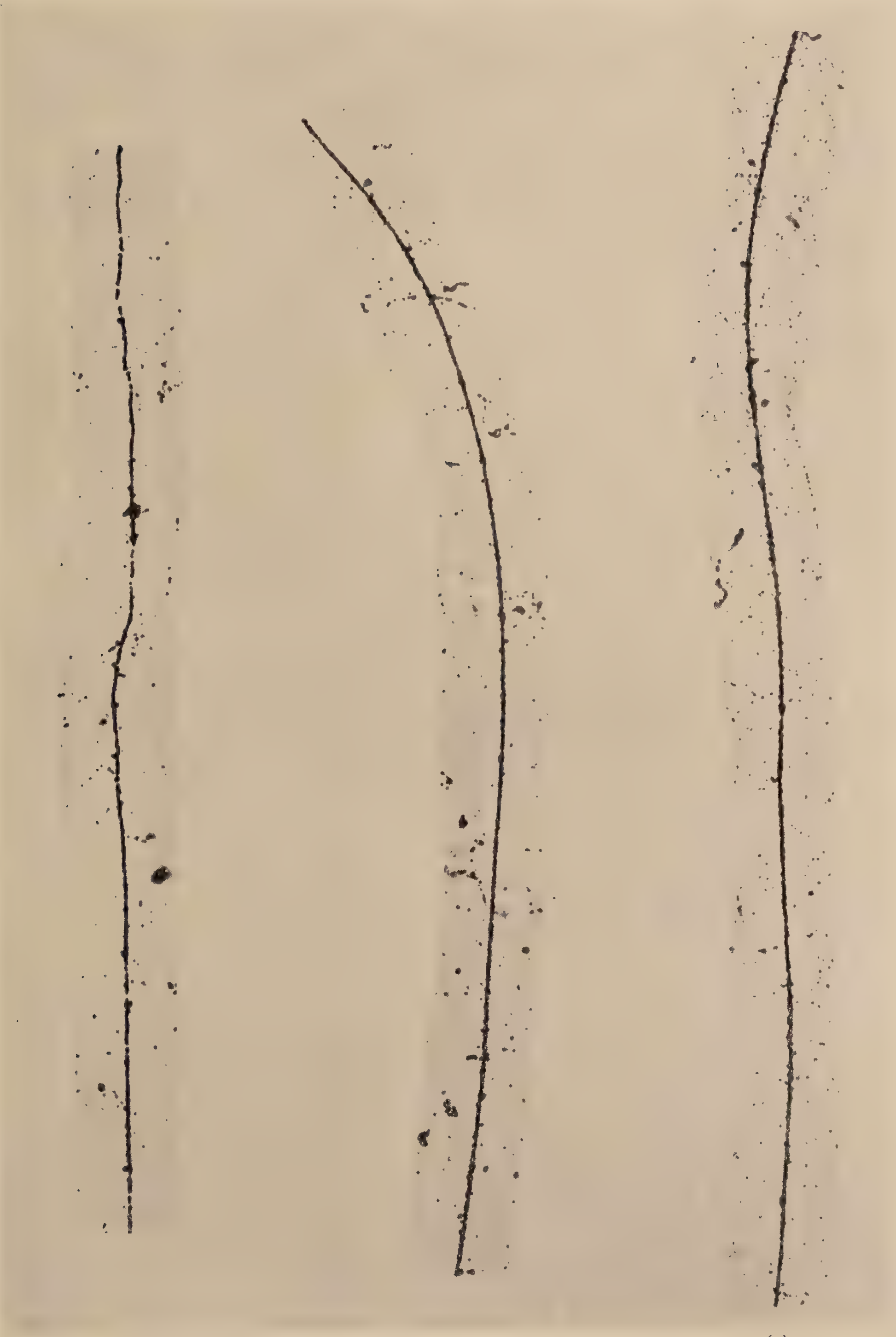

(*a*) (*b*) (*c*)

Examples of (*a*) "chopping", (*b*) C-shaped distortion, and (*c*) S-shaped distortion in 400 $\mu$ G5 emulsions.

## REFERENCES.

BALAGNY, G., 1912, *Bull. Soc. Franc. Photogr.* (3) **3,** 198.
BERRIMAN, R. W., 1948, *Nature, Lond.*, **162,** 992.
BLAU, M., and DE FELICE, J. A., 1948, *Phys. Rev.*, **74,** 1198.
CAMERINI, U., and FRANZINETTI, C., 1948, Private Communication.
COSYNS, M., and VANDERHAEGHE, E., 1950, *Bulletin du Centre de Physique Nucleaire de L'Universite Libre de Bruxelles*, No. 15, February.
DANYSZ, M., 1950 Private Communication.
DILWORTH, C. C., 1950, *Bristol Photographic Conference.*
DILWORTH, C. C., OCCHIALINI, G. P. S., and PAYNE, R. M., 1948, *Nature, Lond.*, **163,** 102.
DILWORTH, C. C., OCCHIALINI, G. P. S., and VERMAESEN, L., 1950, *Bulletin du Centre de physique Nucleaire de L'Universite Libre de Bruxelles.* No. 13 *a*, February.
DODD, E. C., and WALLER, C., 1950, *Bristol Photographic Conference.*
FOWLER, P. H., 1950, *Phil. Mag.*, **41,** 169.
HERZ, A. J., 1950, Private Communication.
MEES, C. E. K., 1942, *The Theory of the Photographic Process* (New York: Macmillan), p. 528.
MUIRHEAD, H., 1950, Private Communication.
PAYNE, R. M., 1949, Private Communication.
POWELL, C. F., and OCCHIALINI, G. P. S., 1947, *Nuclear Physics in Photographs.* (Oxford: Clarendon Press), p. 110.
POWELL, C. F., OCCHIALINI, G. P. S., LIVESEY, D. L., and CHILTON, L. V., 1946, *J. Sci. Instrum.*, **23,** 102.
SMITH, C. L., 1950, Private communication.
WALLER, C., 1951, Private communication.
WILSON, M. J., and VANESLOW, S., 1949, *Phys. Rev.*, **75,** 1144.

# XLVI. *A Theory of the Plastic Distortion of a Polycrystalline Aggregate under Combined Stresses.*

By J. F. W. Bishop and R. Hill,
Wills Physical Laboratory, University of Bristol.*

[Received February 8, 1951.]

## Summary.

A general relationship between stress and plastic strain in a polycrystalline aggregate is derived for any metal in which individual crystals deform by slipping over preferred planes under a critical shear stress. Full account is taken of the non-uniform distortion due to mutual constraints between the grains of an aggregate. It is shown that a plastic potential exists which is identical with the yield function. Upper and lower bounds are obtained for an approximate calculation of this function for any applied system of combined stresses.

## §1. Introduction.

The macroscopic theory of plastic deformation in a polycrystalline metal is based on observations of the behaviour of the metal in bulk. It rests also on the simplifying hypothesis that the material is locally homogeneous (though not necessarily isotropic). The theory so constructed is found to be adequate as a first approximation when applied to many problems in engineering science and metal technology. There remains, however, the task of relating the macroscopic observations to ones more fundamental, for example, the mechanisms by which a single crystal deforms under load. Such an investigation might hope to attain two main objectives: first, to show which of the several microscopic modes of distortion are chiefly responsible for the behaviour of the aggregate as a whole; and second, to indicate, more precisely than experiment at present can, what refinements should be added to the macroscopic theory and what these might be for any particular metal. Several previous writers have dealt with related problems, and the most important papers will be discussed briefly.

In single crystals of many metals it is known that the main mechanism of plastic distortion on a microscopic (though not atomic) scale is simple shear parallel to preferred planes and directions. At ordinary temperatures both the planes and directions are generally those of closest atomic packing. It is observed that pronounced slip (or glide) is initiated along the particular plane and direction for which the corresponding component of shearing stress first reaches a certain critical value under increasing external load. This critical value depends on the temperature and rate of straining, but not on the crystal orientation or the type of load (provided the loading-path is not such as to induce hysteresis effects). This has been established for metals such as copper, aluminium, nickel, magnesium, zinc and cadmium by the experiments of Mark, Polanyi and Schmid (1922), Taylor and Elam (1923), Polanyi and Schmid (1923) and Schmid (1924), among others. Double slipping is observed if the critical shear stress is reached simultaneously on two of the possible planes and directions.

---

* Communicated by the Authors.

The problem of predicting the tensile yield stress of a polycrystalline face-centred cubic metal was considered by Sachs (1928) and by Cox and Sopwith (1937) on the assumptions that (i) each grain is subjected to a uniaxial stress parallel to the specimen axis sufficient to initiate slipping in the most highly stressed direction ; (ii) all orientations are equally likely ; (iii) each grain is in the same state of work hardening. The resultant axial load on the specimen was calculated as the sum of the individual loads in the constituent grains. The value obtained for the macroscopic uniaxial yield stress was $2{\cdot}2\tau$ (approximately), where $\tau$ is the shear yield stress of a single crystal. This treatment is open to the objections that the grains could not form a coherent whole if only a single homogeneous glide occurred in each, and that the necessary conditions of equilibrium could not be satisfied across grain boundaries if the stress in each were a simple tension of varying amount.

Kochendörfer (1941) added the further hypothesis that the grains extend by the same amounts in the direction of the specimen axis. This enabled him to calculate the stress-strain curve of the aggregate. For in each grain

$$\sigma/\tau = d\gamma/d\epsilon = m$$

where $\sigma$ is the axial stress in a grain, $d\epsilon$ is the common axial strain-increment, $d\gamma$ is the increment of shear strain in the slip direction, and $m$ is a dimensionless factor depending only on orientation. (In passing, it may be noted that the virtual work equation $\sigma d\epsilon = \tau d\gamma$ is naturally satisfied). We now interpret the various symbols as mean values over all orientations, so that $m \simeq 2{\cdot}2$ from Sachs' calculations. It follows that the stress-strain curve of the aggregate is

$$\sigma = m\tau(\gamma) = m\tau(m\epsilon)$$

where $\tau(\gamma)$ is the shear-hardening curve (the transition from $d\gamma = m d\epsilon$ to $\gamma = m\epsilon$ is legitimate since $m$ is independent of the amount of strain on the assumption of continuing isotropy). However, the best fit of this $\sigma(\epsilon)$ relation to Taylor's experimental curve for aluminium gives a value of about $3{\cdot}1$ for $m$.

In a recent paper (1950) Calnan and Clews considered the particular directions in which a pure tension would need to be applied to operate simultaneously either 4, 6, or 8 shears in a face-centred cubic lattice. They assumed the stress state in each grain to be a uniaxial tension of this kind and of the requisite amount. Each grain is assumed to undergo the specimen extension (and not the strain as a whole). Thus, the objections raised against previous work with regard to the independent action of the grains apply here, also. Despite this Calnan and Clews' computations led to a stress-strain curve in fair agreement with that measured for polycrystalline aluminium.

A more realistic calculation of the tensile yield stress of a face-centred cubic aggregate is due to Taylor (1938), who assumed that each grain undergoes the same uniform strain (so maintaining cohesion). This requires, in general, the operation of at least 5 independent shears out of the 12 operable at ordinary temperatures. Hence, if only geometry is considered, many choices are possible for a given strain. Taylor introduced the hypothesis that the actual active set of shears is that for which the sum of their separate magnitudes is least. The hypothesis has no obvious *a priori* justification, but Taylor based it on observations of single crystals under uniaxial stress and on a postulated analogy with the dynamics of a non-conservative mechanical system. By adding the further assumption that the shear hardening of a crystal during simultaneous glide depends only on the sum of the absolute shears, Taylor was able to compute a stress-strain curve for an aluminium aggregate in fairly close agreement with the measured curve. There are two main criticisms of this approach: first, it is not proved that a combined stress could always be found to operate any geometrically possible set of shears (without exceeding the critical shear stress in non-active directions); and, second, no account is taken of stress-continuity conditions across grain boundaries.

All these previous investigations have been confined to an aggregate under simple tension or compression. In the present paper no such restriction is placed on the applied load.

## § 2. THE MACROSCOPIC THEORY OF PLASTICITY.

In order to appreciate the aim of the present work it is necessary to be familiar with the premises of the macroscopic theory of plasticity. These will be summarized here; a full discussion has been given by Hill (1950).

The theory assumes a locally homogeneous material (possibly anisotropic) having a sharp yield point after work-hardening. The yield criterion for a metal in a given state of hardening is assumed not to depend on the hydrostatic component $\sigma$ of the applied stress $\sigma_{ij}$, and is usually taken to have the form

$$f(\sigma'_{ij})=c\,;\quad \sigma'_{ij}=\sigma_{ij}-\sigma\delta_{ij}. \quad . \quad . \quad . \quad . \quad . \quad . \quad . \quad . \quad (1)$$

This equation may be regarded as defining a surface in stress hyperspace; the surface is " cylindrical ", with generators parallel to the direction $\delta_{ij}$. An assumption adequate for many applications, though not necessary in principle, is that the function $f$ does not involve parameters depending on the previous strain-history. The dependence of the shape and size of the yield surface on strain-history is thus taken to be expressible through the single parameter $c$. Infinitesimal changes of stress for which $df=0$ maintain the element on the point of yielding, and cause only elastic changes of strain in a hardening material. The sign of $f$ is conventionally chosen so that $df>0$ for an increment of stress producing further plastic strain, while if $df<0$ the element unloads elastically.

The elastic part of the strain is neglected henceforward. The relations between stress and strain are taken to be

$$d\epsilon_{ij}=h\frac{\partial g}{\partial \sigma_{ij}}df\,;\ df\geqslant 0. \quad \ldots\ldots\ldots \quad (2)$$

$g$ (the plastic potential) and $h$ are scalar functions of the reduced stress $\sigma'_{ij}$; parameters in $g$ depending on strain-history are held constant in the differentiation. When the element is isotropic $f$, $g$ and $h$ must be functions only of the two independent invariants of the tensor $\sigma'_{ij}$. Since $g$ does not involve the hydrostatic part of the stress, (2) implies that there is no plastic volume change.

It is normally assumed, in the absence of definite experimental evidence, that the yield function $f$ and the plastic potential $g$ are the same*. With this simplification equation (2) becomes

$$d\epsilon_{ij}=h\frac{\partial f}{\partial \sigma_{ij}}df\,;\ df\geqslant 0. \quad \ldots\ldots\ldots \quad (3)$$

Certain extremum principles (and an associated uniqueness theorem) may then be proved (Hill 1950). The proof of one of them will be repeated here for the sake of a later analogy.

(i) *Maximum Work Principle.*

Equation (2) may be interpreted as asserting that the strain increment (represented in stress hyperspace) is parallel to the corresponding outward normal to the yield surface. In order that a unique state of reduced plastic stress should correspond to a prescribed increment of strain it is evidently necessary for this surface to enclose, and be concave at all points to, the origin.

There will be two generators on the surface where the normals are parallel to a given direction; uniqueness is secured by the condition that the plastic work is positive.

Suppose, now, that an element is in a given state of hardening, defined by a certain yield-surface. Consider a plastic stress state $\sigma_{ij}$ and corresponding strain-increment $d\epsilon_{ij}$. If $\sigma^*_{ij}$ is a stress state lying within or upon the yield surface, the vector $\sigma_{ij}-\sigma^*_{ij}$ is inclined at an acute angle to the outward normal at $\sigma_{ij}$ (the yield surface being cylindrical and concave to the origin). Hence (using the summation convention)

$$(\sigma_{ij}-\sigma^*_{ij})d\epsilon_{ij}\geqslant 0,\quad d\epsilon_{ij}\neq 0, \quad \ldots\ldots\ldots \quad (4)$$

---

* More generally, $g$ is taken equal to any convenient multiple or power of $f$. The resulting stress–strain relations are always the same if $h$ is suitably altered.

the equality holding only when $\sigma_{ij}$ and $\sigma^*_{ij}$ differ by a hydrostatic component. This has the interpretation that the work done by the actual stress in a prescribed strain-increment is greater than that done by any other stress not violating the yield condition. The result does not involve any assumption about the dependence of the yield surface on the strain-history.

Consider, next, a finite mass undergoing plastic deformation at *all* points. Let $\sigma_{ij}$ be the actual stress, satisfying the yield condition and the equilibrium equations

$$\frac{\partial \sigma_{ij}}{\partial x_j}=0, \qquad \ldots \ldots \ldots \qquad (5)$$

at all points. The associated strain-increment must be derived from a continuous displacement increment $du_i$, such that

$$d\epsilon_{ij}=\frac{1}{2}\left\{\frac{\partial}{\partial x_j}(du_i)+\frac{\partial}{\partial x_i}(du_j)\right\}.$$

If $\sigma^*_{ij}$ is any stress state satisfying (5) and lying within or on the yield surface for each point of the mass, we have the virtual work equation

$$\int\{(\sigma_{ij}-\sigma^*_{ij})d\epsilon_{ij}\}\,dV=\int\{(F_i-F^*_i)du_i\}\,dS,$$

where the first integral is taken through the volume, and the second over the surface of the mass, $F_i$ and $F^*_i$ being the *i*th components of the respective outward forces acting on unit surface area. Hence, from (4)

$$\int\{(F_i-F^*_i)\,du_i\}\,dS\geqslant 0, \qquad \ldots \ldots \ldots \qquad (6)$$

the equality holding only when the stress states differ by a uniform hydrostatic stress. Equation (6) is true whether or not the states of hardening and anisotropy are non-uniform, and no assumption is made as to how they depend on strain-history.

(ii) *Converse of Maximum Work Principle.*

Suppose it to be given that, for any prescribed strain-increment, the corresponding state of plastic stress in an element is such that the work done is stationary with respect to infinitesimally near stress states, lying on the yield surface. Then it is evident that the normal to the yield surface at the corresponding point must be parallel to the strain-increment vector. A plastic potential therefore exists and it is identical with the yield function. The latter, moreover, must be cylindrical with generators parallel to the direction $\delta_{ij}$, since any possible strain-increment has zero hydrostatic part (there being no plastic change of volume). If the work done is an absolute maximum, with respect to *all* stress states within or on the yield surface, the surface must be concave to the origin at every point.

This is the basis of the method adopted later to derive equation (3) from the properties of single crystals.

(iii) *Complementary Minimum Principle.*

Consider a mass in an equilibrium plastic state $(\sigma_{ij}, d\epsilon_{ij})$ and let $d\epsilon^*_{ij}$ be any strain-increment; $d\epsilon_{ij}$ and $d\epsilon^*_{ij}$ are derived from continuous displacement increments $du_i$ and $du^*_i$ taking the same values on the surface and having zero divergence everywhere. It may be proved (Hill, *op. cit.*, p. 67) that

$$\int(|\sigma'_{ij}||d\epsilon_{ij}|)\,dV \leqslant \int|(\sigma'_{ij}||d\epsilon^*_{ij}|)\,dV, \quad . \quad . \quad . \quad . \quad . \quad (7)$$

where $$|\sigma'_{ij}|=\sqrt{(\sigma'_{ij}\sigma'_{ij})}, \text{ etc.},$$

provided the material is isotropic and the plastic potential is a *circular* cylinder in principal-stress space; *i.e.* $f=\sigma'_{ij}\,\sigma'_{ij}$ in (3). If the state of hardening is uniform, (7) reduces to Markov's result

$$\int|d\epsilon_{ij}|\,dV \leqslant \int|d\epsilon^*_{ij}|\,dV. \quad . \quad . \quad . \quad . \quad . \quad . \quad . \quad . \quad (8)$$

The analogue of (7) for any plastic potential is

$$\int(\sigma_{ij}\,d\epsilon_{ij})\,dV = \int(\sigma_{ij}\,d\epsilon^*_{ij})\,dV \leqslant \int(\sigma^*_{ij}\,d\epsilon^*_{ij})\,dV,$$

where (4) is used to derive the inequality, $\sigma^*_{ij}$ being the plastic stress-state corresponding to $d\epsilon^*_{ij}$.

## § 3. PLASTICITY OF A SINGLE CRYSTAL.

We assume that the only mechanism of plastic distortion in a single crystal is by glide parallel to preferred planes and directions, and we examine the consequences of such an assumption. Let there be $n$ possible slip directions $a_1, \ldots a_n$. (on associated glide planes), for a certain crystal lattice. The displacement of any point of the crystal, due to simultaneous infinitesimal shears $d\gamma_1, \ldots d\gamma_n$ (positive or negative), in the respective directions may be found by simple geometry. The corresponding tensor representing the homogeneous strain has five independent components (its hydrostatic part being necessarily zero), each of which is found as a certain linear combination of $d\gamma_1, \ldots d\gamma_n$. For given $d\gamma_k$ $(k=1, \ldots n)$ the strain tensor is thereby uniquely determined.

On the other hand, when the components of the strain tensor are given (the hydrostatic part being zero), we have $n$ unknown $d\gamma_k$ and 5 equations between them. If $n$ is less than 5 (as in a hexagonal metal) a combination of shears cannot be found to produce an *arbitrary* strain. If $n$ is equal to 5 there is a unique set of the $d\gamma_k$ if the determinant of the coefficients is non-zero. If $n$ exceeds 5, a set of 5 slip directions can be selected in any one of ${}^nC_5$ ways, but the corresponding set of shears can only be found when the associated determinant is non-zero, *i.e.* when the slip directions form an *independent* set. It may also be possible to find combinations of 6 or more shears to produce the prescribed strain.

In a fully annealed crystal the critical shear stress appears not to depend on which slip-direction is activated, nor on the sense of the shear. During continued deformation active and non-active directions harden equally, to a first approximation (Taylor and Elam 1925). Small differences are observed, however; for example, double slipping does not always begin at the stress which would be expected if the previously non-active direction hardened at the same rate as the active one. Differences between the critical shear stresses may also be due to microscopic internal stresses set up during cold-working. These stresses can be expected to favour slip in certain directions and senses, and they will therefore be effective whenever the load is varied in orientation or sense. At present there is no clear evidence as to the importance of such effects in crystals of *pure* metals, but a Bauschinger effect has been observed in cold-worked brass, from which it could be largely removed by a mild annealing not reducing the average hardening (Sachs and Shoji 1927).

In the subsequent analysis we allow for these possibilities by associating two critical shear stresses with each of the preferred directions: $\tau_k$ for slip in the sense $a_k$, and $\tau'_k$ for slip in the sense $-a_k$. It is assumed that the hydrostatic part of the applied stress is without influence on these critical values; this has been found true in many pure metals (as distinct from alloys) provided the hydrostatic stress is not more than a few times the shear yield stress (*e. g.* Polanyi and Schmid 1923, Taylor 1927).

(i) *Maximum Work Principle for a Single Crystal.*

Let $d\epsilon_{ij}$ be a prescribed increment of strain in a single crystal, and let $\sigma_{ij}$ be a stress (not necessarily unique) which will produce this strain. Let $\sigma^*_{ij}$ be any other stress which does not violate the yield conditions. Then

$$dW-dW^*=(\sigma_{ij}-\sigma^*_{ij})\,d\epsilon_{ij}=\Sigma(\tau-\tau^*)\,d\gamma,$$

where the summation is over all shears of a set equivalent to $d\epsilon_{ij}$ and activated by $\sigma_{ij}$. We take each $d\gamma$ to be the shear (positive or negative) in the sense $a$ of the corresponding slip-direction, so that $\tau$ and $\tau^*$ are then the shear stresses in the same sense. Then, when $d\gamma>0$ in the *kth* direction,

$$\tau-\tau^*=\tau_k-\tau^*\geqslant 0$$

and when $d\gamma<0$ in the *kth* direction,

$$\tau-\tau^*=-\tau'_k-\tau^*\leqslant 0$$

since, by hypothesis $$-\tau'_k\leqslant\tau^*\leqslant\tau_k.$$

All products $(\tau-\tau^*)d\gamma$ are therefore positive or zero, and so

$$(\sigma_{ij}-\sigma^*_{ij})\,d\epsilon_{ij}\geqslant 0. \quad \ldots \ldots \ldots \quad (9)$$

The equality holds only when $\tau$ and $\tau^*$ are equal in all active directions, and, if there are at least 5 of these, $\sigma_{ij}$ and $\sigma^*_{ij}$ will generally differ only by a hydrostatic stress. Particular strains may be obtainable by applying any one of a number of stresses (not differing merely by a hydrostatic component), but these stresses all do the same work. For if $\sigma^*_{ij}$ is also a physically possible stress,

$$(\sigma^*_{ij}-\sigma_{ij})\,d\epsilon_{ij}\geqslant 0,$$

in addition to (9), and therefore $\sigma^*_{ij}d\epsilon_{ij}=\sigma_{ij}\,d\epsilon_{ij}$.

It is also to be remarked that many sets of shears (even associated with the same stress) may produce, in certain cases, the same strain. That is, more than one set of shears may be physically, as well as geometrically, possible. However, since there are only 5 disposable stress components it is clear that only for certain sets of 5 slip-directions is it possible to find a stress to activate them *in prescribed senses*, since the critical shear stress must also not be exceeded in the non-active directions.

### (ii) *Minimum Shear Principle for a Single Crystal.*

Let $d\epsilon_{ij}$ be a prescribed increment of strain and let $\sigma_{ij}$ be a stress which will produce this strain by activating a set of shears $d\gamma$. Let $d\gamma^*$ be any set of shears which are geometrically equivalent to the prescribed strain, but which are not necessarily operable by any stress satisfying the yield conditions. The virtual work equation can be written in two ways :

$$\sigma_{ij}\,d\epsilon_{ij}=\Sigma\tau\,d\gamma=\Sigma\tau\,d\gamma^*.$$

If $\tau_k=\tau'_k$ for each direction (no Bauschinger effect),

$$\Sigma\tau\,d\gamma=\Sigma\tau_k\,|\,d\gamma\,|,\quad\text{and}\quad \Sigma\tau\,d\gamma^*\leqslant\Sigma\tau_k\,|\,d\gamma^*\,|.$$

Hence $$\Sigma\tau_k\,|\,d\gamma\,|\leqslant\Sigma\tau_k\,|\,d\gamma^*\,|. \qquad (10)$$

In particular, when all directions are equally hardened,

$$\Sigma\,|\,d\gamma\,|\leqslant\Sigma\,|\,d\gamma^*\,|. \qquad (11)$$

This states that the sum of the absolute values of a physically possible set of shears producing a given strain is less than that for a set which is only geometrically possible. If more than one set is physically possible the sums of their absolute values are equal.

We have thereby proved the hypothesis (11) suggested by Taylor (1938), and extended it (10) to the case when the hardening is unequal.

## § 4. POLYCRYSTALLINE AGGREGATE.

The experimental laws of plastic deformation in an aggregate (as a whole) express relations between macroscopic measures of stress and strain. An ideal experiment is designed so that the measuring device gives an average value of stress or strain over a large number of crystal grains. In the interpretation of such measurements the following two assumptions are involved.

(*a*) The measuring device extends over a volume of such size that the distribution of orientations and hardnesses of crystals (or perhaps fragmented " crystallites ") does not vary significantly from one part to another. That is, the specimen is regarded as homogeneous in the macroscopic sense. This does not preclude a macroscopic state of anisotropy, since the actual orientations are not necessarily randomly distributed over all possible ones.

It is convenient to refer to the smallest cubical volume possessing this property as a " unit " cube.

(*b*) No correlation exists between microscopic stress and position over any plane section of " unit " area. This is the necessary and sufficient condition for the stress resultant over such a unit section to be a single force through the centroid of the section. The Cartesian components of the resultant force per unit area are, of course, the conventional measures of the corresponding components of macroscopic stress. These form a tensor (as a direct consequence of the conditions for linear equilibrium) and the tensor is symmetric if the stress resultant on a plane is a force, and not a force and irreducible couple. If a correlation did exist between microscopic stress and position (and this appears possible in principle), the macroscopic stress tensor would not necessarily be symmetric, and the conditions for angular equilibrium would take another form. These remarks are equally pertinent, of course, to the concept of *microscopic* stress in a single crystal and its dependence on the distribution of interatomic forces.

The definition of a normal component of an infinitesimal *homogeneous* strain is the increment of distance between two points initially unit distance apart in the direction under consideration. The definition of a component of shearing strain is based on the total relative tangential displacements of two pairs of perpendicular planes at unit distance apart. The analogous definition of the macroscopic strain-increment components for a " unit cube " of an aggregate is

$$dE_{ij}=\tfrac{1}{2}\int(l_i\,du_j+l_j\,du_i)\,dS, \quad . \quad . \quad . \quad . \quad . \quad . \quad (12)$$

where the integral is taken over the surface of the unit cube, $l_i$ being the unit outward normal, and $du_i$ the incremental microscopic displacement (the coordinate axes are taken parallel to the cube edges). When the microscopic displacement is a continuous function of position (no opening of cavities or sliding of one grain over another), Green's theorem gives

$$dE_{ij}=\frac{1}{2}\int\left\{\frac{\partial}{\partial x_i}(du_j)+\frac{\partial}{\partial x_j}(du_i)\right\}dV,$$

$$=\int(d\epsilon_{ij})\,dV,$$

taken through the volume of the unit cube, where $d\epsilon_{ij}$ is the microscopic strain-increment. Since the latter is a symmetric tensor with zero hydrostatic part so also is $dE_{ij}$.

Consider the work of deformation within a unit cube. It is

$$dW=\int(\sigma_{ij}\,d\epsilon_{ij})\,dV=\int(\sigma_{ij}\,du_i l_j)\,dS, \quad . \quad . \quad . \quad . \quad (13)$$

provided the displacement function is continuous and the equilibrium equations are satisfied. At grain boundaries, or elsewhere, the microscopic stress is not necessarily continuous in all its components, and only the stress resultants acting on opposite sides of such a surface must be the same for equilibrium.

We now postulate that the grains are distributed in the unit cube in such a way that there is no correlation between any component of the microscopic stress and any component of the displacement over any plane section of unit area. This is so provided that

$$\int\sigma_{ij}\,dA\times\int du_k\,dA=\int(\sigma_{ij}\,du_k)\,dA(i, j, k=1, 2, 3), \quad . \quad . \quad (14)$$

where the integration extends over the unit section. In particular, this is satisfied when the stress is uniform or when the strain is uniform (the stress being distributed according to (*b*) above). Applying (14) to each face of the unit cube, we find from (13) that

$$dW=\int(\sigma_{ij}\,d\epsilon_{ij})\,dV=S_{ij}\,dE_{ij}, \quad . \quad . \quad . \quad . \quad . \quad (15)$$

where $S_{ij}$ is the macroscopic stress tensor defined in (*b*).

(i) *Maximum Work Principle for an Aggregate.*

Let $S^*_{ij}$ be any macroscopic stress corresponding to an equilibrium microscopic distribution $\sigma^*_{ij}$ not violating the yield conditions at any point of a unit cube. Then, from (15),

$$(S_{ij}-S^*_{ij})\,dE_{ij}=\int\{(\sigma_{ij}-\sigma^*_{ij})\,d\epsilon_{ij}\}\,dV\geqslant 0, \quad . \quad . \quad . \quad . \quad (16)$$

since (9) holds at every point. We have thereby derived (4) from assumed properties of a single crystal. It is worth noting that (16) is still true even if $du_i$ is tangentially discontinuous across certain surfaces provided the corresponding frictional stress vanishes. This is approximately true in high-temperature creep where relative slip occurs between grains.

(ii) *Minimum Shear Principle for an Aggregate.*

Let $du_i$ and $du^*_i$ be two continuous displacement distributions, with zero divergence, taking the same values on the surface of a unit cube. $du_i$ is associated with an equilibrium distribution of stress $\sigma_{ij}$ satisfying the yield conditions. Then

$$\int(\sigma_{ij}\,d\epsilon_{ij})\,dV=\int(\sigma_{ij}\,d\epsilon^*_{ij})\,dV \quad \text{or} \quad S_{ij}\,dE_{ij}=S_{ij}\,dE^*_{ij},$$

and so $$\int(\Sigma\tau\,d\gamma)\,dV=\int(\Sigma\tau\,d\gamma^*)\,dV.$$

If $\tau_k=\tau'_k$ for each direction at any point (no Bauschinger effect),

$$\Sigma\tau\,d\gamma=\Sigma\tau_k\,|d\gamma|, \quad \Sigma\tau\,d\gamma^*\leqslant\Sigma\tau_k\,|d\gamma^*|.$$

Hence $$S_{ij}\,dE_{ij}=\int(\Sigma\tau_k\,|d\gamma|)\,dV\leqslant\int(\Sigma\tau_k\,|d\gamma^*|)\,dV. \quad . \quad . \quad . \quad (17)$$

When the critical shear stress is uniform throughout the aggregate:

$$\int (\Sigma |d\gamma|)\, dV \leqslant \int (\Sigma |d\gamma^*|)\, dV. \quad . \quad . \quad . \quad . \quad . \quad . \quad (18)$$

This is true whether or not the aggregate has the properties ascribed to the unit cube. There is a close formal analogy between (17) and (7), and between (18) and (8).

On combining (16) and (17) we have for a unit cube, when $\tau_k = \tau_k'$

$$S_{ij}^* dE_{ij} \leqslant S_{ij} dE_{ij} \leqslant \int (\Sigma \tau_k |d\gamma^*|)\, dV. \quad . \quad . \quad . \quad . \quad . \quad (19)$$

Another inequality that will be used later is

$$S_{ij}\, dE_{ij}^* \leqslant \int (\Sigma \tau_k |d\gamma^*|)\, dV, \quad . \quad . \quad . \quad . \quad . \quad . \quad . \quad (20)$$

where $du_i^*$ is *any* continuous distribution.

It is to be noticed carefully that in establishing these extremum principles for an aggregate there is an implicit assumption, not merely that slip is the only mechanism of distortion, but that it is also a *sufficient* mechanism. In other words, it is assumed that the equations of equilibrium (5) can be satisfied throughout an aggregate by a stress distribution which, at the same time, will everywhere operate sufficient shears to produce a continuous displacement. For this to be mathematically possible, it may well be that the microscopic stress and strain must be allowed to vary *continuously*, and not be restricted to take constant values within each of a finite number of regions (which may be grains or parts of grains). If a continuous variation is envisaged, the relations between microscopic stress and strain, established for a crystal of a certain finite size, must be assumed to apply *at a point*. This, of course, is a procedure that is adopted in every branch of mechanics.

## § 5. CALCULATION OF THE YIELD SURFACE.

In § 4 (i) a maximum work principle for an aggregate has been shown to hold when slipping under a critical shear stress is the only microscopic mechanism of distortion. It follows from § 2 (ii) that a plastic potential governs the relation between macroscopic stress and strain-increment, and that the plastic potential is identical with the yield function. If, therefore, the yield function can be calculated for any particular metal the relationships between the ratios of the stress components and the ratios of the strain-increment components follow immediately from (3).

We consider first what general properties of the yield function follow from the assumption of deformation by slip. It is evident that the hydrostatic part of the applied stress has no influence on yielding; that is, the yield surface is cylindrical (though not, of course, necessarily circular). This follows since the superposition of a uniform hydrostatic stress throughout a plastic aggregate does not disturb the equilibrium of the microscopic stresses, nor does it alter the active slip-directions at any point, when the influence of elasticity is disregarded. In reality, however, a certain effect of hydrostatic stress would be expected in an aggregate of elastically anisotropic grains.

If the critical shear stress does not depend on the sense of slip, and if the aggregate is free from internal stress when the applied loads are removed after cold-work, the yield surface for that state is symmetrical about the origin. That is, if $S_{ij}$ produces yielding when the aggregate is reloaded under constant stress-ratios so also will $-S_{ij}$. For the elastic compatibility equations are linear in the stresses, and hence if a microscopic distribution $\sigma_{ij}$ corresponding to $S_{ij}$ can be established by monotonic loading from a stress-free state so also can a distribution $-\sigma_{ij}$ corresponding to $-S_{ij}$. Furthermore, if $\sigma_{ij}$ satisfies the yield conditions at any point so does $-\sigma_{ij}$, and if $d\epsilon_{ij}$ is the increment of strain associated with $\sigma_{ij}$, $-d\epsilon_{ij}$ is the increment associated with $-\sigma_{ij}$. Plastic deformation would therefore be initiated under the stress $-S_{ij}$.

When the aggregate is macroscopically isotropic the yield surface can be shown to possess a six-fold symmetry in principal-stress space (Hill 1950, p. 18). Since this symmetry does not depend on any particular mechanism of plastic distortion, we do not need to discuss it here.

The exact calculation of the yield surface appears to be a matter of some difficulty. In the present paper we shall merely show that it is possible to calculate, with comparative ease, two cylindrical surfaces between which the yield surface must certainly lie when there is no Bauschinger effect. For this purpose we use the inequalities established in the last section. In one case we consider an aggregate in which the stress is uniform but displacement continuity is violated, and in the other case we consider an aggregate in which the strain is uniform but equilibrium is violated.

Take first the uniform stress distribution

$$\sigma^*_{ij}=\lambda^* r_{ij}, \quad r_{ij}=S_{ij}/(S_{ij}S_{ij})^{1/2}, \qquad \dots\dots \quad (21)$$

where, for given stress-ratios $r_{ij}$, $\lambda^*$ is to be chosen so that the critical shear stress corresponding to $\sigma^*_{ij}$ is just attained in one slip-direction at the "weakest" point of the aggregate. It is then certain that $\sigma^*_{ij}$ does not violate the yield conditions anywhere in the aggregate. $\sigma^*_{ij}$ is therefore an equilibrium distribution such as is envisaged in (16) (the displacement function being continuous) which leads to

$$(S_{ij}S_{ij})^{1/2}=|S_{ij}|\geqslant\lambda^*. \qquad \dots\dots\dots \quad (22)$$

Hence, for each direction $r_{ij}$ in stress hyperspace, (22) supplies a lower limit to the length of the corresponding "radius" to the yield surface. Since we know that the surface is cylindrical we need only take stresses $S_{ij}$ with zero hydrostatic part in (21).

Next take any *uniform* strain distribution $d\epsilon^*_{ij}=dE^*_{ij}$ with zero hydrostatic part, and such that $r_{ij}\,dE^*_{ij}>0$. Let $d\gamma^*$ be any of the sets of shears which are equivalent to the strain $dE^*_{ij}$. $d\gamma^*$ is a function of position since the lattice orientation varies through the aggregate. Let a quantity $\mu^*$ be defined such that

$$\mu^*=\int(\Sigma\tau_k\,|d\gamma^*|)\,dV/r_{ij}\,dE^*_{ij}, \qquad \dots\dots \quad (23)$$

where $r_{ij}$ is defined in (21) and the integration extends through the unit cube. Then, by (20),

$$|S_{ij}| \leqslant \mu^* . \qquad (24)$$

According to (10) the least possible value of $\mu^*$ for any choice of $dE^*_{ij}$ is to be obtained by taking $d\gamma^*$ to be a *physically* possible set of shears for each orientation, the "crystallites" being supposed completely independent. Then

$$\mu^* = (dE^*_{ij} \int \sigma^*_{ij} \, dV)/(r_{ij} \, dE^*_{ij}), \qquad (25)$$

where $\sigma^*_{ij}$ is a stress which would produce the strain $dE^*_{ij}$ in a free crystal. An advantageous choice of $dE^*_{ij}$ appears to be $dE^*_{ij} = r_{ij}$ (an arbitrary scale factor can obviously be omitted for convenience). Then, since $r_{ij} r_{ij} = 1$,

$$\mu^* = r_{ij} \int \sigma^*_{ij} \, dV. \qquad (26)$$

This value of $\mu^*$ is equal to the work which would be done if a unit cube of aggregate were split into its constituent regions of uniform orientation and each were separately given the strain $r_{ij}$.

## § 6. DEPENDENCE OF YIELD SURFACE ON STRAIN-HISTORY.

We have not yet considered how the shape and size of the yield surface depend on the previous strain-history. For simplicity let us disregard possible Bauschinger effects both in a crystal grain and in the aggregate as a whole, and suppose also that the critical shear stress is the same in all slip directions. If there were no work-hardening it is evident that the shape and size of the yield surface would be preserved during continued deformation, provided the distribution of orientations did not vary. (This last condition will not be satisfied whenever a preferred orientation is developed during cold-working). When work-hardening occurs the grains harden by different amounts, due partly to the non-uniform distortion and partly to their different orientations. However, to a first approximation, it seems reasonable to expect that the yield surface will simply increase in size without changing shape. The size will be proportional to some mean value of the critical shear stress.

There is some evidence (Taylor 1927) that the shear yield stress of a crystal is, very roughly, a function only of the total shear. That is,

$$\tau = F(\Sigma \gamma),$$

where the function F is the hardening curve in simple slip. Now we have seen that the work done on the aggregate unit cube during an increment of strain is

$$dW = \int (\tau \Sigma |d\gamma|) \, dV,$$
$$= \tau \Sigma |d\gamma|,$$

say, where $\tau$ and $\gamma$ now denote mean values over the aggregate. Hence, approximately

$$dW = \tau \, d\tau / F'$$

where F′ is the slope of the shear-hardening curve. Since F′ is a function of $\tau$ only, so also is W. Conversely, the mean critical shear stress is a function only of the total plastic work.

These qualitative considerations lead, therefore, to the conclusion that the size of the yield surface is mainly a function of the total plastic work, and that other factors are secondary (in the absence of Bauschinger effects). This, indeed, is observed for face-centred cubic metals (see Hill 1950, pp. 27–32).

## ACKNOWLEDGMENT.

We wish to thank the Director of the Mechanical Engineering Research Organization, D.S.I.R., for permission to publish this paper, one of us (J. F. W. B.) being seconded by D.S.I.R. to the Wills Physical Laboratory.

## REFERENCES.

CALNAN, E. A., and CLEWS; C. J. B., 1950, *Phil. Mag.*, **41**, 1085.
COX, H. L., and SOPWITH, D. G., 1937, *Proc. Phys. Soc.*, **49** (ii), 134.
HILL, R., 1950, *The Mathematical Theory of Plasticity* (Oxford: Clarendon Press).
KOCHENDÖRFER, A., 1941, *Reine und angewandte Metallkunde* (Berlin: Springer).
MARK, H., POLANYI, M., and SCHMID, E., 1922, *Z. f. Phys.*, **12**, 58.
POLANYI, M., and SCHMID, E., 1923, *Z. f. Phys.*, **16**, 336.
SACHS, G., 1928, *Z. d. Ver. deut. Ing.*, **72**, 734.
SACHS, G., and SHOJI, H., 1927, *Z. f. Phys.*, **45**, 776.
SCHMID, E., 1924, *Proc. Int. Congr. App. Mech.* (*Delft*), 342.
TAYLOR, G. I., 1927, *Proc. Roy. Soc.* A, **116**, 39; 1938, *Journ. Inst. Met.*, **62**, (i), 307; 1938, *S. Timoshenko Anniversary Volume*, 218 (New York: Macmillan).
TAYLOR, G. I., and ELAM, C. F., 1923, *Proc. Roy. Soc.* A, **102**, 643; 1925, *Ibid.*, **108**, 28.

# XLVII. ABSTRACT.

## *The Capacitance of a Parallel-Plate Condenser with an Anisotropic Dielectric Cylinder in Torsion between its Plates.*

By C. Mack,
The British Cotton Industry Research Association,
Shirley Institute, Manchester*.

[Received February 1, 1951.]

An abstract of the above paper is given here.

[The full paper will be published in the Shirley Institute Memoirs and copies may be obtained from the Director, Shirley Institute, Manchester, 20.]

### 1. Problems Solved.

The solution to this problem is important in estimating the accuracy of the capacitance method of measuring the irregularity of cotton yarn (Boyd 1949 and Walker 1950). The dielectric properties of cotton fibres are such that (Balls 1946) a singles cotton yarn may be represented by a uniformly twisted cylinder which, in the untwisted state, has one dielectric constant value along its length but a different, though axially symmetric, transverse value.

We first find the field when the cylinder is placed in a general type of field $F(R)$ [$\cos n\phi i$—$\sin n\phi j$] (see equation (1)). This calculation is carried out by using a molecular model and mathematical process akin to that of Lorentz's molecular dielectric theory, thus obtaining a pair of simple simultaneous integral equations (see (3)). If the twist is not too great a series solution is obtained when $F(R)=R^n$. With this series the field when the cylinder is placed parallel to and between two infinite conducting planes at different potentials is found by means of multipliers which can be determined to any required accuracy. By assuming that finite plates do not alter the field, the charge on the plates is calculated and finally the capacity. For non-midway positions the calculated capacity is not quite exact but is a good approximation if the plates are wide compared with their distance apart. An approximate solution valid for most midway cases is given (see (10)).

Acknowledgments are due to Mr. C. Illingworth of Manchester University for many helpful discussions and to Miss M. Castle of the Shirley Institute who has checked much of the mathematics and carried out the numerical work.

---

* Communicated by the Author.

## 2. Results.

We consider an infinitely long circular cylinder of radius W which has a dielectric constant $K_2$ parallel to its axis but an axially symmetric transverse value $K_1$. It is then twisted so that a line of molecules originally parallel to OZ, the axis, lies along the helix $x=R\cos bt$, $y=R\sin bt$, $z=t$, where $b$ is a constant, $0\leqslant R<W$ and $-\infty\leqslant t<+\infty$ (fig. 1).

We then prove that an externally applied field

$$F(R)\,[\cos N\phi i-\sin N\phi j] \quad . \quad . \quad . \quad . \quad . \quad . \quad . \quad . \qquad (1)$$

Fig. 1.

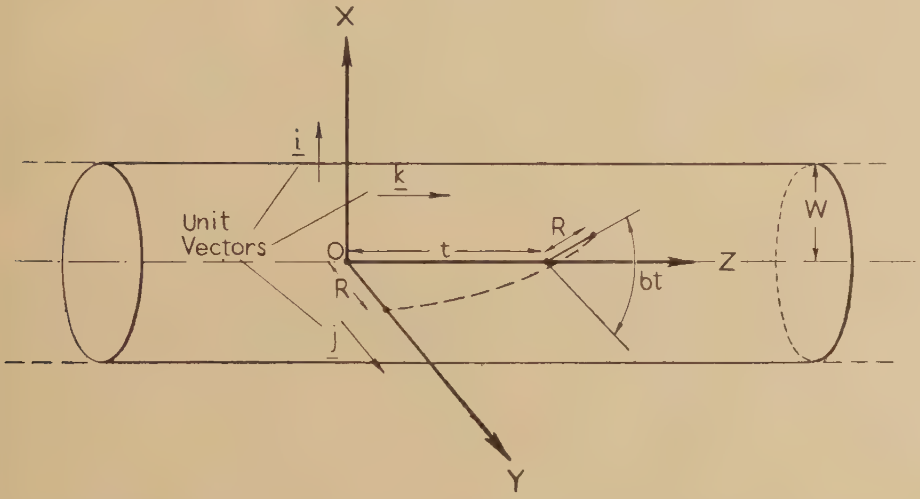

where $N=0, 1, 2 \ldots\ldots$, $x=R\cos\phi$ and $y=R\sin\phi$, produces a distribution of molecular dipoles of density

$$[A'\cos N\phi+B'\cos(N+2)\phi]\,i+[-A'\sin N\phi+B'\sin(N+2)\phi]j$$
$$+C'\sin(N+1)\phi k \quad . \quad . \quad . \qquad (2)$$

where $A'=k_1A+bRJ$, $B'=k_1B-bRJ$, $C'=k_1C-2J$

$$4\pi k_2(K_2+2)=3(K_2-1),\ 4\pi k_1(K_1+2)=3(K_1-1)$$
$$2J(1+b^2R^2)=(k_2-k_1)\,[bR(A-B)-C],\ 3C=4\pi C'$$
$$A-F(R)=-2\pi\left[A'(R)/3+B'(R)-2(N+1)R^N\int_R^W\left\{B'(S)/S^{N+1}\right\}dS\right]$$
$$B=-2\pi\left[B'(R)/3+A'(R)-2(N+1)R^{-(N+2)}\int_0^R A'(S)S^{N+1}\,dS\right].$$
$$. \quad . \quad . \qquad (3)$$

Outside the cylinder the field resulting from (2) is

$$D'[\cos(N+2)\phi i-\sin(N+2)\phi j]/R^{N+2},\quad D'=4(N+1)\pi\int_0^W A'(S)S^{N+1}\,dS$$
$$. \quad . \quad . \qquad (4)$$

Straightforward expansions solve the simultaneous integral equations (3) when $F(R)=2\pi(bR)^N$. Writing $bR=u$, $bW=U$

$$A'=u^N \sum_0^\infty a_m u^{2m}=A'_N, \text{ say}; \quad B'=u^N \sum_1^\infty b_m u^{2m}=B'_N, \text{ say};$$

$$C'=u^{N-1} \sum_1^\infty c_m u^{2m}=C'_N \text{ say}; \quad D'=2\pi(N+1)W^{2N+2} \sum_0^\infty a_m U^{2m}/(N+m+1)$$

$$=D'_N, \text{ say}$$

$$6K_1 a_m=J_{m-1}(K_1+2)\ [2K_1+(N+1)\ (K_1-1)/m],\ 3c_m=-2J_{m-1}(K_1+2),$$

$$6K_1 b_m=-J_{m-1}(K_1+2)\ [2K_1-(N+1)\ (K_1-1)/(m+N+1)],$$

$$m=1, 2, 3 \ldots, \ |U| \leqslant 1,$$

$$J_m/J_{m-1}=-1+(K_2-K_1)\ (N+1)^2/[4K_1 m(m+N+1)],$$

$$3(K_1-1)J_0=2(K_2+2)a_0$$

$$a_0(K_1+1)-(N+1)\ (K_1-1)\ [b_1U^2+b_2U^4/2+b_3U^6/3+ \ldots]=K_1-1 \ldots \quad \ldots \quad (5)$$

Fig. 2.

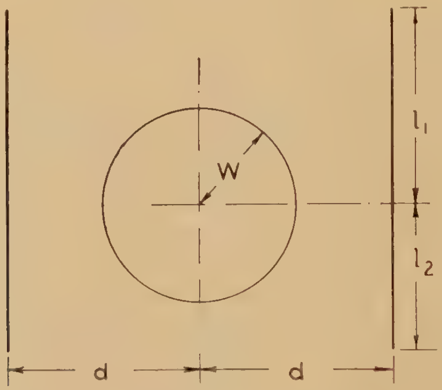

All quantities are first expressed in terms of $a_0$ then from the last equation the value of $a_0$ is found.

When the cylinder is placed between two infinite parallel conducting planes kept at different potentials we assume the dipole density to be

$$\sum_{N-0}^{\infty} \mu_N R^N[\{A'_N \cos N\phi+B'_N \cos (N+2)\phi\}i+\{-A'_N \sin N\phi$$
$$+B'_N \sin \times (N+2)\phi\}j+C'_N \sin (N+1)\phi k] \quad \ldots\ldots \quad (6)$$

At each image of the cylinder we imagine a cylinder with the same distribution (6) except that, for odd N, the $\mu_N$ change sign. At the images of these images we assume (6) with unchanged sign. At the images of these, odd $\mu_N$ change sign and so on. We then calculate the field at the original cylinder due to the original field and these images and we expand it thus

$$\sum_{N=0}^{\infty} F_N R^N [\cos N\phi i-\sin N\phi j] \quad \ldots\ldots \quad (7)$$

where the $F_N$ are infinite linear combinations of the $\mu_N$. From (5) the dipole density (7) would generate is calculated and must equal (6). By neglecting $\mu_N$ for $N \geqslant M$ we obtain a finite number of linear equations for the $\mu_N$. Numerical results indicate that by taking M large enough any desired accuracy can be achieved.

The case of the cylinder midway between the plates is considered in detail (Fig. 2). Provided the potential difference between the plates is $2d$; we have, writing

$$\sum_{1}^{\infty} (1/s)^r = S_r$$

$$\pi\mu_0 = \tfrac{1}{2} + \sum_{0}^{\infty} \mu_{2m} D'_{2m} S_{2m+2} (2d)^{-(2m+2)}, \quad \pi b^2 \mu_2 = \sum_{0}^{\infty} {}^{2m+3}C_2 \mu_{2m} D'_{2m} S_{2m+4} (2d)^{-2m-4}$$

$$\pi b^4 \mu_4 = \sum_{0}^{\infty} {}^{2m+5}C_4 \mu_{2m} D'_{2m} S_{2m+6} (2d)^{-2m-6} \text{ etc.}; \ \mu_1 = \mu_3 = \mu_5 = \ldots . = 0. \quad . \quad (8)$$

The charge per unit length induced on the width AB (fig. 2) is

$$\tfrac{1}{2} \sum_{m=0}^{\infty} (-1)^m \frac{\mu_{2m} D'_{2m} W^{4m+2}}{(2m+1)\,!} \left(\frac{\pi}{2d}\right)^{2m+1} \left[\frac{d^{2m} \tanh \beta}{d\beta^{2m}}\right]_{\beta = \pi l_1 (2d).} \quad . \quad (9)$$

The charge induced on AB′ is the same with $l_1$ replaced by $l_2$. In the case of finite plates we assume that the charge induced is not materially altered. Dividing by the potential difference we obtain the increase in capacity per unit length $\delta C$. For fig. 2 a good approximation is

$$\delta C \doteqdot \frac{3D'_0 \{\tanh[\pi l_1/(2d)] + \tanh[\pi l_2/(2d)]\}}{4\,(24\pi d^2 - \pi^2 D'_0)} . \quad . \quad . \quad . \quad (10)$$

A method of successive approximations is also given which may be applicable to other problems.

The solution, in the form of an expansion, to an applied field

$$R^M [\cos N\phi i - \sin N\phi j], \quad M \neq N$$

is also found (hence the more general case $\Sigma f_M R^M [\cos N\phi i - \sin Nj\phi]$ can be solved).

## References.

Balls 1946, *Dielectric Properties of Raw Cotton*, *Nature*, 1946, **158,** 9–11.

Boyd 1949, *An Electronic Instrument for Measuring Weight Variations in Silvers, Rovings and Yarn*, Journal of the Textile Institute (*Transactions*), July, 1949.

Walker 1950, *The Electronic Measurement of Sliver, Roving and Yarn Irregularity*, Annual Conference of the Textile Institute, 1950.

# XLVIII. CORRESPONDENCE.

---

## *The Resistance-Minimum in Gold.*

By D. K. C. MacDonald and I. M. Templeton,
The Clarendon Laboratory, Oxford*.

[Received February 1, 1951.]

The definite observation of a minimum in the electrical resistance of gold at low temperatures was first made by de Haas, de Boer and van den Berg (1933) and has so far received no satisfactory theoretical explanation. Later measurements by de Haas and van den Berg (1936, 1937) and Giauque, Stout, Clark (1937); Stout and Barieau (1939) have given evidence that the temperature of the minimum was a unique function of the relative resistance at the minimum (usually measured as $(R_{\text{min}}/R_{0^\circ\text{ C.}})$) for annealed specimens and that for an ideally pure specimen the minimum would occur at absolute zero. It has been suggested (*cf.* Gorter 1938) that the resistance of any specimen would rise towards infinity if the temperature were lowered sufficiently far, but this suggestion hardly seems feasible particularly in view of the remarkable behaviour then to be expected at extremely low temperatures in a specimen of vanishingly small impurity.

Two very tentative theories by one of us (D. K. C. McD.) suggest that the resistance would pass through a point of inflexion below the minimum and then flatten off ultimately on approach to absolute zero at a higher value than the minimum. Both theories suggest, however, that the nature of the particular impurity atoms present would affect the situation of the minimum. Since it appears likely that the major impurity present in the specimens available to the Dutch and American workers would generally be silver (the latter workers in fact worked specifically in one case with a range of Au–Ag alloys and report silver as the major impurity in the later work) it seemed profitable to investigate some prepared alloys containing other specific impurities. At the same time specimens with *no* intentionally inserted impurity were examined by us.

Alloys containing respectively 0·05 per cent (by weight) of Cu and Ni and 0·2 per cent of Ni were made for us by Messrs. Johnson, Matthey and Co. Ltd., and we also experimented with a sample of fine gold which we drew down to a suitable diameter and a sample of "spectrographically pure" gold. As may be seen from the accompanying graph which also displays the data obtained elsewhere, the latter two specimens agree rather well with the curve of $R_{\text{min}}$ against $T_{\text{min}}$ suggested by the other workers. (It should be noted that the minima derived in America are only

---

* Communicated by the Authors

approximate since they do not have experimental results above ~4° K. or below ~10° K.). However the results for our "alloys" do not agree at all and this suggests very strongly that the presumption of a simple variation with residual resistance alone cannot be accepted. In fact, it seems tempting to assume that there is a characteristic curve for each type of impurity atom.

Fig. 1.

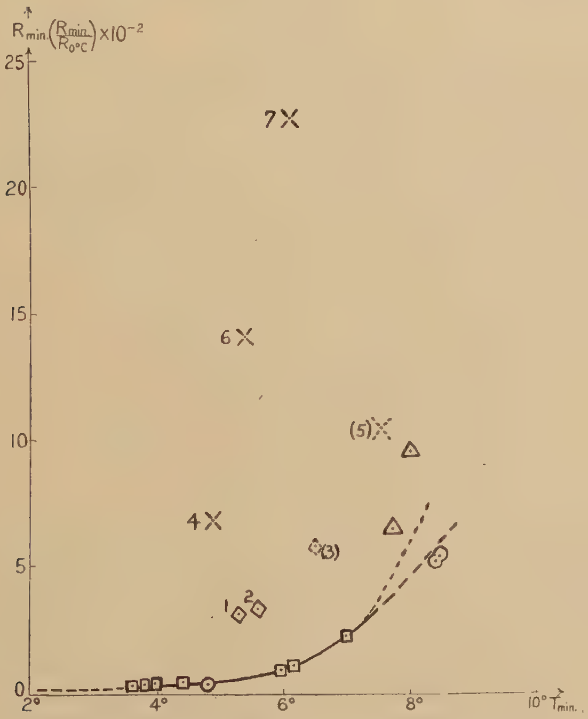

⊡ : Data of : de Haas and v. d. Berg. △ : Data of Giauque, Stout *et al.*
⊙ : Data of : Present work—"Specpure" and "fine" gold.

◇: Data of : Present work—0·05% Cu/Au
- 1. "Hot" annealed.
- 2. "Cold" annealed.
- 3. Unannealed.

╳: Data of : Present work—Ni/Au
- 4. 0·05% "Hot" annealed.
- 5. 0·05% Unannealed.
- 6. 0·2% "Hot" annealed.
- 7. 0·2% "Cold" annealed.

Since it was thought that the precise method of annealing might be critical (*e. g.* Stout and Barieau annealed their wire for three hours at 450° C.) we have annealed specimens at ~400° C. for 2–3 hours and also at ~850° C. (onset of bright red heat) for about the same period. There appears to be little difference in the cases of the "pure" gold specimens and Cu/Au alloy but in the 0·2 per cent Ni/Au alloy a considerable improvement in residual resistance occurred with the "*hot*" annealing over the "cold" process with a slight shift of the minimum to a lower temperature. We may also mention that in the 0·05 per cent Ni and Cu alloys annealing by either method produced a considerable minimum shift to a lower temperature—the points for the unannealed specimens are shown by dotted characters on the graph.

Further experiments are in progress and it is hoped to publish the work in more detail later.

## REFERENCES.

GIAUQUE, STOUT and CLARK, 1937, *Phys. Rev.*, **51,** 1108.
GORTER, 1938, *Physica*, **5,** 483.
*DE HAAS, DE BOER, and V. D. BERG, 1933, *Physica*, **1,** 1115.
* DE HAAS and V. D. BERG, 1936, *Physica*, **3,** 440 ; 1937, *Ibid.*, **4,** 683.
STOUT and BARIEAU, 1939, *Journ. Amer. Chem. Soc.*, **61,** 238.

---

## *The Range-Energy Relation for Slow Alpha-Particles in Air.*

By JOAN M. FREEMAN and W. E. BURCHAM,
Cavendish Laboratory, Cambridge[†].

[Received February 13, 1951.]

DURING some recent work on ($p\alpha$) reactions (Burcham and Freeman 1949 a, b) the ranges in air of a number of groups of alpha-particles with energies between 1 and 2·5 MeV. were compared. The measured range differences were used to obtain the energy differences for the corresponding groups of alpha-particles, with the aid of the range-energy relation given by Holloway and Livingston (1938). This range-energy relation was constructed on the assumption that the number of ions formed by an alpha-particle stopping in air was strictly proportional to its energy ; this assumption has recently been shown to be incorrect (Jesse and Sadauskis 1950), and a new range-energy relation has been given by these authors and also by Bethe (1950). The difference between the new and old range-energy curves is most significant for energies below about 2·5 MeV., and the new relation is in good agreement with observations on the $^6$Li($n\alpha$) and $^{10}$B($n\alpha$) reactions, for which the alpha-particle ranges have been measured, and the energy releases are also accurately known as a result of magnetic deflection experiments (see Bethe 1950). The number of points on the range-energy curve for energies less than 2·5 MeV., for which direct measurements of range and energy have been made is however small. It was therefore thought

---

[*] Or see : V. D. BERG, 1938, *Thesis*, Leiden, "De Electrische Weerstand van zuivere Metalen bij lage . . . Temperaturen ".

[†] Communicated by the Authors.

to be of some interest to use the range measurements made during the work on ($p\alpha$) reactions to check the slope of the range-energy curve in the region from 2·5 down to 1·0 MeV.

The measurements were made by a method previously described (Burcham and Freeman 1949 a, § 3 (*a*)). The reactions studied, together with the energy releases deduced from recent magnetic deflection measurements are shown below (Table I.).

### Table I.

Energy Releases in ($p\alpha$) reactions.

| Reaction | $Q$ (MeV.) | Reference |
|---|---|---|
| $^9$Be($p\alpha$)$^6$Li | 2·121 ± 0·012<br>2·142 ± 0·006 | Tollestrup, Fowler and Lauritsen (1949)<br>Strait *et al.*, quoted by Hornyak, Lauritsen, Morrison and Fowler (1950) |
| $^{10}$B($p\alpha$)$^7$Be | 1·148 ± 0·006<br>1·152 ± 0·004<br>1·147 ± 0·010 | Brown, Chao, Fowler and Lauritsen (1950)<br>Van Patter, Sperduto, Strait and Buechner (1950)<br>Burcham and Freeman (1950) |
| $^{19}$F($p\alpha_1$)$^{16}$O* | 1·977 ± 0·008<br>1·979 ± 0·009 | Chao, Tollestrup, Fowler and Lauritsen (1950)<br>Freeman (1950) |
| $^{19}$F($p\alpha_2$)$^{16}$O* | 1·204 ± 0·008<br>1·200 ± 0·010 | Chao, Tollestrup, Fowler and Lauritsen (1950)<br>Freeman (1950) |
| $^{19}$F($p\alpha_3$)$^{16}$O* | 1·002 ± 0·008<br>0·996 ± 0·010 | Chao, Tollestrup, Fowler and Lauritsen (1950)<br>Freeman (1950) |

At the time at which the measurements were made the Q-value for $^9$Be($p\alpha$) seemed the best known, and all range comparisons were made with the alpha-particles from this reaction taken as standard. We have now chosen the $^{19}$F($p\alpha_1$) reaction with $E_p = 873{\cdot}5$ keV. and angle of observation 83°, as the standard, giving alpha-particles of energy 2·272 ± 0·010 MeV. ; the corresponding mean range, from the curve given by Bethe (1950), is 1·157 cm. The observed range differences then lead, after small corrections for differences of straggling and target thickness, to the mean ranges given in Table II. The energies shown in this Table were calculated, for the given conditions of bombardment, from the Q-values listed in Table I.; for the $^{19}$F($p\alpha$) reactions the Q-values given by Chao, Tollestrup, Fowler and Lauritsen were used, since the values obtained by Freeman, although in good agreement, were based on a spectrometer calibration which involved the Q-value of the $^9$Be($p\alpha$)

reaction. This was assumed at the time to be 2·121 MeV., but the more recent measurement gives an appreciably higher value (see Table I.). The weighted mean of the two Q-values was used to calculate the energy given in Table II. for the alpha-particles from the $^9$Be($p\alpha$) reaction.

TABLE II.

Range Energy Relation.

| Reaction | $E_p$ (keV.) | $E_\alpha$ (MeV.) (Angle of observation 83°) | Mean range cm. of air at 15° C., 760 mm. |
|---|---|---|---|
| $^{19}$F($p\alpha_1$)$^{16}$O* | 669 | 2·113 ± 0·010 | 1·068 ± 0·008 |
| $^9$Be($p\alpha$)$^6$Li | 860 | 1·774 ± 0·015 | 0·895 ± 0·008 |
| $^{19}$F($p\alpha_2$)$^{16}$O* | 873·5 | 1·649 ± 0·010 | 0·812 ± 0·008 |
| $^{19}$F($p\alpha_3$)$^{16}$O* | 669 | 1·326 ± 0·010 | 0·651 ± 0·008 |
| $^{10}$B($p\alpha$)$^7$Li | 630 | 1·113 ± 0·007 | 0·559 ± 0·011 |

Fig. 1.

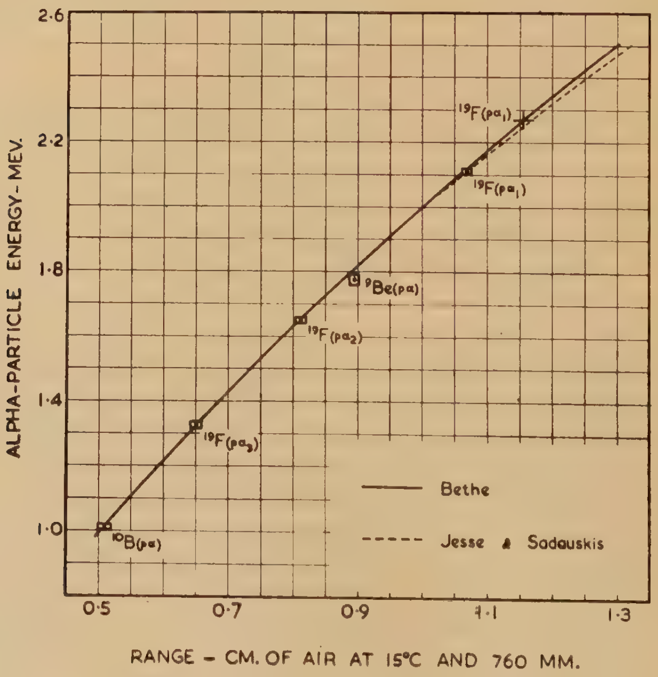

These results are plotted in fig. 1, together with the curves proposed by Bethe (1950) and Jesse and Sadauskis (1950). The standard point for $^{19}$F($p\alpha_1$) at $E_p$=873·5 keV. has been placed on the former curve, and all the other points, except that for $^9$Be($p\alpha$), lie within 10 keV. of the curve. The position of the point for $^9$Be($p\alpha$) suggests that the higher Q-value of the two given in Table I. is the more nearly correct.

The results confirm the slope of the new range-energy curves over the energy range 1·0–2·3 MeV. ; they are in slightly better agreement with the curve given by Bethe (1950) than with the figures given by Jesse and Sadauskis in the region where these differ.

## REFERENCES.

BETHE, H. A., 1950, *Rev. Mod. Phys.*, **22,** 213.
BURCHAM, W. E., and FREEMAN, J. M., 1949 a, *Phil. Mag.*, **40,** 807 ; 1949 b, *Phys. Rev.*, **75,** 1756 ; 1950, *Phil. Mag.*, **41,** 337.
BROWN, A. B., CHAO, C. Y., FOWLER, W. A., and LAURITSEN, C. C., 1950, *Phys. Rev.*, **78,** 88.
CHAO, C. Y., TOLLESTRUP, A., FOWLER, W. A., and LAURITSEN, C. C., 1950, *Phys. Rev.*, **79,** 108.
FREEMAN, J. M., 1950, *Phil. Mag.*, **41,** 1225.
HOLLOWAY, M. G., and LIVINGSTON, M. S., 1938, *Phys. Rev.*, **54,** 18.
HORNYAK, W. F., LAURITSEN, T., MORRISON, P., and FOWLER, W. A., 1950, *Rev. Mod. Phys.*, **22,** 291.
JESSE, W. P., and SADAUSKIS, J., 1950, *Phys. Rev.*, **78,** 1.
TOLLESTRUP, A., FOWLER, W. A., and LAURITSEN, C. C., 1949, *Phys. Rev.*, **76,** 428.
VAN PATTER, D. M., SPERDUTO, A., STRAIT, E. N., and BUECHNER, W. W., 1950, *Phys. Rev.*, **79,** 900.

# XLIX. *Notices of New Books and Periodicals received.*

*Weltsystem, Weltather, und die Relativitaetstheorie.* By K. JELLINCK. Pp. 450. (Verlag, Basel: Wepf and Co., 1949.) Price 45 S.Fr.

*Verstandlische Elemente der Wellenmechanik.* By K. JELLINCK. 1 Teil. Pp. 304. (Verlag, Basel: Wepf and Co., 1950.) Price 34 S.Fr.

PROFESSOR JELLINCK may be known to many readers as the author of an extensive work on Physical Chemistry. In the preface to the book on the Theory of Relativity he confides that he has always wanted to understand this theory, but not finding a suitable textbook, he decided to write one both for himself and for the great number of experimental physicists and chemists.

As the title suggests the author believes that the Theory of Relativity can be understood only by postulating an absolute frame of reference with respect to which all galaxies are, on the average, at rest (*Weltbezugs system*). The General Theory of Relativity states that even if it could be found, it must in no way be distinguishable from any other inertial frame of reference. It therefore seems unnecessary to introduce the Weltbezugs system in the first place. But this concept has, apparently, helped Professor Jellinck to a better understanding of the theory, and it may likewise help many others. Apart from this special attitude the book is easy to read and abounds in detailed discussions of particular problems. The tensor calculus is made familiar by working out many examples. This is probably the best way of becoming used to a new method. A discussion of the electro-magnetic equations, which should appeal strongly to experimentalists by showing at once the power and simplicity of the Special Theory of Relativity is unfortunately not included.

The other book by Professor Jellinck is the first of two volumes on the principles and methods of wave mechanics. The demands on the reader with regard to mathematical knowledge are very small, as all necessary concepts are developed in the book. An attractive feature of the book is the discussion of various examples, such as harmonic oscillator, spinning top, and Kepler problem, from the points of view of Classical Mechanics, of the old Quantum Theory, and of Wave Mechanics. The final section is devoted to the problem of potential barriers and its applications.

The text is amply illustrated and very readable.

One unsatisfactory feature of the book must, however, be mentioned. It concerns the interpretation of some results of Wave Mechanics. For instance, in the case of the harmonic oscillator, Professor Jellinck asks: How is it possible for a particle with a definite energy to be found with a finite probability outside the classically allowed range? The answer is, of course, that as long as the energy is known exactly the position of the particle is completely unknown, but as soon as the position of the particle has been determined by experiment its energy is no longer known precisely.

Professor Jellinck, however, argues as follows: The particle apparently can get to a place where its potential energy is greater than its total energy; but its kinetic energy cannot be negative. Therefore the total energy as calculated by Wave Mechanics is only the constant average of the rapidly fluctuating actual energy of the particle. This fluctuating energy comes from the ether, which Professor Jellinck introduces very early in the book, together with the absolute frame of reference (Weltbezugs system). The ether has the property not only to propagate the wave function but also to interact energetically with the dynamical system.

This way of explaining the " paradoxes "of Wave Mechanics is contrary to the logical scheme of Wave Mechanics, and misleading for the student.

*Ultrasonics.* By P. Vigoureux. Pp. 163. (Chapman and Hall, 1950.) Price 25*s.*

The author has dealt with the technique and with the theory of ultrasonics in simple terms which brings the work within the scope of a wide circle of readers including undergraduates.

Readers may remember the standard of work of Bergmann to which the author refers and which appeared in 1937. The author gives a good account of the progress which has been made since then in the study of attenuation, and in the effects associated with the vibrational states of molecules both in gases and in liquids.

*The Mathematical Theory of Plasticity.* By R. Hill. [Pp. 354.] (Oxford: University Press.) Price 35*s.*

The mathematical theory of plasticity has undergone great development in the past dozen years or so, not only in its extension to more complex problems of industrial interest, but in its fundamental concepts and techniques. Much has been done to remove the reproach that it was one of the unrealistic branches of applied mathematics. This book is principally concerned with the behaviour of a model substance with the following properties: (i.) it is and remains isotropic; (ii.) it has a yield point; (iii.) this depends on the kind of stress in accordance with von Mises' hypothesis (the yield surface in " principal stress space " is a right circular cylinder) or, as an occasional alternative, with Tresca's hypothesis of critical shear stress; (iv.) work hardening occurs as a function of the irrecoverable work done, or of Odquist's integral plastic strain, or not at all; (v.) the principal axes of the plastic strain increment are parallel to the principal axes of the stress, frequently with the simplification that the principal strain increments are proportional to the deviatoric principal stresses; (vi.) the superimposed effects of elasticity are consistently regarded throughout.

Considerable care is given to showing that these are the best assumptions, within the range of those capable of mathematical treatment, for conformity with the requirements of metal physics: and they lead to results in very satisfactory conformity with experimental measurements. The weakest of the assumptions is clearly (i.), and a final chapter on plastic anisotropy develops the attack against this weakness. The author, who has been intimately concerned with the modern developments of the subject, has been in the fortunate position of being able to write what is simultaneously a complete text-book and a report of recent advancements.

F. C. F.

*Mathematical Snapshots.* By Prof. Hugo Steinhaus, Oxford University Press. [Pp. 265, with 295 illustrations.] (London: Geoffrey Cumberlege.) Price 27*s.* 6*d.* net.

This book attempts with notable success to present mathematical ideas and theorems attractively to the layman with the help principally of illustrations. These are many and imaginative, while the text is always clear and to the point, if occasionally perhaps too brief. The author ranges widely, without evident design, from pursuit paths to polyhedra, from longimeters to loxodromes, from tesselations to topology, from counterfeit coins to cartography. Really difficult theorems are included, for example ones due to Minkowski and Lebesgue. A few results are proved; most are stated with a challenge to the reader, but a bibliography of original papers is thoughtfully provided. Even a mathematical specialist, whatever his field, will surely find much in this book to divert him.

R. H.

*Electromagnetic Theory.* By OLIVER HEAVISIDE. [Pp. xxx+386.] (New York, Dover Publications Inc. British Agents: Interscience Publishers, Ltd.). Price 60*s*.

THIS is a photographic reproduction in one volume (12 in. by 9 in.) of the three volumes which appeared in 1883, 1899 and 1912. Four pages of the original appear on one page of the reproduction. Despite the reduction in size the print is quite as readable as in the reprint of 1925. Besides the original text there are a portrait of the author, a biographical sketch and an appraisal of Heaviside's contribution to vector analysis, electromagnetism and communication theory. J.D.E.

---

[*The Editors do not hold themselves responsible for the views expressed by their correspondents.*]